

NAVAL POSTGRADUATE SCHOOL

Monterey, California

②

AD-A237 028




DTIC
ELECTE
JUN 18 1991
S B D

THESIS

IMPACT OF ION PROPULSION ON PERFORMANCE,
DESIGN, TESTING AND OPERATION
OF A GEOSYNCHRONOUS SPACECRAFT

by

Spotrizano Descanzo Lugtu

June 1990

Thesis Advisor:
Co-Advisor

Brij N. Agrawal
Oscar Biblarz

Approved for public release; distribution unlimited

91-02174


91 6 14 040

Unclassified

Security Classification of this page

REPORT DOCUMENTATION PAGE

1a Report Security Classification Unclassified		1b Restrictive Markings	
2a Security Classification Authority		3 Distribution Availability of Report	
2b Declassification/Downgrading Schedule		Approved for public release; distribution is unlimited.	
4 Performing Organization Report Number(s)		5 Monitoring Organization Report Number(s)	
6a Name of Performing Organization Naval Postgraduate School	6b Office Symbol (If Applicable) 39	7a Name of Monitoring Organization Naval Postgraduate School	
6c Address (city, state, and ZIP code) Monterey, CA 93943-5000		7b Address (city, state, and ZIP code) Monterey, CA 93943-5000	
8a Name of Funding/Sponsoring Organization	8b Office Symbol (If Applicable)	9 Procurement Instrument Identification Number	
8c Address (city, state, and ZIP code)		10 Source of Funding Numbers	
		Program Element Number	Project No
		Task No	Work Unit Accession No

11 Title (Include Security Classification) IMPACT OF ION PROPULSION ON PERFORMANCE, DESIGN, TESTING AND OPERATION OF A GEOSYNCHRONOUS SATELLITE			
12 Personal Author(s) Spotrizano D. Lugu			
13a Type of Report Master's Thesis	13b Time Covered From To	14 Date of Report (year, month, day) June 1990	15 Page Count 177
16 Supplementary Notation The views expressed in this thesis are those of the author and do not reflect the official policy or position of the Department of Defense or the U.S. Government.			
17 Cosati Codes		18 Subject Terms (continue on reverse if necessary and identify by block number)	
Field	Group	Subgroup	
		Ion Propulsion; Geosynchronous Satellite; North-South Station Keeping	

19 Abstract (continue on reverse if necessary and identify by block number)	
<p>This thesis presents the implementation issues of an ion propulsion subsystem (IPS) on a geosynchronous communications satellite. As an example, Ultra High Frequency (UHF) Follow-On class satellite is selected for this study. The issues include: 1) impact of integration of IPS with other subsystems, such as the electrical power subsystem to take care of the heavy demand of power requirements and location of the subsystem with least impact on attitude control and plume impingement on solar arrays, 2) environmental considerations- particulate contamination, electrostatic discharge (ESD), and electromagnetic interference (EMI), and finally risks and benefits. Ion propulsion offers significant advantages over chemical propulsion due to its high specific impulse and the advent of xenon thruster technology, multikilowatt spacecraft, and nickel-hydrogen (Ni-H₂) batteries with demonstrated high cycle life have combined to make the ion thruster attractive for North-South Station Keeping (NSSK).</p>	
20 Distribution/Availability of Abstract	21 Abstract Security Classification
<input checked="" type="checkbox"/> unclassified/unlimited <input type="checkbox"/> same as report <input type="checkbox"/> DTIC users	Unclassified

22a Name of Responsible Individual Brij N. Agrawal	22b Telephone (Include Area code) (408) 646-3338	22c Office Symbol AA/Ag
--	--	-----------------------------------

DD FORM 1473, 84 MAR

83 APR edition may be used until exhausted

security classification of this page

All other editions are obsolete

Unclassified

Approved for public release; distribution is unlimited.

Impact of Ion Propulsion on Performance,
Design, Testing and Operation
of a Geosynchronous Spacecraft

by

Spotrizano D. Lugtu
Lieutenant, United States Navy
B.S., FEATI University, 1975

Submitted in partial fulfillment of the
requirements for the degree of

MASTER OF SCIENCE IN ASTRONAUTICAL ENGINEERING

from the

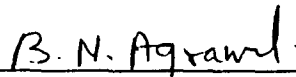
NAVAL POSTGRADUATE SCHOOL

June 1990

Author:

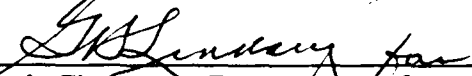

Spotrizano Descenzo Lugtu

Approved By:



B. Agrawal, Thesis Advisor


O. Bielacz, Second Reader


E. Roberts Wood, Chairman, Department of Aeronautical and
Astronautical Engineering

ABSTRACT

This thesis presents the implementation issues of an ion propulsion subsystem on geosynchronous communications satellites. As an example, Ultra-High Frequency (UHF) Follow-On class satellite is selected for this study. The issues include: 1) impact of integration of ion propulsion subsystem with other subsystems, such as the electrical power subsystem to take care of the heavy demand of power requirements and location of the subsystem with least impact on attitude control and plume impingement on solar arrays, 2) environmental considerations- particulate contamination, electrostatic discharge (ESD), and electromagnetic interference (EMI), and finally 3) risks and benefits. Ion propulsion offers significant advantages over chemical propulsion due to its high specific impulse and the advent of xenon thruster technology, multikilowatt spacecraft and nickel-hydrogen (Ni-H₂) batteries with demonstrated high cycle life have combined to make the ion thruster attractive for North-South Station Keeping (NSSK).

Accession For	
NTIS GRA&I	<input checked="" type="checkbox"/>
DTIC TAB	<input type="checkbox"/>
Unannounced	<input type="checkbox"/>
Justification	
By _____	
Distribution/	
Availability Codes	
Dist	Avail and/or Special
A-1	

TABLE OF CONTENTS

I.	INTRODUCTION.....	1
A.	OBJECTIVE	2
B.	SCOPE OF STUDY	2
II.	SELECTION OF GEOSYNCHRONOUS SPACECRAFT.....	4
A.	SATELLITE DESCRIPTION	4
1.	Station Keeping Considerations	4
B.	LAUNCH VEHICLE.....	9
III.	TYPES OF ELECTRIC PROPULSION THRUSTERS	12
A.	ION THRUSTER.....	14
1.	Field-Emission Ion Thruster (FEIT).....	16
2.	RF Ionization Thruster.....	17
3.	Electron Bombardment Ion Thruster (EBIT).....	19
B.	ELECTROTHERMAL	20
1.	Resistojet.....	20
2.	Arcjet.....	20
3.	Pulsed Electrothermal Thruster	21
4.	Laser.....	22
5.	Microwave.....	24
C.	ELECTROMAGNETIC	25
1.	MPD Thruster.....	26
2.	Pulsed Plasma Thruster (PPT).....	27
3.	Pulsed Inductive Thruster (PIT).....	27
E.	PERFORMANCE COMPARISON OF ELECTRIC PROPULSION..	28

IV.	XENON ION PROPULSION SUBSYSTEM DESCRIPTION	33
A.	PERFORMANCE CHARACTERISTICS OF XENON	33
B.	XENON ION THRUSTER OPERATION.....	37
C.	SELECTION OF ION THRUSTER	38
1.	Trade-offs Between Ion Thrusters.....	38
2.	Selection of Thrust Level	39
3.	Available Ion Thrusters.....	39
E.	LOCATION OF ION THRUSTERS.....	42
1.	Ion Thrusters on Gimbals.....	55
V.	STATION KEEPING	60
A.	NORTH-SOUTH STATION KEEPING (NSSK)	60
1.	Perturbation Forces	62
B.	EAST-WEST STATION KEEPING (EWSK).....	62
C.	STATION REPOSITIONING	63
D.	NSSK STRATEGY	64
VI.	SOLAR ARRAY/BATTERY TRADE-OFF AS POWER SOURCE FOR ION THRUSTER	66
A.	SOLAR ARRAY.....	67
1.	Solar Array Description.....	68
2.	Solar Array as Power Source for IPS	68
B.	BATTERY.....	69
1.	Battery Description.....	70
2.	Battery as Power Source for IPS.....	70
VII.	BIPROPELLANT AND ION PROPULSION TRADE-OFF	72
VIII.	IMPLEMENTATION IMPACT ON PRESENT SUBSYSTEMS	80
A.	PROPULSION.....	80

B.	ELECTRIC POWER.....	80
C.	THERMAL CONTROL.....	81
D.	STRUCTURES.....	82
E.	TELEMETRY, TRACKING AND CONTROL (TT&C).....	82
F.	ATTITUDE CONTROL.....	83
IX.	ENVIRONMENTAL IMPACT	85
A.	PARTICULATE CONTAMINATION.....	85
1.	Contamination Process.....	85
a.	Production of Positive Ions.....	87
B.	ELECTROMAGNETIC INTERFERENCE (EMI).....	88
C.	ELECTROSTATIC CHARGING AND DISCHARGING (ESD).....	89
1.	Neutralization of the Beam.....	90
2.	The Acceleration and Deceleration Concept.....	91
3.	Charge-Exchange Plasma Flow	91
X.	RISKS AND BENEFITS OF ION PROPULSION.....	92
A.	REQUIREMENTS FOR GROUND TESTING.....	92
B.	UNCERTAINTIES IN FLIGHT OPERATION.....	93
C.	COST AND BENEFITS	94
XI.	SUMMARY AND CONCLUSIONS	97
A.	BIPROPELLANT AND ION PROPULSION TRADE-OFF.....	97
B.	IMPACT ON OTHER SUBSYSTEMS	97
C.	ENVIRONMENTAL IMPACT	98
D.	RISKS AND BENEFITS	99
APPENDIX A: BIPROPELLANT AND ION PROPULSION TRADE-OFF FOR NORTH-SOUTH STATION KEEPING USING HUGHES 13CM ION THRUSTER		100

A.	CASE I: PURE XENON ION PROPULSION.....	101
1.	For 10 Year Mission.....	101
a.	Assume ETR Launch	102.....
b.	Assume Ariane IV Launch	103 .
2.	For 15 Year Mission.....	104
a.	Assume ETR Launch	105
b.	Assume Ariane IV Launch	105
3.	For 20 Year Mission.....	106
a.	Assume ETR Launch	107
b.	Assume Ariane IV Launch	107
B.	CASE II: ION AND BIPELLANT COMBO	108
1.	For 10 Year Mission.....	108
2.	For 15 Year Mission.....	108
3.	For 20 Year Mission.....	109
a.	Assume ETR Launch	109
b.	Assume Ariane IV Launch	110
 APPENDIX B. BIPELLANT AND ION PROPULSION TRADE-OFF		
FOR NORTH-SOUTH STATION KEEPING USING UK-10 ION		
	THRUSTER	111
A.	USING PURE XENON ION PROPULSION	112
1.	For 10 Year Mission.....	112
a.	Assume ETR Launch	113
b.	Assume Ariane IV Launch	114
2.	For 15 Year Mission.....	114
a.	Assume ETR Launch	115
b.	Assume Ariane IV Launch	115

3.	For 20 Year Mission.....	116
a.	Assume ETR Launch	117
b.	Assume Ariane IV Launch	117
APPENDIX C. BIPROPELLANT AND ION PROPULSION TRADE-OFF		
FOR NORTH-SOUTH STATION KEEPING USING MELCO ION		
	THRUSTER	119
A.	USING PURE XENON ION PROPULSION	120
1.	For 10 Year Mission.....	120
a.	Assume ETR Launch	121
b.	Assume Ariane IV Launch	122
2.	For 15 Year Mission.....	122
a.	Assume ETR Launch	123
b.	Assume Ariane IV Launch	124
3.	For 20 Year Mission.....	124
a.	Assume ETR Launch	125
b.	Assume Ariane IV Launch	126
APPENDIX D. EAST-WEST STATION KEEPING.....		
	A. USING ION PROPULSION.....	127
	A. USING ION PROPULSION.....	128
APPENDIX E. STATION REPOSITIONING.....		
	A. USING PURE XENON ION PROPULSION	129
APPENDIX F. ORBIT VELOCITIES.....		
	APPENDIX F. ORBIT VELOCITIES.....	131
APPENDIX G. NORTH-SOUTH STATION KEEPING.....		
	A. FOR 10 YEAR MISSION	137
	A. FOR 10 YEAR MISSION	138
	B. FOR 15 YEAR MISSION	139
	C. FOR 20 YEAR MISSION	139

APPENDIX H. BIROPELLANT MASS BUDGET FOR 10, 15 AND 20

YEAR MISSION..... 141

A. FOR 10 YEAR MISSION 142

 1. For Station Repositioning 142

 2. For East-West Station Keeping..... 142

 3. For North-South Station Keeping 142

 4. Assuming the Spacecraft is Launched at French Guiana 143

 5. Assuming the Spacecraft is Launched at ETR..... 143

B. FOR 15 YEAR MISSION 144

 1. For Station Repositioning 144

 2. For East-West Station Keeping..... 144

 3. For North-South Station Keeping 145

 4. Assuming the Spacecraft is Launched at ETR..... 145

 5. Assuming the spacecraft is Launched at French Guiana..... 146

C. FOR 20 YEAR MISSION 147

 1. For Station Repositioning 147

 2. For East-West Station Keeping..... 147

 3. For North-South Station Keeping 147

 4. Assuming the Spacecraft is Launched at ETR..... 148

 5. Assuming the spacecraft is Launched at French Guiana..... 148

APPENDIX I. DETERMINATION OF INCLINATION DRIFT RATES..... 150

A. DRIFT RATE DUE TO SUN'S PERTURBATION..... 150

B. DRIFT RATE DUE TO MOON'S PERTURBATION 151

LIST OF REFERENCES..... 153

INITIAL DISTRIBUTION LIST 157

LIST OF TABLES

TABLE 1.	INCLINATION STATION KEEPING [REF. 3].....	8
TABLE 2.	LONGITUDINAL STATION KEEPING [REF. 3].....	8
TABLE 3.	ARIANE IV GEOSYNCHRONOUS TRANSFER ORBIT DELIVERY [REF. 4].....	9
TABLE 4.	THRUSTER'S PARAMETER	42
TABLE 5.	UK-10 IPS MASS BUDGET [REF. 15].....	44
TABLE 6.	HUGHES 13-CM ION THRUSTER MASS BREAKDOWN [REF. 20].....	45
TABLE 7.	RITA MASS BUDGET [REF. 15].....	45
TABLE 8.	SUMMARY OF CALCULATIONS OF APPENDIX A AND APPENDIX H COMPARING ION AND BIPROPELLANT PROPULSION SUBSYSTEM MASS FOR NSSK USING HUGHES ION THRUSTER.....	46
TABLE 9.	SUMMARY OF CALCULATIONS FROM APPENDIX A AND APPENDIX H FOR ION PROPULSION WITH BIPROPELLANT BACKUP DURING ECLIPSE USING HUGHES ION THRUSTER.....	47
TABLE 10.	THE INFLUENCE OF DUAL THRUSTER FAILURES ON THE SYSTEM CAPABILITY OF PERFORMING NSSK (+), EWSK (+) OR BOTH (+) [REF. 27]	56
TABLE 11.	INCLINATION DRIFT RATES.....	61
TABLE 12.	SUMMARY OF CALCULATIONS OF APPENDIX B AND APPENDIX H COMPARING ION AND BIPROPELLANT	

	PROPULSION SYSTEMS MASS FOR NSSK USING UK-10 THRUSTER.....	78
TABLE 13.	SUMMARY OF CALCULATIONS OF APPENDIX C AND APPENDIX H COMPARING ION AND BIPROPELLANT PROPULSION SYSTEMS MASS FOR NSSK USING MELCO THRUSTER.....	79
TABLE 14.	SPECIFIC IMPULSE (SECONDS) OF VARIOUS PROPULSION [REF. 3].....	103

LIST OF FIGURES

Figure 1.	Exploded View of UHF Follow-On Class Satellite	5
Figure 2.	UHF Follow-On Satellite in Flight Configuration	6
Figure 3.	Ariane IV Envelope Configuration [Ref. 4].....	10
Figure 4.	Ariane IV Payload Compartment Configuration.....	11
Figure 5.	Simple Ion Thruster Diagram [Ref. 11].....	15
Figure 6.	Ion Propulsion Schematic Diagram [Ref. 14]	16
Figure 7.	RIT Ion Propulsion Schematic Diagram [Ref. 15].....	18
Figure 8.	Resistojet Heater Configuration [Ref. 11].....	21
Figure 9.	Cutaway View of 30-kW Regeneratively Cooled Arcjet Thruster [Ref. 11]	22
Figure 10.	Pulsed Electrothermal Thruster (PET) [Ref. 7].....	23
Figure 11.	Laser-Heated Thruster [Ref. 7]	24
Figure 12.	Microwave-Heated Thruster [Ref. 7]	25
Figure 13.	Magnetoplasmadynamic (MPD) Thruster [Ref. 7].....	26
Figure 14.	Pulsed Plasma Thruster Using Teflon as Propellant [Ref. 8]	28
Figure 15.	Pulsed Inductive Thruster [Ref. 7]	29
Figure 16.	Specific Impulse (Isp) Ranges [Ref. 1]	30
Figure 17.	Isp and Efficiencies of Different Thrusters [Ref. 1]	31
Figure 18.	Hughes Ion Thruster [Ref. 21]	34
Figure 19.	Xenon Feed System [Ref. 21].....	35
Figure 20.	Xenon Thruster Power Processing Unit Schematic Diagram [Ref. 21].....	36
Figure 22.	Different Electrostatic Ion Thrusters [Ref. 9].....	41

Figure 23.	Hughes Thruster Beam Divergence Characteristics [Ref. 21]...	48
Figure 24.	Plume Impingement Geometry	49
Figure 25.	Thruster Configuration with Plume Shield and Sputtering Resistant Material.....	50
Figure 26.	Thrusters at Ends of Solar Panels [Ref. 14].....	51
Figure 27.	Possible Configuration for NSSK Ion Thrusters [Ref. 27]	53
Figure 28.	NSSK Thruster Location without EW Station Keeping Capability.....	54
Figure 29.	Eccentricity Buildup Due to Diagonal Thruster Firing [Ref. 27] .	57
Figure 30.	Ion Thruster Location with EW Station Keeping Capability [Ref. 22].....	58
Figure 31.	Ion Thrusters with Gimbals.....	59
Figure 32.	NSSK Strategy.....	65
Figure 33.	Eclipse Season in Geosynchronous Orbit [Ref. 32].....	67
Figure 34.	Projected Output of Solar Array.....	69
Figure 35.	Battery Cycle Capability [Ref. 14].....	71
Figure 36.	Power/Thrust Ratios for Ion Thrusters [Ref. 24]	77
Figure 37.	Ariane GTO Capability vs Spacecraft Lifetime.....	95
Figure 38.	ETR GTO Capability vs Spacecraft Lifetime	96
Figure 39.	Orbital Parameters for Parking Orbit and Transfer Orbit [Ref. 3]	132
Figure 40.	Velocity Vector Diagram.....	135

LIST OF ABBREVIATIONS AND ACRONYMS

AKM	Apogee Kick Motor
ATS	Applied Technology Satellite
AUSAT	Australian Satellite
BOL	Beginning of Life
BPS	Bipropellant Propulsion Subsystem
DOD	Depth of Discharge
ΔV	Change in Velocity
EBIT	Electron Bombardment Ion Thruster
EMI	Electromagnetic Interference
EOL	End of Life
EPEX	Electric Propulsion Experiment
ESD	Electrostatic Discharge
ETR	Eastern Test Range
ETS	Engineering Test Satellite
EURECA	European Retrievable Carrier
EWSK	East-West Station Keeping
FEIT	Field-Emission Ion Thruster
GTO	Geosynchronous Transfer Orbit
η	Efficiency
HAC	Hughes Aircraft Corporation
Hg	Mercury
HRL	Hughes Research Laboratories
INTELSAT	International Telecommunications Satellites Corporation

IPS	Ion Propulsion System
I_{sp}	Specific Impulse
kg	Kilogram
kW	Kilowatt
MELCO	Mitsubishi Electric Company
MHz	Megahertz
MLI	Multilayer Insulation
MPD	Magnetoplasmadynamic
N	Newton
NASA	National Aeronautics and Space Administration
NASCAP	NASA Charging Analyzer Program
Ni-H ₂	Nickel Hydrogen
NSSK	North-South Station Keeping
PIT	Pulsed Inductive Thruster
PMU	Power Management Unit
PPT	Pulsed Plasma Thruster
PPU	Power Processor Unit
RD&E	Research Development and Testing
RF	Radio Frequency
RIT	Radio frequency Ion Thruster
SERT	Space Electric Rocket Test
SFU	Space Flyer Unit
TT&C	Telemetry, Tracking and Control
UHF	Ultra High Frequency
Xe	Xenon
Xe ⁺	Ionized Xenon

XIPS

Xenon Ion Propulsion Subsystem

ACKNOWLEDGMENT

I would like to give my special thanks to my wife, Letty, and my two daughters, Royce and Kim, for their love and unending support during this intensive period.

I. INTRODUCTION

Ion propulsion is a technique of space propulsion which involves the conversion of electrical power into the kinetic power (thrust) of the exhaust beam [Ref. 1: p. 1]. To reach higher exhaust velocities, the source of energy must be decoupled from the propellant. This is where ion propulsion systems (IPS) provide an alternative to chemical propulsion systems. In ion propulsion, electric power is used to accelerate propellant to much higher velocities in the range of 30 to 40 km/s. Higher velocity means higher specific impulse (I_{sp}). The ion thruster selected in this study has an I_{sp} of 2718 seconds compared to 285 seconds for bipropellant. Since the I_{sp} of the ion thruster is almost an order of magnitude higher than the bipropellant thruster, the propellant required by the ion thruster will be approximately an order of magnitude lower than that required by bipropellant thruster. The dry mass of the IPS is higher than that of the bipropellant because of the additional parts required to operate it, such as separate xenon propellant tank, feed system, and power processor unit (PPU) that takes care of the high electric power demand.

As an example, on a spacecraft with 1200 kg dry mass and a 20 year mission, 94% (514 kg) of the total bipropellant at beginning of life (BOL) is allocated for north-south station keeping (NSSK) using bipropellant propulsion subsystem (BPS). If IPS is used instead of BPS for NSSK, 139 kg IPS mass (this includes the 54 kg xenon propellant) will be required, which will only be 23% of the BPS mass.

Therefore, IPS becomes more attractive and advantageous over BPS especially for heavier spacecraft with long mission years. The mass saving derived from this can be used for low launch cost or increased revenues in the

case of commercial satellites due to additional transponders and/or longer operational capability of the satellite.

A. OBJECTIVE

The purpose of this thesis is to evaluate: 1) the implementation feasibility of IPS on Ultra High Frequency (UHF) Follow-On class satellite, 2) the risks and benefits due to the addition of IPS, and 3) the impact of IPS to other spacecraft subsystems.

B. SCOPE OF STUDY

This thesis is organized to cover the aspects of IPS implementation on a geosynchronous spacecraft. Chapter II describes the satellite chosen for the study. Due to high dry mass requirement of the ion propulsion, not all geosynchronous satellites will benefit from its implementation. BOL mass and mission years are primarily the driving factors.

In Chapter III, types of electric propulsions are explored and their advantages and disadvantages compared. Emerging from the comparison, electrostatic (ion) type comes out on top primarily because of the mature technology as a result of long years of research, development and experiments (RD & E) associated with it. Chapter IV explains in detail the operation of the xenon ion propulsion subsystem (XIPS) selected for this study. This chapter also includes the trade-offs in using different sizes of thrusters and possible locations on the spacecraft.

To make this study complete, Chapter V describes the requirements of NSSK and east-west station keeping (EWSK) corrections to maintain proper station for a geosynchronous satellite. To make these corrections, thrusters are used to compensate for the drift.

Chapter VI explains the need for large electrical power to support the IPS. Trade-offs between the battery and solar array power as the source of IPS power is also presented in this chapter. In Chapter VII, bipropellant and ion thrusters are compared in terms of propellant mass consumption to determine the savings derived from using ion thrusters over the bipropellant thrusters.

Chapter VIII presents the implementation impacts of XIPS on other subsystems. Also, cost and benefits are analyzed in this chapter to provide some dollar figures on launch cost for a spacecraft using bipropellant and ion propulsion subsystem. Environmental impacts are considered in Chapter IX. These include: particulate contamination as a result of sputtering of the thruster grids, electromagnetic interference during XIPS operation, and electric discharge due to the charge-exchange plasma that is generated in the main beam downstream of the thruster.

II. SELECTION OF GEOSYNCHRONOUS SPACECRAFT

In order to evaluate the net reduction in satellite mass obtainable by using IPS instead of BPS to perform NSSK, it is necessary to first specify an equivalent satellite that uses BPS to perform all maneuvers [Ref 2: p. 308].

A. SATELLITE DESCRIPTION

The satellite selected for this study is a UHF Follow-On class communications satellite, as shown in Figure 1. The UHF Follow-On satellite is a U. S. Navy satellite being built by Hughes Aircraft Corporation (HAC) and is scheduled for launch in 1992. The bus (mainframe) used is similar to that of the Australian Satellite (AUSAT).

The dimensions are 2.58 m wide, 2.93 m high, and 18.45 m long (solar array deployed), as illustrated in Figure 2, and has a 1200 kg dry mass. The 1200 kg dry mass includes the bipropellant tanks' mass that can accommodate a baseline of 990 kg for the apogee kick motor (AKM). Therefore, additional dry mass must be considered when the total bipropellant mass exceeds 990 kg, as shown in Appendix A, Appendix B, Appendix C, and Appendix H. When calculating the additional dry mass, the allowances are 16% for BPS (10% for structural support and 6% for tankage) and 17% for IPS (11% for structures and 6% for tankage). The IPS has 1% more allowance for structures because of its complexity.

1. Station Keeping Considerations

Unlike commercial communications satellites in geosynchronous orbit, the present mission of the UHF Follow-On satellite does not require periodic

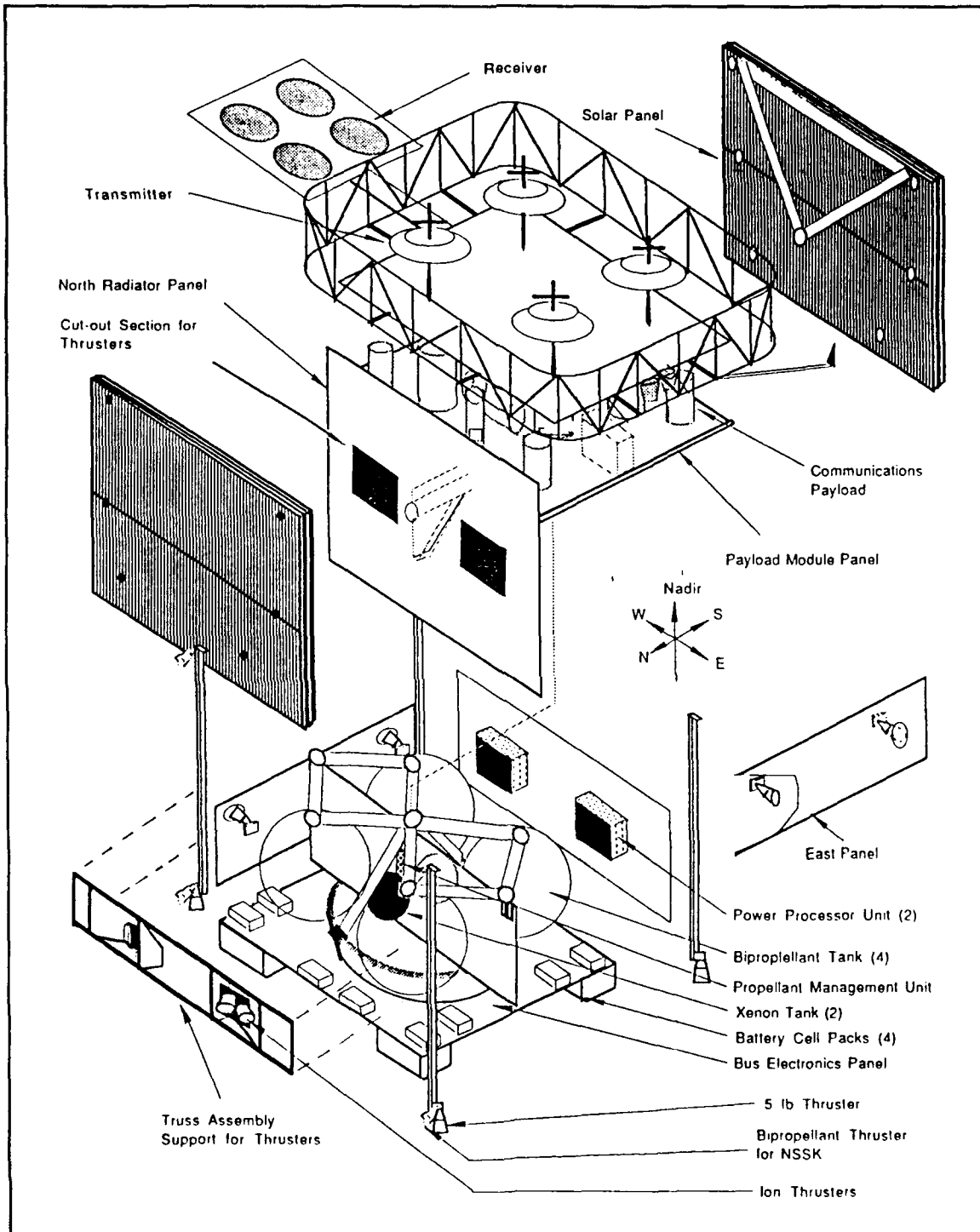


Figure 1. Exploded View of UHF Follow-On Class Satellite

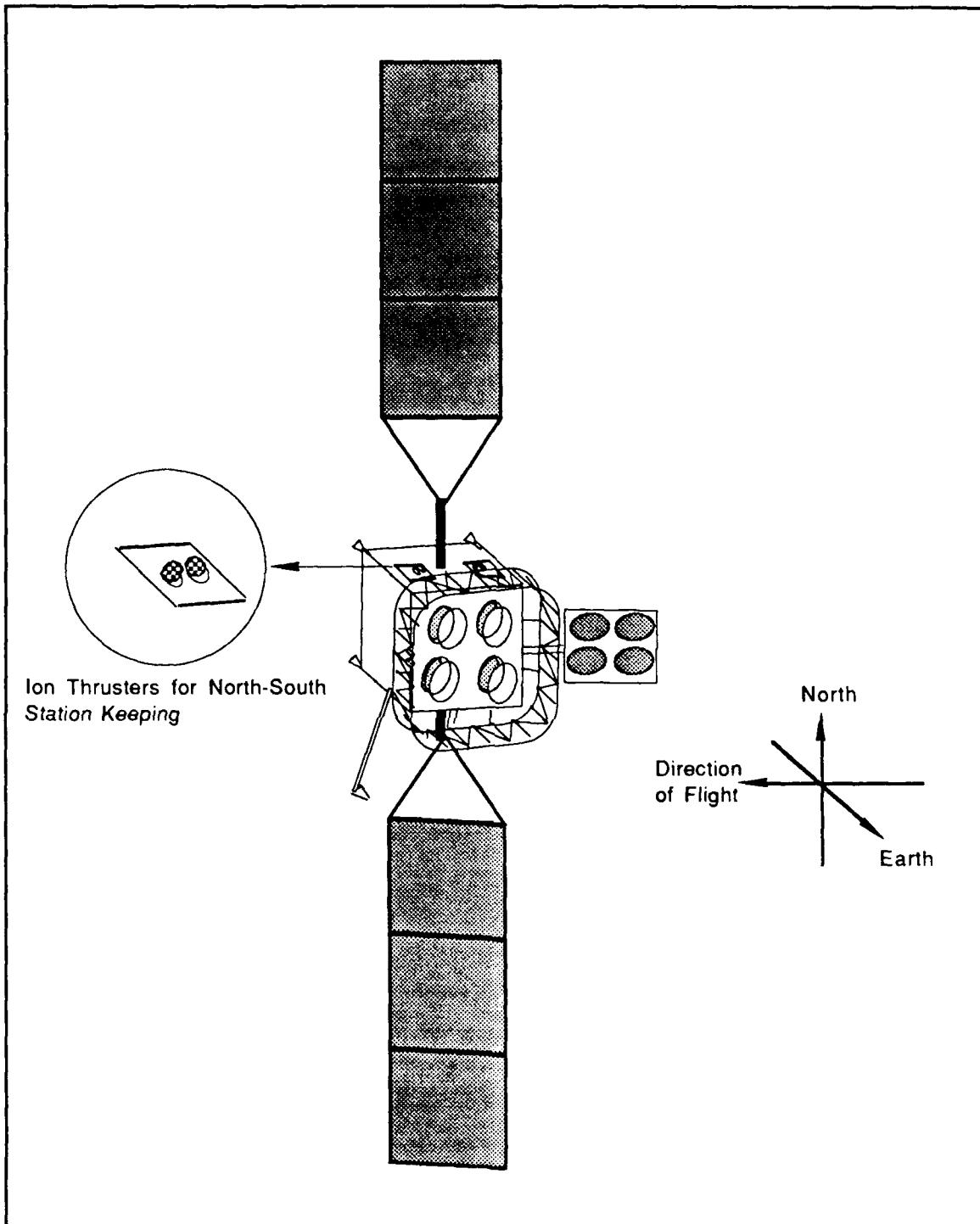


Figure 2. UHF Follow-On Satellite in Flight Configuration

NSSK maneuvers. Table 1 and Table 2 show the typical values of velocity change requirements (ΔV s) for given drift tolerances and the number of days before the satellite must perform the correction without incurring further drift. The actual drift rates depend mainly on the time (month and year) when the spacecraft is launched into orbit, as further discussed in Chapter V.

For fine pointing accuracy of the antennas, the allowable drifts are small. If this is to be considered for a UHF Follow-On class satellite, additional propellant for NSSK is required to provide corrections for the inclination drifts. For this study, it is assumed that the inclination tolerance is 0.1° of the equator and $\pm 0.1^\circ$ for longitudinal drift.

In order to evaluate the net reduction in satellite mass by using IPS, it is necessary to evaluate which of these maneuvers will require more bipropellant to offset the addition of IPS dry mass. The total ΔV s required for NSSK are 429.21, 676 and 912.1 m/s for 10, 15 and 20 year missions respectively, as shown in Appendix G. For EWSK the required ΔV is only 1.74 m/s per year, as shown in Appendix D. Appendix E shows that the ΔV required for a one time 180° longitudinal change of station is 33.96 m/s. If all these ΔV s are translated into bipropellant mass, as shown in Appendix A, NSSK maneuvers need more than three times an order of magnitude of bipropellant than the EWSK and a change of longitudinal station for a 20 year mission. As can be seen, replacing BPS with IPS is only beneficial for NSSK and not for EWSK or station repositioning. Another unfavorable factor using ion thrusters for station repositioning is the length of time to perform the maneuver. Since ion thrusters are only rated in millinewton (mN), it will take a substantial amount of time (320

TABLE 1. INCLINATION STATION KEEPING [REF. 3]

Inclination Limit (deg)	ΔV per Maneuver (m/s)	Average Time between Maneuver (days)
0.1	10.7	86.14
0.5	53.65	430.7
1.0	107.30	861.4
2.0	214.56	1,722.8
3.0	321.76	2,584.2

TABLE 2. LONGITUDINAL STATION KEEPING [REF. 3]

Longitude Tolerance	ΔV_{\max} / Maneuver (m/sec)	Minimum Time Interval Between Maneuvers (days)
± 0.1	0.15	31
± 0.2	0.21	43
± 0.5	0.30	69
± 1.0	0.46	97
± 2.0	0.66	138
± 3.0	0.80	169

thruster firing hours) to accomplish the maneuver using two 17.7 mN thrusters, as shown in Appendix E.

B. LAUNCH VEHICLE

The launch vehicle chosen for the spacecraft is the Ariane IV (French Guiana as launch site); however, an analysis is also included in Appendix F showing the Eastern Test Range (ETR) in Florida as launch site. The Ariane IV fairing has a payload envelope as shown in Figure 3 and Figure 4. Table 3 shows the geosynchronous transfer orbit (GTO) capabilities of different Ariane IV configurations.

As shown in Appendix H, launching the satellite from Guiana Space Center (French Guiana), will result in lower spacecraft launch mass due to a smaller transfer orbit inclination of 8° instead of 24.5° for ETR launch.

TABLE 3. ARIANE IV GEOSYNCHRONOUS TRANSFER ORBIT DELIVERY [REF. 4]

Configuration	Kilogram
AR40	1900
AR42P	2600
AR44P	3000
AR42L	3200
AR44LP	3700
AR44L	4200

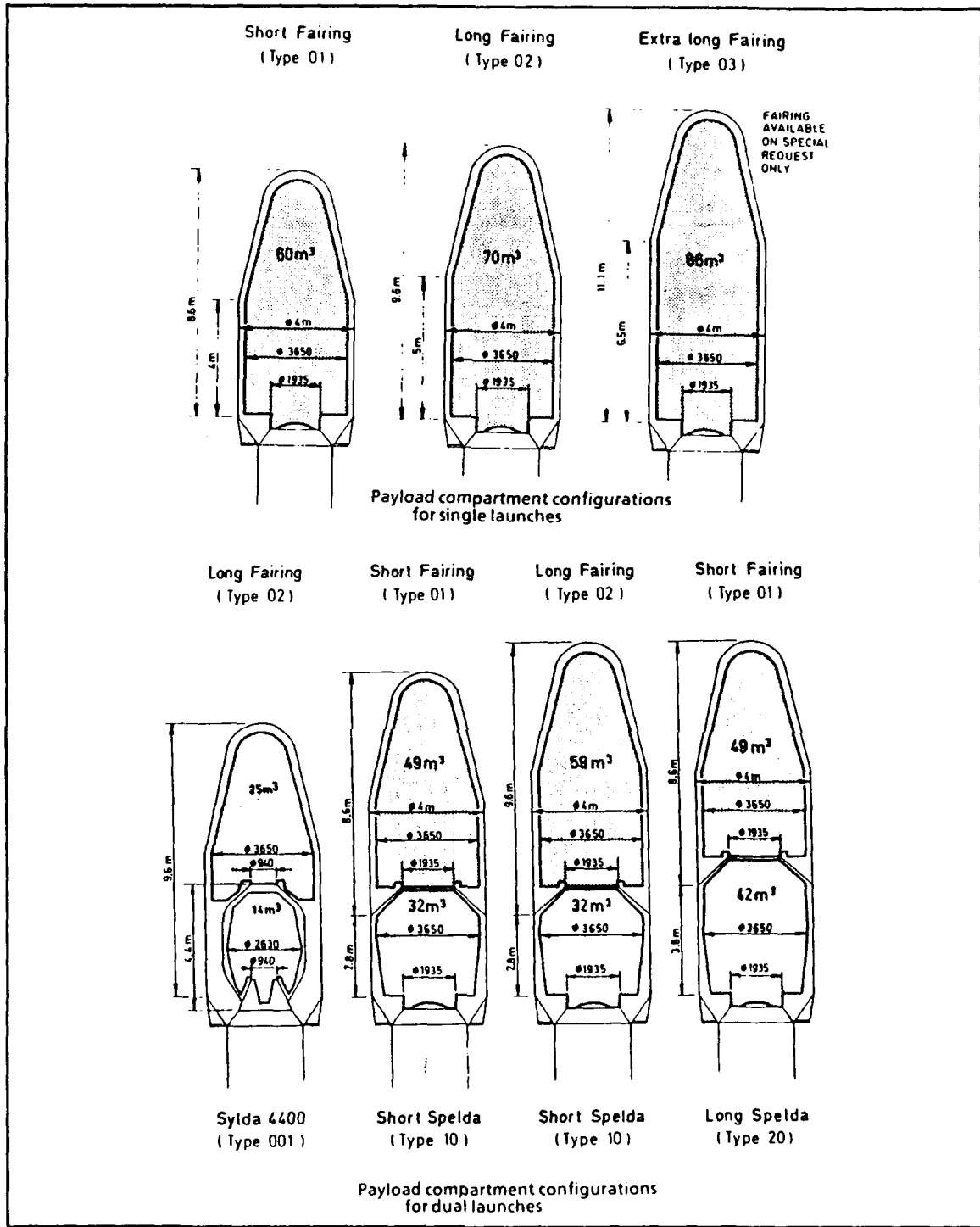


Figure 3. Ariane 4 Envelope Configuration [Ref. 4]

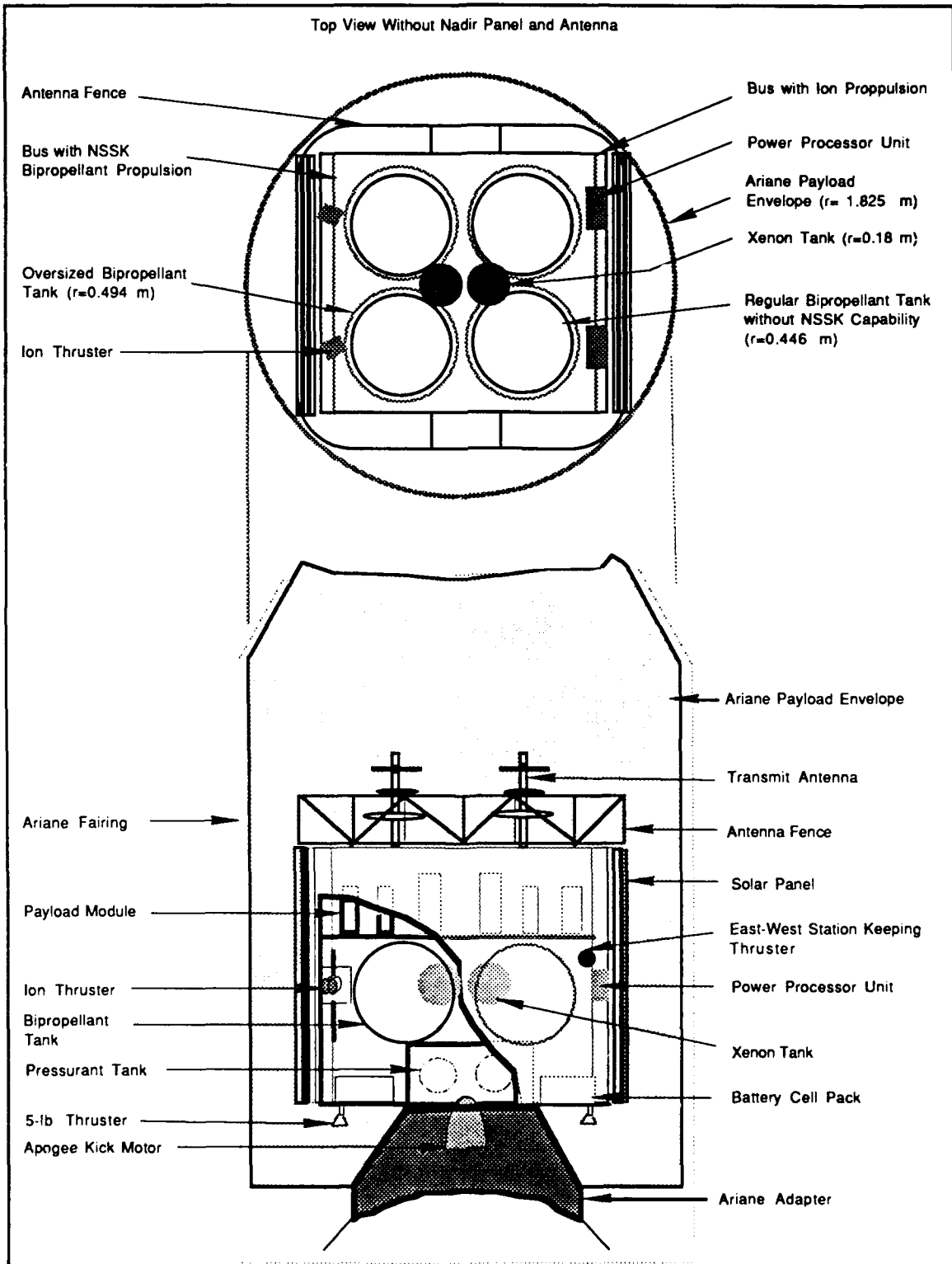


Figure 4. Ariane IV Payload Compartment Configuration

III. TYPES OF ELECTRIC PROPULSION THRUSTERS

There are three basic types electric propulsion: electrostatic (ion thruster), electrothermal (resistojet, arcjet, laser, microwave and pulsed electrothermal), and electromagnetic (magnetoplasmadynamic (MPD), pulsed plasma, and pulsed inductive).

Electrostatic thrusters use electric body forces established between an ion source and a negative electrode to accelerate a collisionless beam of positive atomic ions which subsequently joins a stream of electrons producing a beam of zero net charge, which in turn can provide high I_{sp} . The term I_{sp} is defined [Ref. 5: p. xviii] as

$$I_{sp} = \frac{v}{g_0} \quad (3-1)$$

where

I_{sp} = specific impulse, sec

v = exhaust velocity, m sec⁻¹

g_0 = 9.806 m sec⁻²

Aside from the United States, several countries are involved in the development of ion thrusters, such as Japan, West Germany, France, the USSR and the United Kingdom (UK). The Japanese Mitsubishi Electric Company (MELCO) xenon ion thruster will be used for NSSK when the Engineering Test Satellite (ETS-VI) is launched in 1992. West Germany's European Retrievable Carrier (EURECA) free flyer spacecraft, equipped with a radio frequency xenon ion thruster (RIT-10), is scheduled to be launched by the Shuttle in 1992. Both the RIT-10 and the UK's UK-10 xenon ion thrusters are planned for launch on

the European Space Agency's SAT-2 technology satellite in 1993. Ford Aerospace, on the other hand, initiated a study under contract to International Telecommunications Satellites Corporation (INTELSAT) to analyze in detail the feasibility of incorporating xenon ion thrusters on INTELSAT-VII for NSSK. [Ref. 6: p. 78]

Electrothermal propulsion enhances the I_{sp} by injecting thermal energy into a gaseous exhaust. It includes electromagnetic energy beamed from a remotely located source using an electric resistance heater or heat exchanger and thus is termed electrothermal [Ref. 7: p. 374]. A 1989 decision by GE-Astro Space Division to utilize arcjet thrusters for station keeping on the AT&T Telstar 4 commercial communications satellite marked a major milestone for electrothermal propulsion. The 1.8 kW arcjet, under development and qualification at Rocket Research Company, with funding from NASA-Lewis and GE Astro Space, provides an I_{sp} of over 500 seconds with monopropellant hydrazine [Ref. 6: p. 78].

Electromagnetic propulsion utilizes a magnetic field acting on an electric current to accelerate an ionized gas by means of the Lorentz body force, the vector cross product of the magnetic and the discharge current [Ref. 7: p. 374]. Electromagnetic thrusters can operate in either steady or pulsed modes. In Japan, electromagnetic propulsion development has progressed to the flight test of a pair of micronewton (μN) Pulsed Plasma Thruster (PPT) on Engineering Test Satellite (ETS-IV) in 1981 [Ref. 8: p. 15], the magnetoplasmadynamic (MPD) system on Spacelab-1 [Ref. 9: p. 5], and a 1 kW class quasi-steady MPD thruster is planned for the Electric Propulsion Experiment (EPEX) onboard Space Flyer Unit (SFU) in the early 1990's [Ref. 10: p. 315].

A. ION THRUSTER

The basic thermal limitations on attainable exhaust speeds and thrusts associated with the heating and subsequent expansion of a propellant gas through a nozzle can be circumvented if the gas is directly accelerated by electric body forces. The simplest concept for the application of electric body forces to a propellant stream is the ion thruster, wherein a collisionless beam of positive atomic ions is accelerated by a suitable electrostatic field. As shown in Figure 5, a stream of ions, released from the ionizing surface, is accelerated by an electric field established between the source and a negative grid electrode. Subsequently, a stream of electrons from the neutralizer joins the ion stream, producing a beam of zero net charge, which leaves the accelerator with a velocity determined by the total potential drop between the source and the exit electrode and by the charge-to-mass ratio of the ions employed. The thrust attainable in this manner depends on the exhaust speed, mass of the ion, and total ion flux that can be accommodated by the source-accelerator-neutralizer system. Thermal limitations of the ionizing source must not be neglected, but these pose far less severe constraints on attainable exhaust speed and efficiency than do those inherent in electrothermal accelerators. [Ref. 11: p. 143]

In electrostatic ion propulsion, propellant is accelerated by electric forces to high velocities to produce thrust [Ref. 12: p. 240]. The propellant must have the electrons removed from its atoms, leaving positive ions. By far the most flexible means of ionization is for electrons to hit or bombard the propellant atoms and knock off electrons, as shown in Figure 6. Ions are extracted from the plasma chamber by the acceleration (accel) grid. Because the grids (screen, accel and decel) are made of molybdenum (high sputtering resistance material), there is

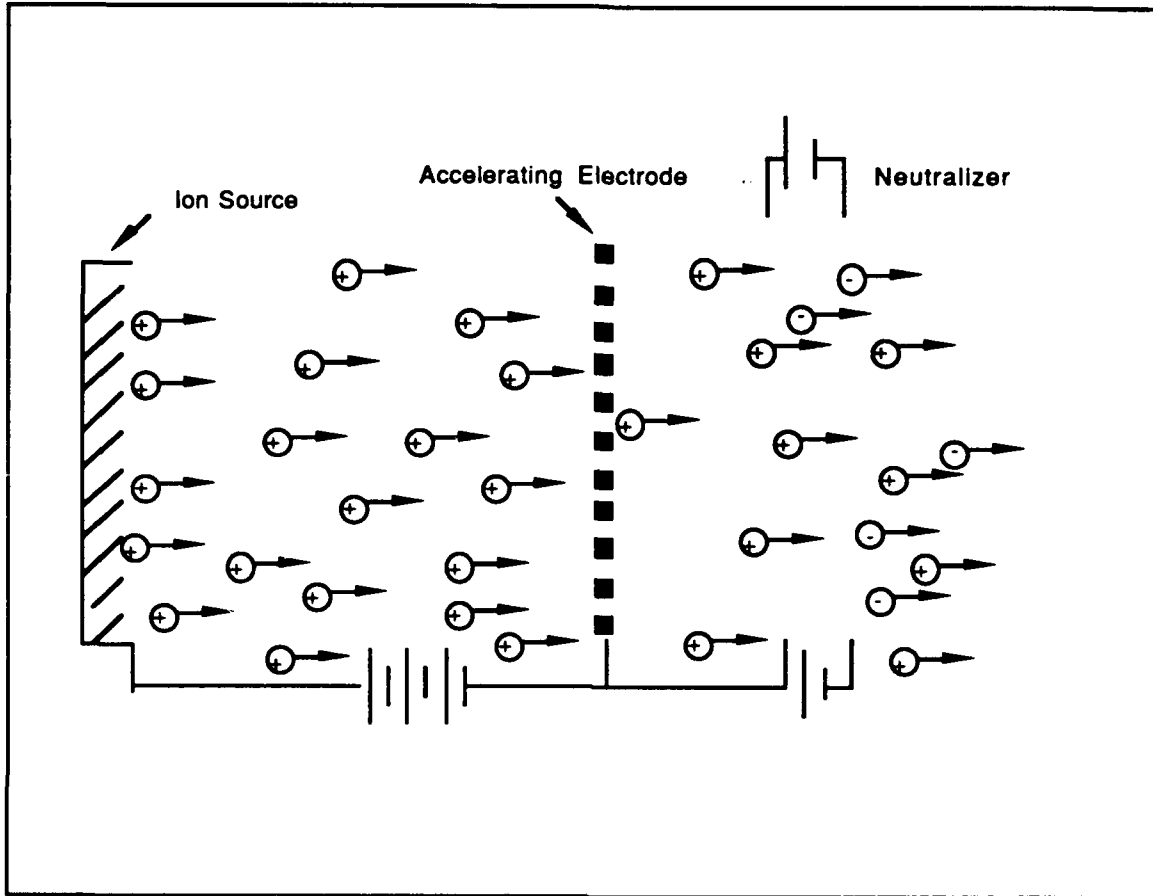


Figure 5. Simple Ion Thruster Diagram [Ref. 11]

minimal sputtering problem at expected temperatures. Reference values of creep indicate negligible dimensional changes on the grids even at temperatures of 1900°K over several thousands of hours of operation. [Ref. 13: pp. 648-654]

The input power to the thruster consists of three major elements: the beam (ion acceleration), power discharge (propellant ionization) power, and a small additional (other) power used to control the thruster which is relatively insensitive to thruster size [Ref. 13: p. 650].

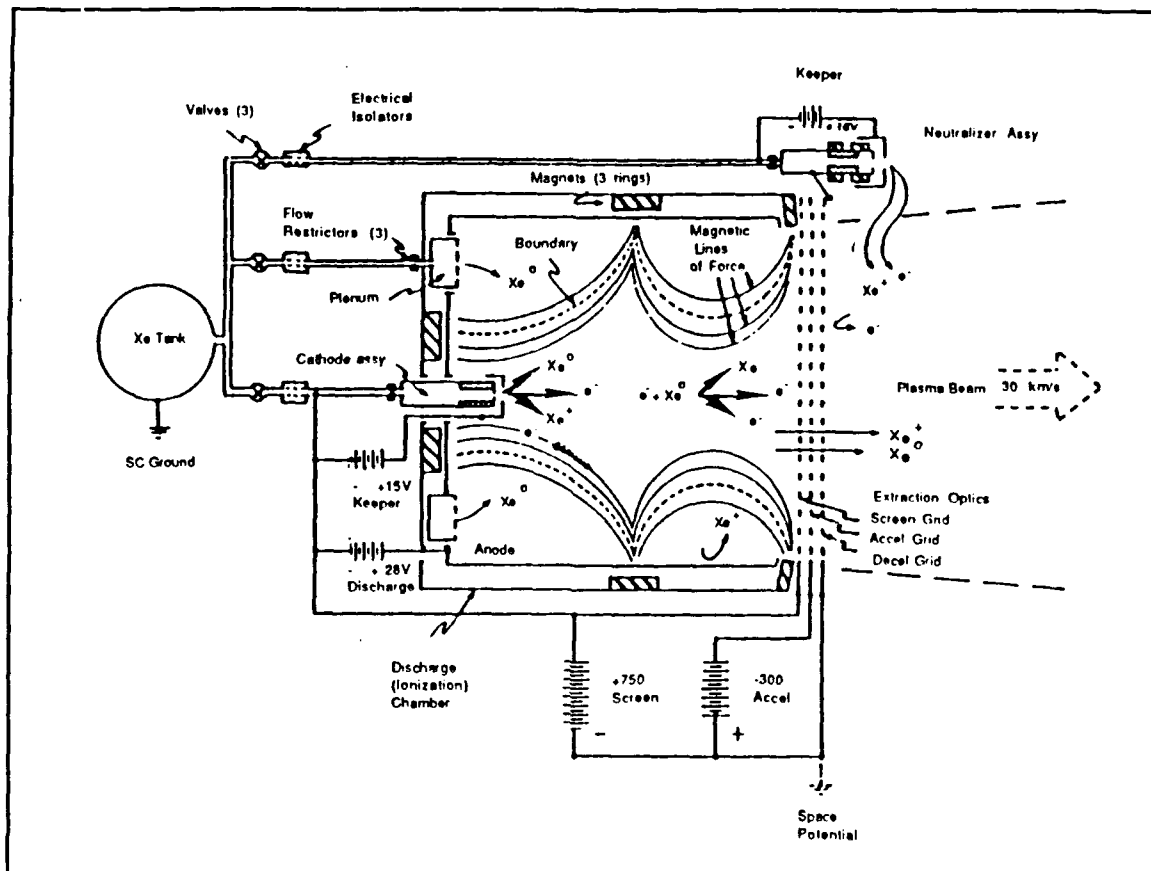


Figure 6. Ion Propulsion Schematic Diagram [Ref. 14]

1. Field-Emission Ion Thruster (FEIT)

The concept states that by subjecting a liquid metal to a sufficiently strong electric field at the atomic level (of the order of 0.5 V/\AA), electrons can be repelled into the bulk of the liquid and ions are left at its surface. These ions are then accelerated by the same electric field that created them, and this constitutes the basic process of ion field-emission. [Ref. 8: p. 37]

With contamination and environmental effects of electric thrusters becoming increasingly more important, the use of inert gases is a big advantage for any thruster. To date, only the Kaufman and radio frequency (RF) thrusters

can use inert gases while FEIT cannot. Cesium, used as FEIT propellant, is sufficiently reactive to discourage most users in using it. Similarly, benign plume properties and environmental concerns appear to be the reason why inert gas ion thrusters are being developed today. However, the FEIT has an advantage the other two do not have, namely, mechanical and electrical simplicity. This simplicity should make for very low system fabrication costs, which should favor field-emission's applications not only for primary propulsion, but also for NSSK and attitude control. [Ref. 8: pp. 37-41]

2. RF Ionization Thruster

RF thruster couples a radio frequency (low megahertz (MHz)) electromagnetic field to a gaseous or vaporized propellant to affect ionization and create a plasma within the thruster [Ref. 14: p. 3]. Developed in West Germany, the RF thruster differs from the Kaufman thruster in two basic functions: 1) an electrodeless, annular, self-sustaining RF discharge is used to generate the low pressure plasma, and 2) special ion-optics consisting of the extracting anode and of a three grid system provides for improved focusing.

The propellant is fed into a quartz discharge chamber where it is ionized with an RF discharge, typically around 1 MHz [Ref 14: p. 3]. The ionization vessel is located inside the induction coil of the 1 MHz RF generator, as illustrated in Figure 7, which supplies the plasma with the discharge energy (i.e., accelerates the ionizing electrons by means of the induced electrical eddy field). A low pressure plasma is generated by collision between accelerated electrons and neutral atoms. The ions are then accelerated by a strong electrostatic field which is imposed between the grids and the discharge chamber plasma, and thus form a well-collimated ion beam that produces thrust. The positive space is then

neutralized by electrons emitted by the external hollow cathode fed with the same propellant as employed by the thrusters. [Ref 8: p. 37]

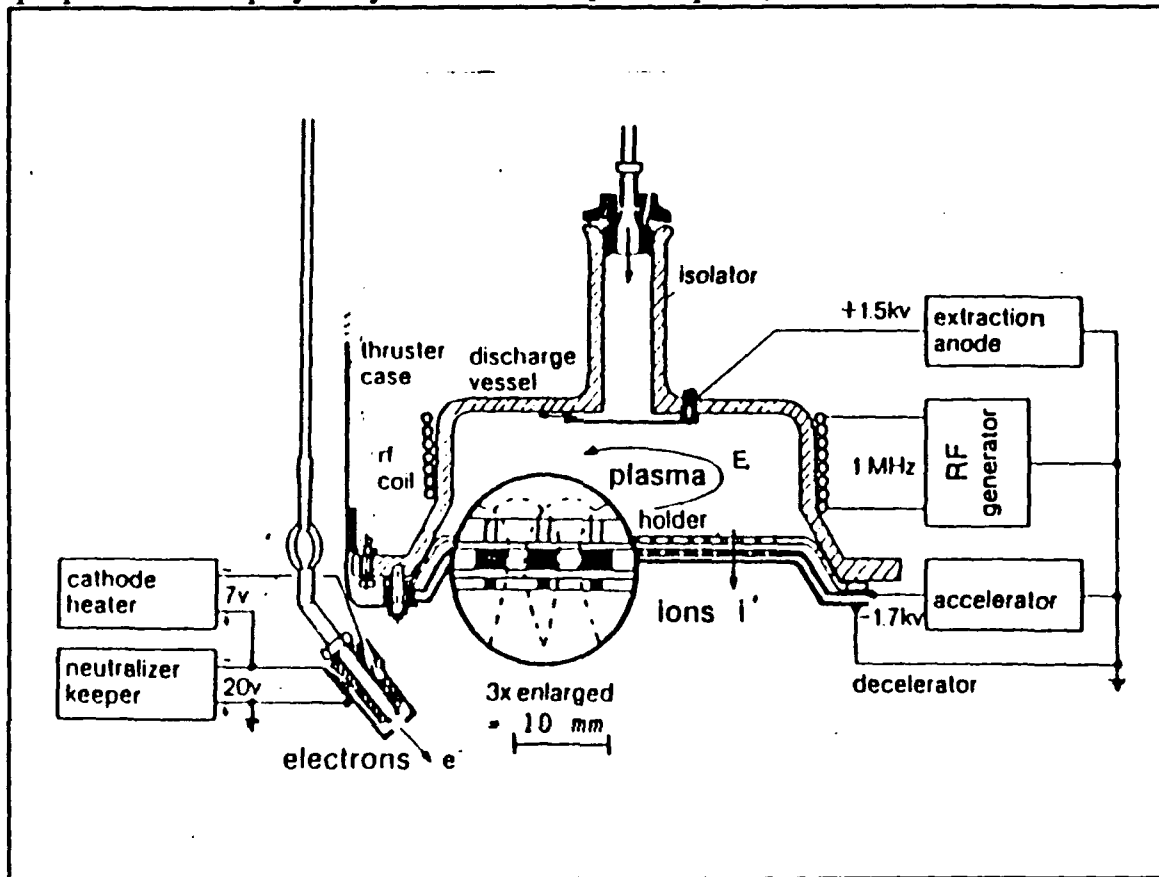


Figure 7. RIT Ion Propulsion Schematic Diagram [Ref. 15]

An example of RF thruster is the RIT-10 which is now ready and qualified for an experiment onboard the EURECA. EURECA will be flown on a Space Shuttle mission in 1992. An application of the commercialized system is also planned on the European Technology Satellite SAT-2 for a 1993 launch. For the SAT-2, UK-10 (electron bombardment type) will also be flown and this will give the unique opportunity to integrate and compare both technologies under the same conditions. [Ref. 15: p. 1]

3. Electron Bombardment Ion Thruster (EBIT)

In an EBIT (Kaufman type), as shown in Figure 6, electrons are emitted from a cathode [Ref. 14: p. 4] and accelerated to cylindrical anode, colliding on the way with propellant which is fed into the discharge chamber, where these processes are occurring. At the front of the chamber is the ion extraction system, consisting of grids with many small holes. If the ions accelerated into space, then the satellite would quickly build up a large negative charge. Therefore, a neutralizer is provided to eject electrons to balance the charge on the spacecraft.

To improve the efficiency of the plasma source and protect the anode from damage from energetic ions, a weak magnetic field is imposed upon the discharge. This causes the electrons to follow a very much longer path between electrodes, increasing the probabilities of collision with a propellant atom, producing ionization. Baffles are also included to protect the cathode and to control gas flow and the electron energy in the main chamber. A complete propulsion system has a propellant monitoring and control system, and an electrical power supply and control system.

Most early works used mercury (Hg) as a propellant, which from a propulsion point of view was excellent because it is easily stored with a very low tankage fraction and yields high thruster efficiency; however, environmental considerations prevent its use [Ref. 16: p. 18]. Xenon (Xe), a noble gas with 131 atomic mass units (amu), replaces Hg as the primary propellant for ion thrusters in the 80's. Such a change has many advantages even to the propulsion system, removing the need to vaporizers and avoiding problems with zero gravity management of a dense liquid and the possibility of solidification in eclipse. In

addition, non-corrosive and long lifetime storage present no problems, and gas control system is very mature, reliable technology. [Ref. 17: p. 16]

B. ELECTROTHERMAL

In electrothermal thrusters, a propellant gas is electrically heated and then expanded through an appropriate nozzle to convert its thermal energy into a thrust beam of directed energy [Ref. 7: p. 5]. The five electrothermal propulsion systems are resistojet, pulsed electrothermal, microwave and laser propulsion systems.

1. Resistojet

Resistojet is the simplest of the electrothermal propulsion systems. The propellant gas is heated by passing it over an electrically heated surface. As shown in Figure 8, the heat transfer to the propellant gas is primarily by conduction; convection and radiation have secondary effects. The limiting factors are increased stress, both mechanical and thermal, on the chamber wall and increased nozzle throat erosion. Resistojet thrusters have been developed for auxiliary propulsion applications. The specific mass for resistojet is 19 kg/kW and can have an I_{sp} as high as 385 seconds for hydrogen. [Ref. 7: p. 375]

2. Arcjet

The arcjet thruster uses an electric arc to heat a propellant, which then expands to generate thrust. The arc transfers its energy to the gas by means of radiation, convection, and conduction, and establishes the desired temperature profile across the gas stream where an intensely hot central core is surrounded by a relatively cold gas stream, as shown in Figure 9. The test of 30 kW-class arcjets provided an I_{sp} of 950 seconds with an overall specific mass of 1.8 kg/kW. The life limiting factors are erosion of the cathode tip, constrictor wall, and the propellant injection nozzle. [Ref. 7: p. 375]

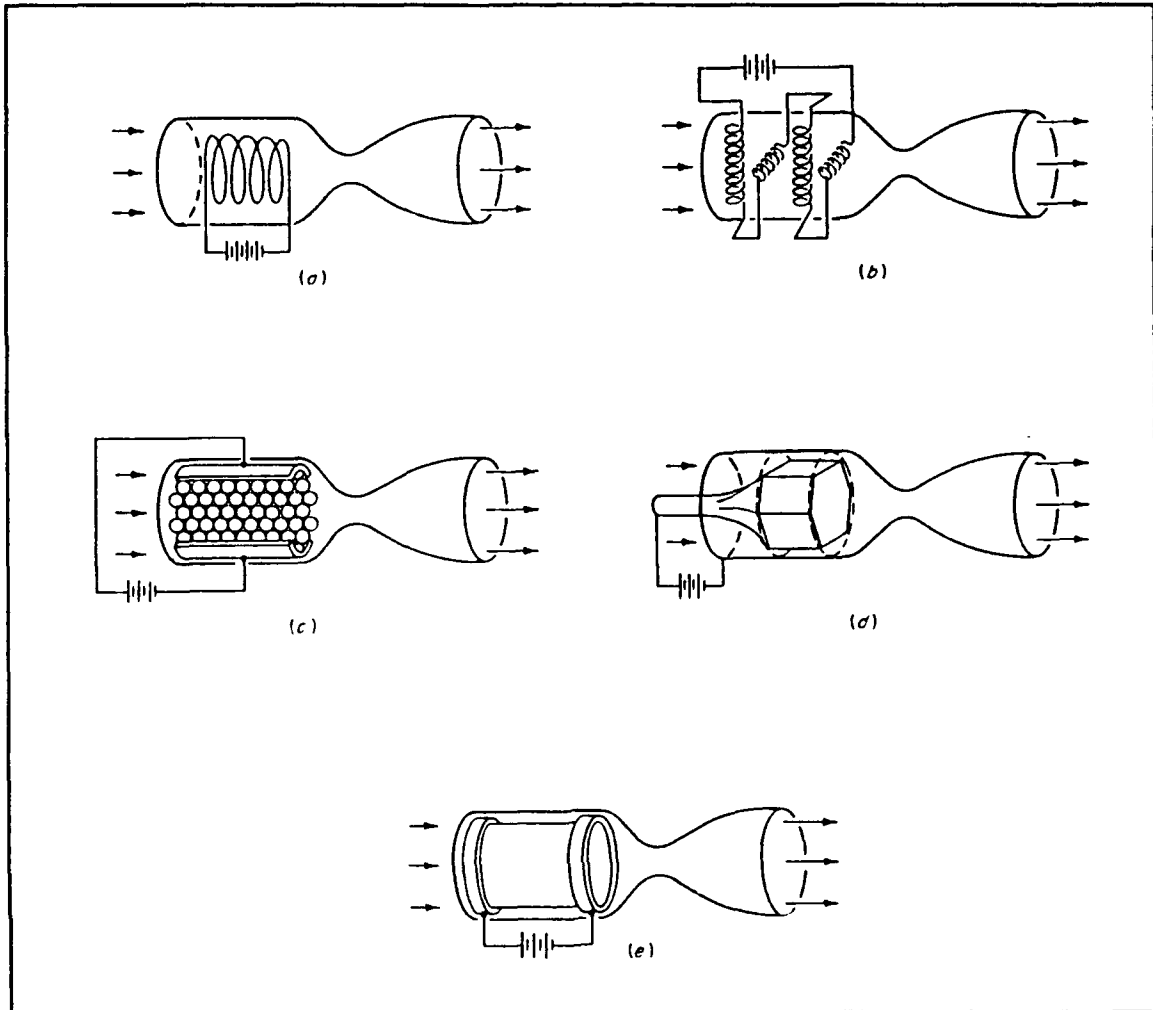


Figure 8. Resistojet Heater Configuration [Ref. 11]

3. Pulsed Electrothermal Thruster

The pulsed electrothermal thruster, as shown in Figure 10, uses a high pressure (approximately 100 atmospheres) and temperature (approximately 10,000° K) plasma generated in a capillary-confined electric discharge. A liquid propellant (water) is injected into the capillary chamber through a small orifice

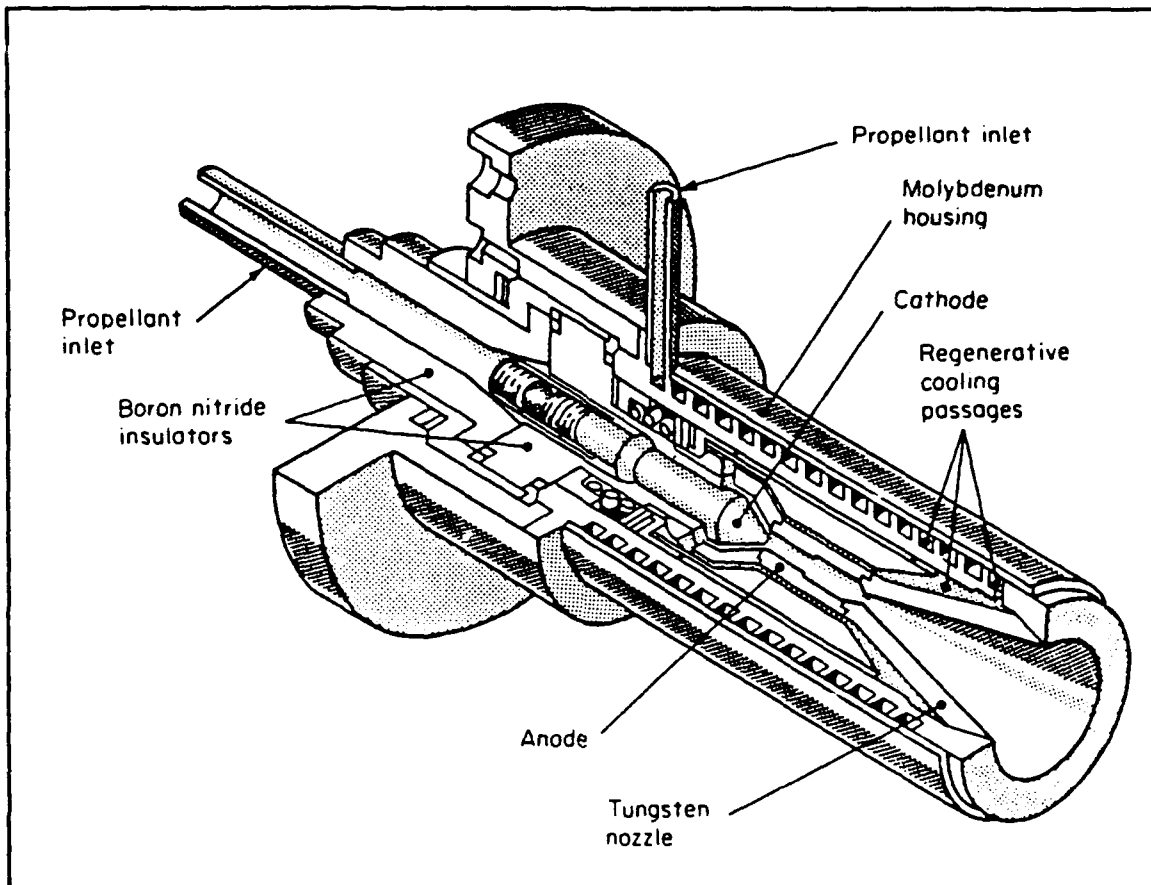


Figure 9. Cutaway View of 30-kW Regeneratively Cooled Arcjet Thruster [Ref. 11]

at the cathode. Using water as the propellant has shown that the pulsed electrothermal thruster can achieve an I_{sp} of 1700 seconds with a specific mass of 14 kg/kW. [Ref. 7: p. 375]

4. Laser

Laser propulsion consists of using energy from a remotely located laser to heat a low molecular gas to an extremely high temperature followed by a gas

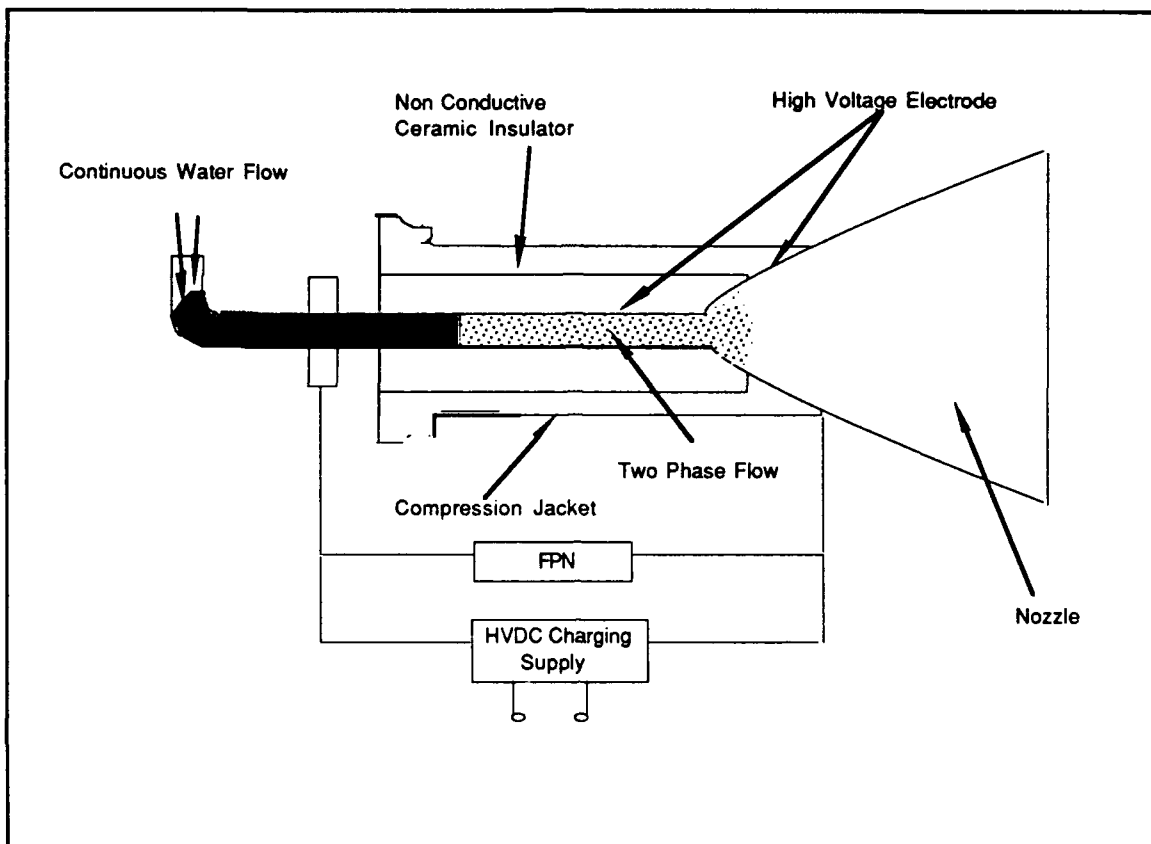


Figure 10. Pulsed Electrothermal Thruster (PET) [Ref. 7]

dynamic expansion through a nozzle to provide a thrust, as shown in Figure 11. The laser source can be either on the ground or in space. If the working gas is argon, an I_{sp} of 1000 seconds can easily be obtained with a specific mass of 0.0265 kg/kW, assuming the source of the laser is not from the spacecraft itself. [Ref. 7: p. 376]

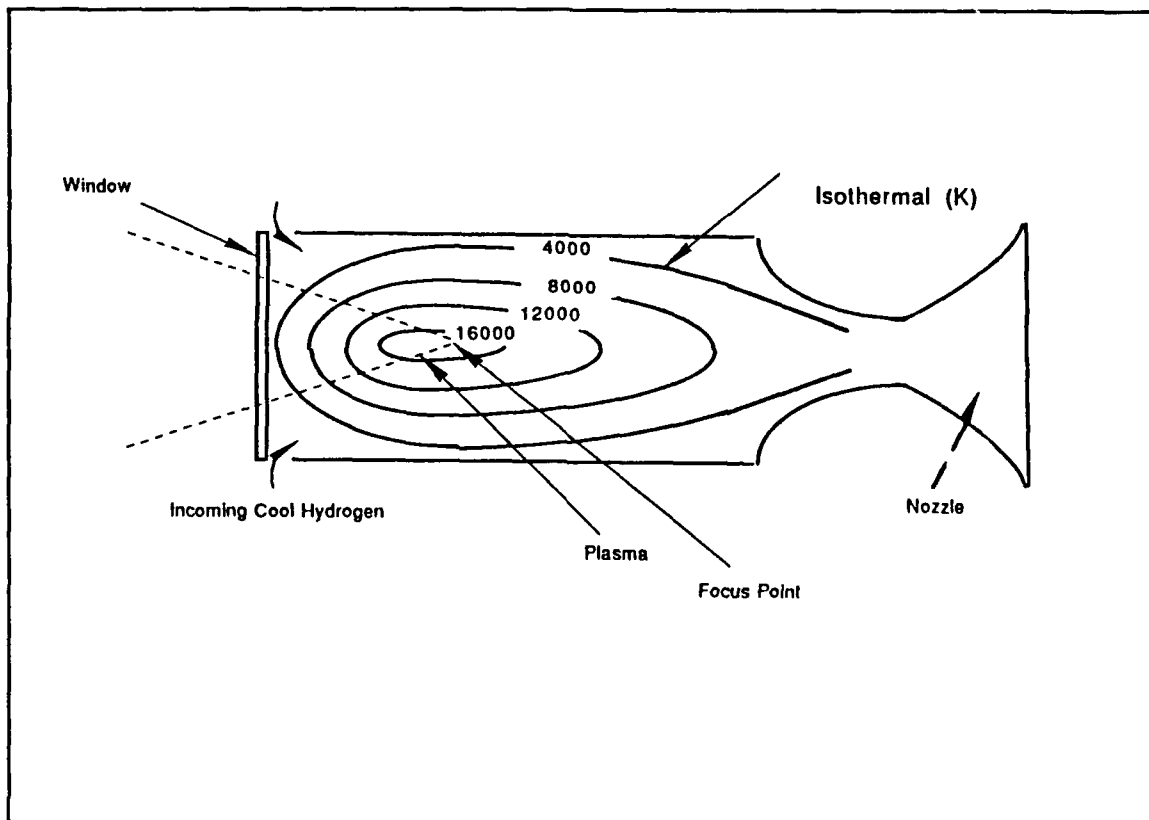


Figure 11. Laser-Heated Thruster [Ref. 7]

5. Microwave

Microwave propulsion is an alternative continuous beam propulsion system. The microwave energy, as shown in Figure 12, is absorbed by a gas in a resonant cavity, coaxial microwave plasmatron, or a plasma flame front region in a microwave waveguide, similar to a combustion wave. The microwave energy can be transmitted into the cavity through a dielectric window which, along with the cavity, can form the gas containing rocket chamber. An I_{sp} of 307 seconds was measured for nitrogen gas and specific mass of 0.0265 kg/kW, if the microwave energy source is other than the spacecraft itself. [Ref. 7: p. 376]

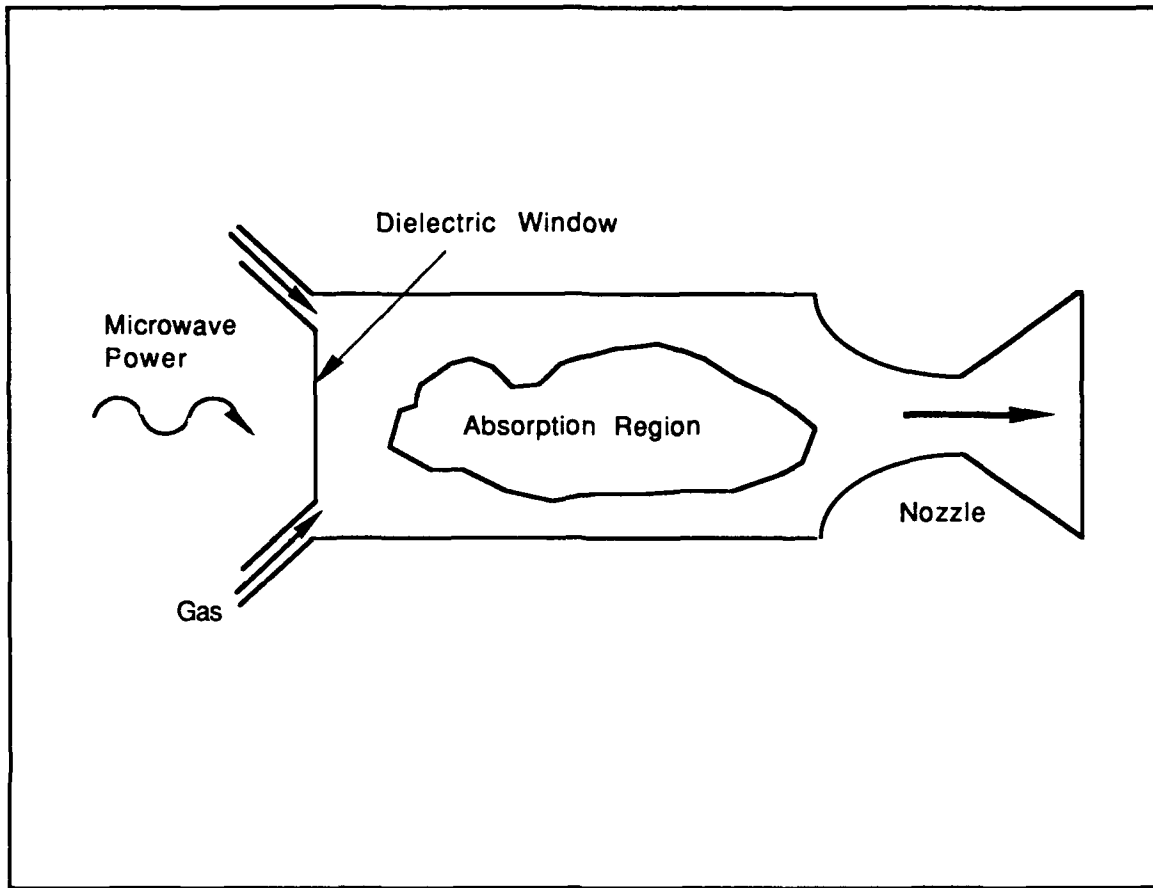


Figure 12. Microwave-Heated Thruster [Ref. 7]

C. ELECTROMAGNETIC

Electromagnetic propulsion system operating condition and performance characteristics are quite different from electrothermal propulsion because they operate at a much lower pressure (on the order of 10 torr or below) and high power (on the order of megawatt) with an I_{sp} of up to 4000 seconds at 20 to 40% efficiency.

1. MPD Thruster

The MPD thruster, as shown in Figure 13, utilizes a single discharge between concentric electrodes, with interaction of the discharge current and a magnetic field providing the thrust. More efficient operation is obtained at high power and thrust densities so that, for most applications, pulsed operation is required to reduce the average power to achieve the value. At high power, the magnetic field involved in thrust generation is usually provided by the discharge current, rather than a separate field coil or permanent magnets. Pulsed operation requires energy storage between the power source and the thruster, as well as some mechanism for generating and controlling pulse or propellant flow.

[Ref. 16: p. 181]

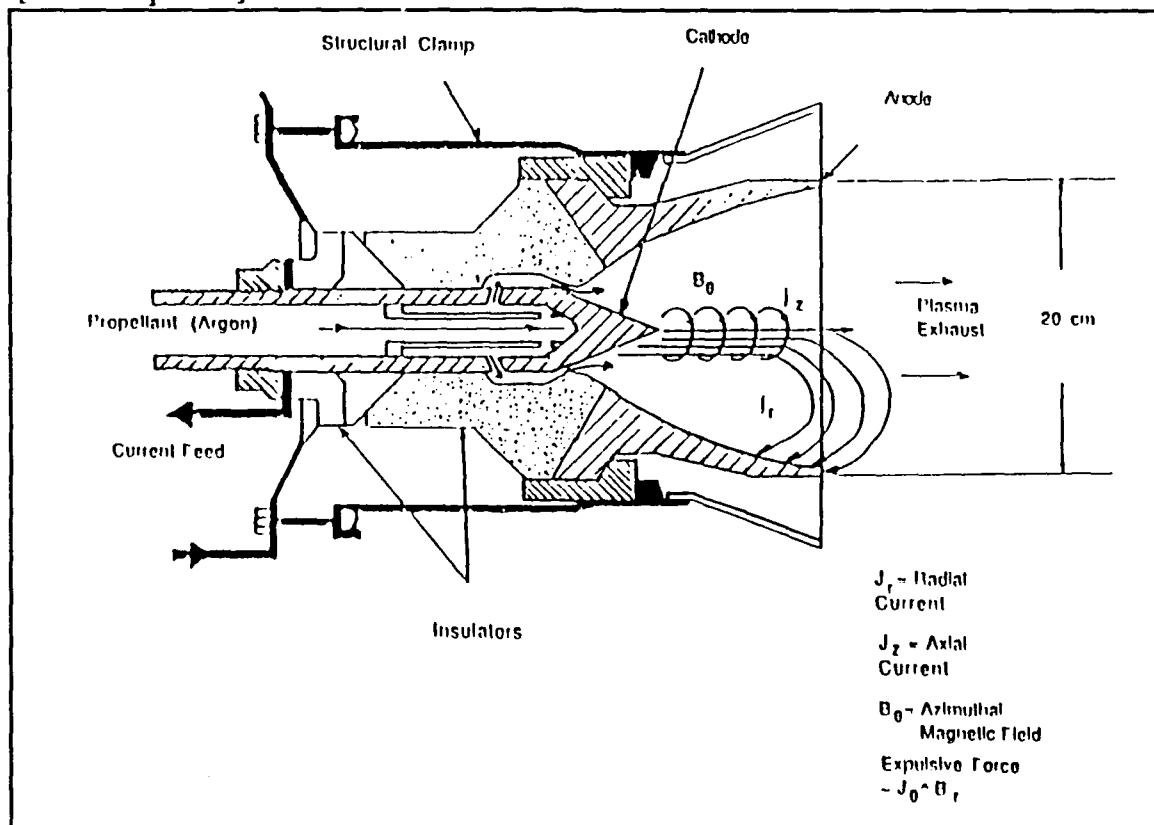


Figure 13. Magnetoplasmadynamic (MPD) Thruster [Ref. 7]

For acceptable performance characteristics, the discharge current should exceed several thousand amperes. This current level requires operating power levels in excess of 500 kW, therefore MPD thrusters are considered high power devices. With argon as a propellant, an I_{sp} of 1800 seconds was measured with a specific mass of 0.15 kg/kW. [Ref. 7: p. 377]

2. Pulsed Plasma Thruster (PPT)

PPT uses a burst electrical energy to produce, accelerate and eject a plasma wave or slug, as shown in Figure 14. It differs from most propulsive devices in that it inherently produces discrete impulse bits. The thruster consists of a set of rail-shaped electrodes connected to an energy storage system through closely paired strip-lines or parallel flanges. A high current, high power pulse is provided by a capacitor once the gap between electrodes starts conducting by the discharge of a small ignitor plug mounted in the cathode. Once ignited, the current flows along the solid propellant (usually Teflon but other thermoplastics such as Celcon, Halar, Halon and Tefzel can be used) [Ref. 8: p. 17] surface and vaporizes a thin sheet of solid fuel which is subsequently accelerated downstream by the self-generated electromagnetic field. [Ref. 7: p. 377]

3. Pulsed Inductive Thruster (PIT)

PIT consists of a flat spiral coil that is periodically pulsed from a capacitor, as shown in Figure 15. Prior to each pulse, a layer of propellant gas is transiently injected over the coil surface; the rapid rise of the radial magnetic field in the propellant induces electrical breakdown in the azimuthal direction and drives a large circulating plasma current that repels the gas from the coil at a useful I_{sp} . [Ref. 7: p. 377]

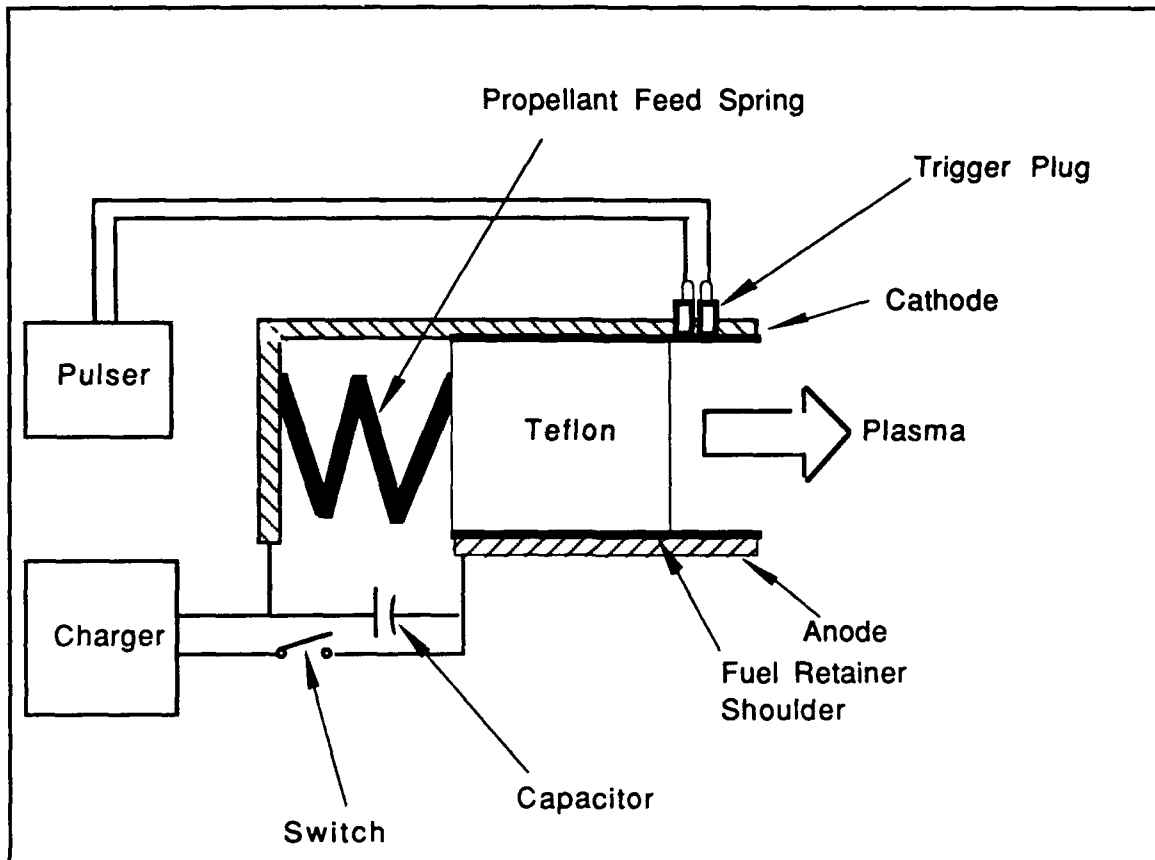


Figure 14. Pulsed Plasma Thruster Using Teflon as Propellant [Ref. 8]

E. PERFORMANCE COMPARISON OF ELECTRIC PROPULSION

Since the voltage-current characteristics of the satellites and that required of the electric propulsion are different, PUs are used to convert the electrical power generated by the power supply to the voltage-current characteristics required by the specific thruster. For example, ion thrusters require high voltages (1000 volts) at low currents (1 Amp) while electrothermal thrusters require lower voltages (100 volts) at higher currents (20 Amps). Magnetoplasmadynamic thrusters require current on the order of kiloamps to operate in the steady state mode and pulsed devices such as the pulsed

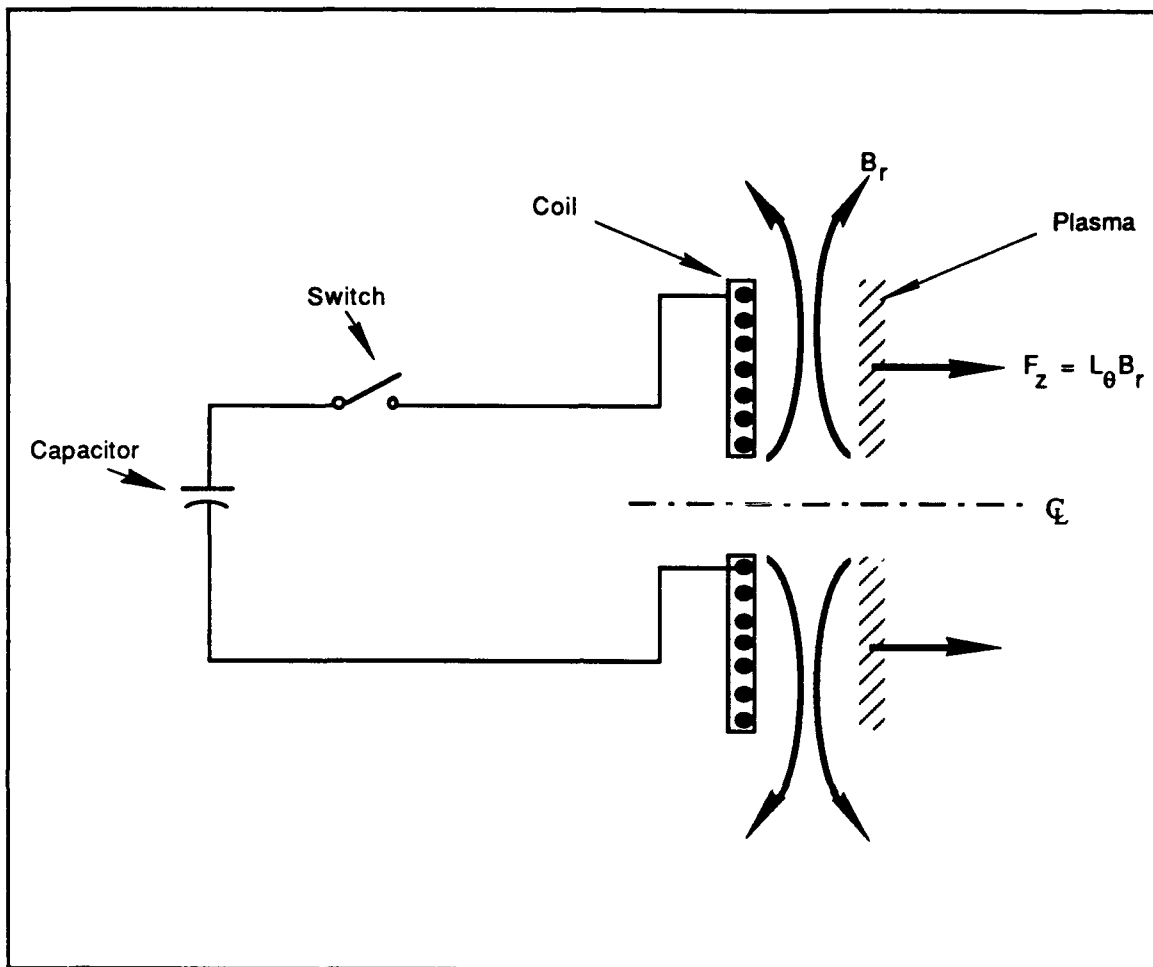


Figure 15. Pulsed Inductive Thruster [Ref. 7]

electrothermal and pulsed inductive thrusters require a means to rapidly switch a large amount of stored electrical power. [Ref. 7: p. 373]

Figure 16 shows a sample of general ranges of I_{sp} and the thrust range attainable by single thruster [Ref. 1: p. 8], while Figure 17 shows how ion thrusters become more efficient, far better than MPD, as I_{sp} increases.

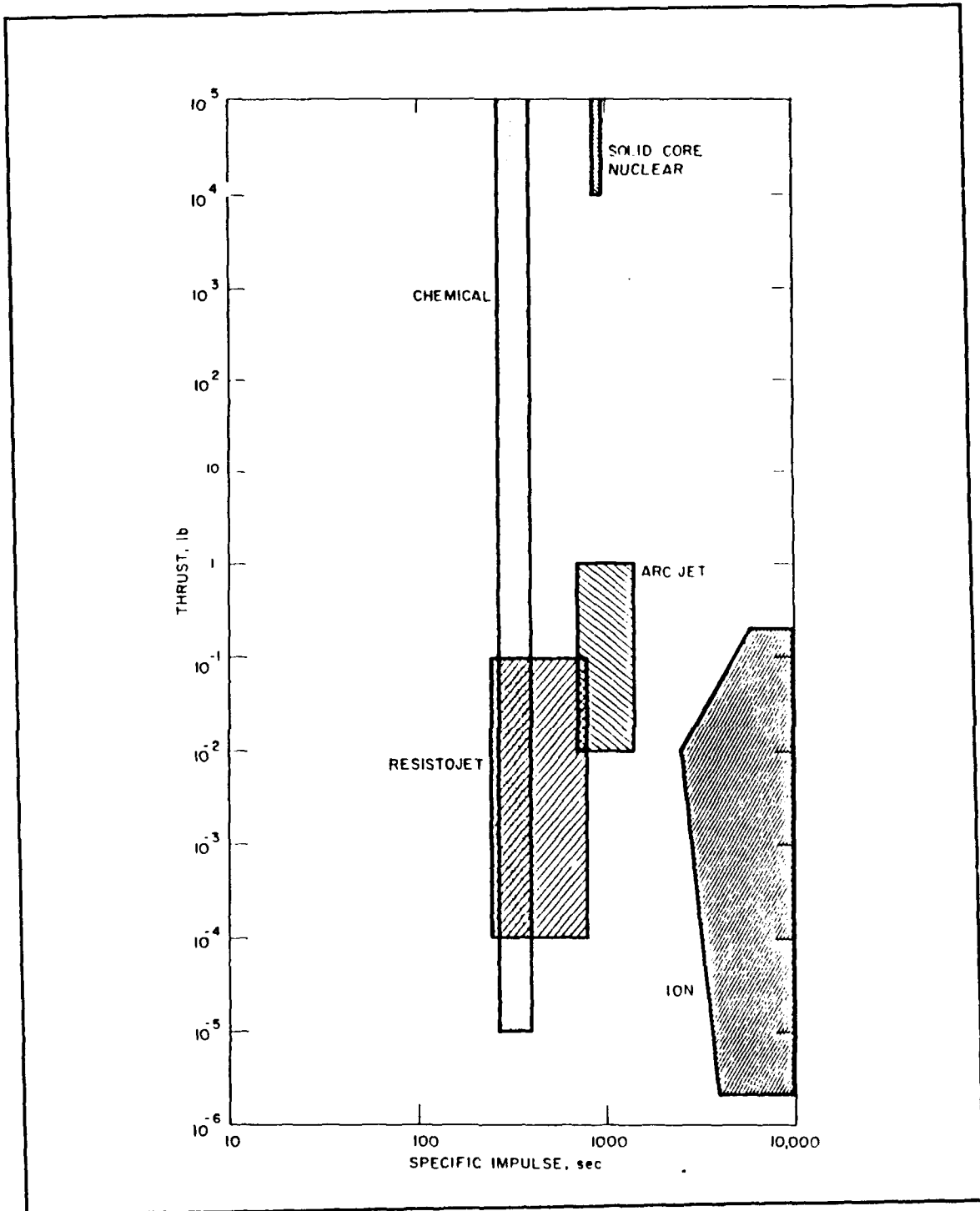


Figure 16. Specific Impulse (I_{sp}) Ranges [Ref. 11]

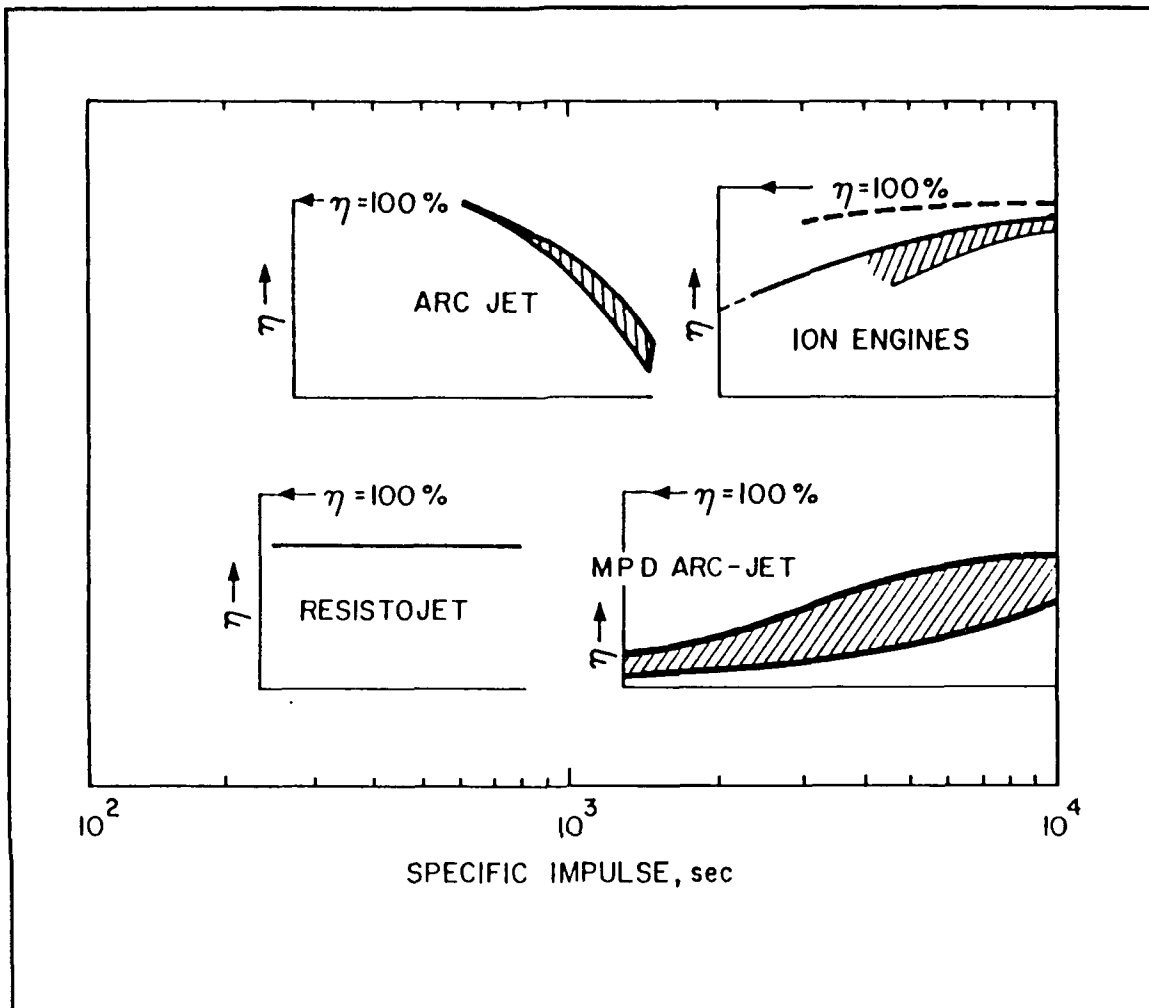


Figure 17. Isp and Efficiencies of Different Thrusters [Ref. 1]

Although lacking in commercial satellites application because of the involved risks, ion propulsion is one of the mainstream technologies within the electric propulsion field. Hundreds of reports and papers detail the advances, setbacks and tribulations experienced during innumerable analytic studies, experimental projects and a number of flight programs [Ref 16: p. 1]. Clearly, the successful demonstrations of the upcoming Japanese ETS-VI and the European SAT-2 ion

propulsion subsystems will open the door of commercial industries to IPS as the primary NSSK propulsion system.

IV. XENON ION PROPULSION SUBSYSTEM DESCRIPTION

Xenon has been chosen as the propellant because of its high molecular weight (resulting in high I_{sp}) and convenient handling properties. It is a noble gas that is inert to all normal chemical reactions. [Ref 19: p. 353]

The three major parts of the subsystem are: 1) the xenon ion thruster, as shown in Figure 18, which ionizes and accelerates xenon atoms to achieve station keeping thrust at a very high I_{sp} (2718 seconds) [Ref. 20: p. 8], 2) the xenon propellant feed system, as shown in Figure 19, which consists of xenon at a regulated pressure and flow rate to the thrusters [Ref. 21], and 3) the PPU, the schematic diagram as shown in Figure 20. The PPU, provides the high voltage power conditioning for the xenon thrusters, input current from spacecraft buses, the timing and control sequencer required to provide thruster start-up and automatic recycle sequences, and command and telemetry interfacing for the entire thruster subsystem.

A. PERFORMANCE CHARACTERISTICS OF XENON

The combined use of xenon and flight qualified solenoid valves allows rapid ON/OFF cycling with a single command bringing the thruster to full operation in 3 minutes [Ref. 22: p. 6]. The use of inert gas eliminates thruster shorts and plugging due to condensation, as well as the need for vaporization and flow control heaters as in the case of the mercury propellant [Ref. 18: p. 1].

Xenon's critical temperature (17°C) allows storage as a high density (2.2 g/cc) supercritical fluid at a reasonable pressure (4200 psia) and spacecraft temperature (25°C). By maintaining tank temperature above critical, no (liquid) propellant management devices are needed in the tank. Conventional qualified fluid components, as seen in the schematic in Figure 19, such as pressure

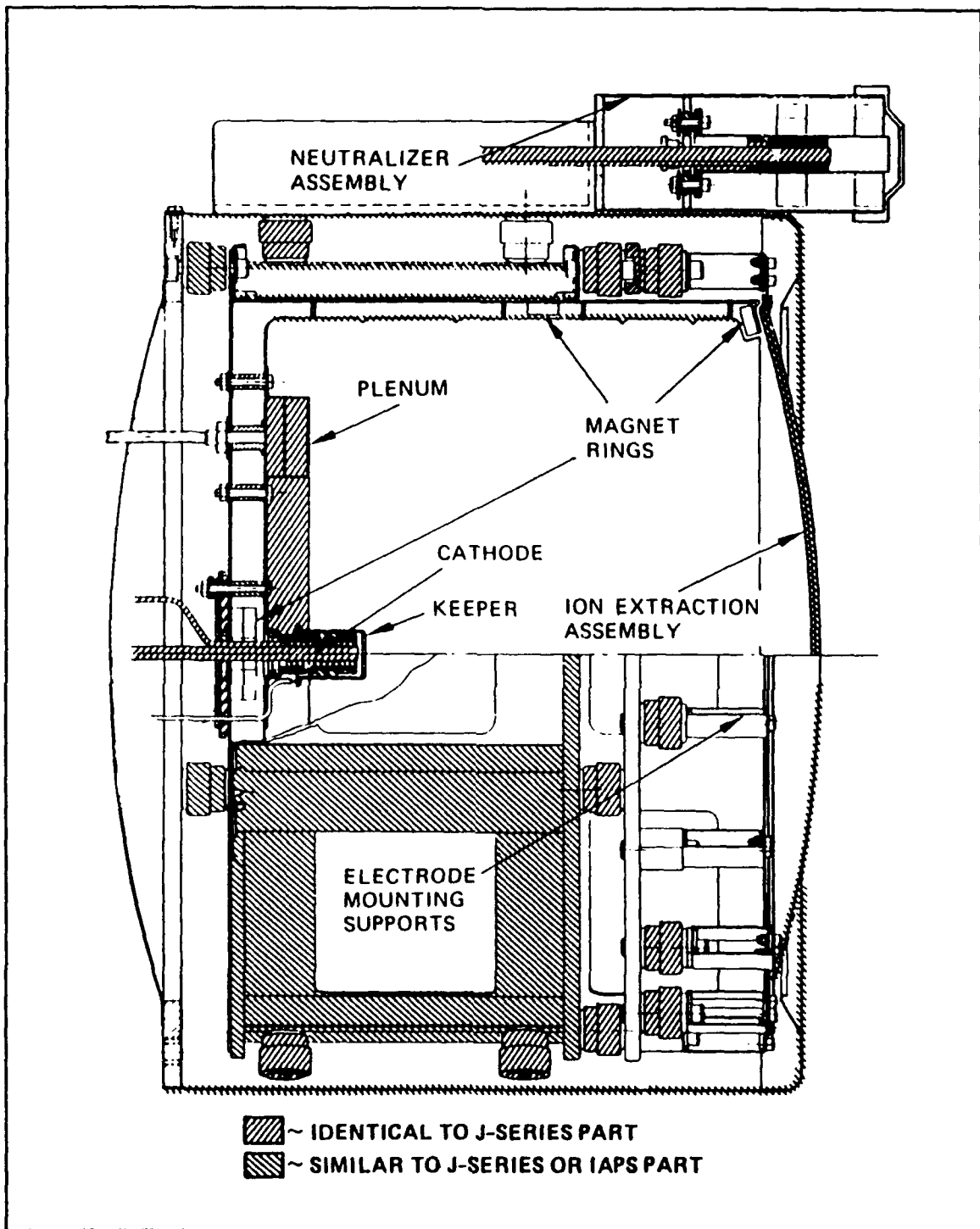


Figure 18. Hughes Ion Thruster [Ref. 21]

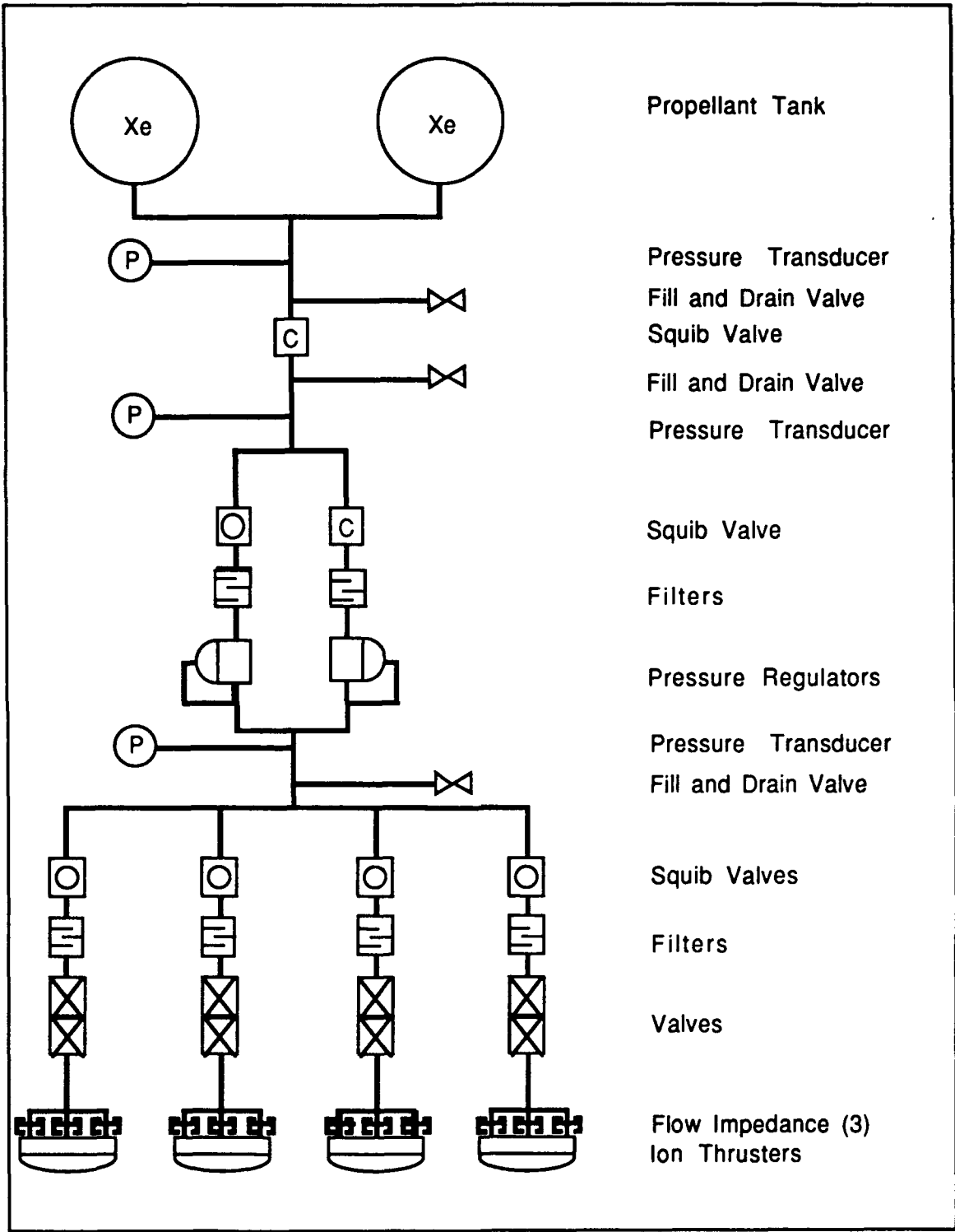


Figure 19. Xenon Feed System [Ref. 21]

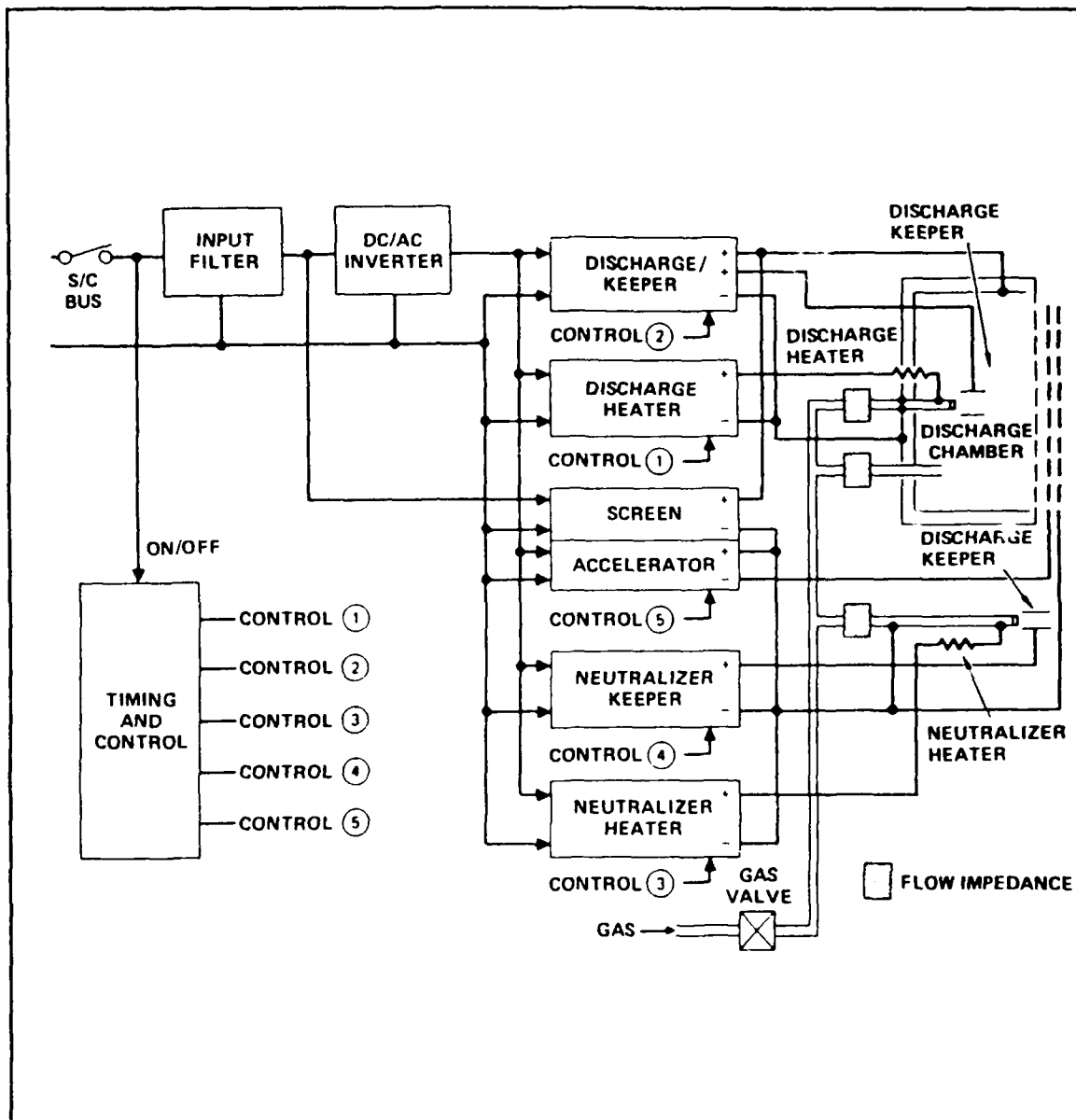


Figure 20. Xenon Thruster Power Processing Unit Schematic Diagram [Ref. 21]

regulators, isolation valves, and sensors [Ref. 18: p. 1], are readily available to support the operation of the xenon feed system. Although liquid helium must be used for cryopumping in combination with increased diffusion pumping capacity,

testing with xenon greatly reduces contamination problems in ground test vacuum tanks [Ref. 18: p. 2].

The disadvantages cited for the xenon are: 1) its cost (\$1200/kg, approximate cost in 1984) [Ref. 18: p. 2], and 2) low production rate (air contains 8.7 xenon parts per million), but for the quantities to be used in earth satellites this would not be a problem.

B. XENON ION THRUSTER OPERATION

As shown in Figure 6, the thruster consists of a short cylindrical ionization chamber closed on the left, with the three extraction grids on the right. Xenon (Xe) is fed from its supply through a pressure regulator to the neutralizer ($\approx 3\%$ of the total flow), the distribution plenum ($\approx 92\%$) and to the main cathode ($\approx 5\%$). The uncharged (neutral) xenon (Xe^0) within the chamber is ionized to (Xe^+) by "bombarding" electrons (e^-) streaming from the central cathode under the $\approx 30\text{V}$ cathode to anode potential (via a plasma bridge formed by the partially ionized xenon within the cathode). The three rings of magnets, behind the cathode, at mid chamber and at the grid opening, form a "cusped" magnetic field that confines the electrons by reflection from the strong peripheral magnetic field, enhancing the probability of collisions with xenon. [Ref. 13: p. 5]

About 90% of the xenon is ionized and the resulting positive ions are accelerated out of the chamber by the electrostatic field established between the closely spaced grids. The inner screen grid at +750 V is slightly negative of the internal plasma potential to prevent axial loss of electrons from the discharge region [Ref. 11: p. 153]. The middle accel (acceleration) grid is at -300V while the decel (deceleration) grid is at the neutralized beam potential, of about zero V. First the xenon ions are driven by the +750 to -300 electrostatic potential

gradient, leaving the chamber at a velocity of about 26.6 km sec^{-1} ($I_{sp} = 2718$ seconds), the result of a net potential drop. The high negativity of the accel grid also prevents neutralizing electrons from entering the chamber. The neutralization process occurs when the excess electrons within the chamber flow to the neutralizer cathode and via a plasma bridge join the exiting positive ions. The extraction/acceleration process occurs at each set of aligned grid holes, forming a beamlet, and it is the combined action/reaction forces of all the beamlets that produces the resultant mN level thrust. [Ref. 14: p. 5]

C. SELECTION OF ION THRUSTER

1. Trade-offs Between Ion Thrusters

Bombardment thrusters with diameters of 2.5, 8, 5, 10, 13, 15, 20, 25, 30 and 150 cm have been tested. Whenever the size of the thruster was varied, the performance obtained at that particular time was nearly as expected based on developed scaling laws [Ref. 13: p. 652]. Most bombardment thrusters are cylindrical in shape, and therefore their volume may be defined by a length and a diameter. In addition, Kauffman [Ref. 22: p. 267] has noted that optimized thruster length changes little as the diameter is varied. Thus, to scale the operating or performance parameters of various size thrusters, only the diameter need be varied [Ref. 13: p. 652].

While larger thrusters of a given type are more efficient due to the fewer number of warm-up times and shorter firing time at the orbital nodes, the more important things to consider are the reduced thruster life and qualification requirement, principally from a cost point of view [Ref. 14: p. 6]. Consideration must also be given to the electrical power requirement of the thruster. Larger thrusters require more electrical power to produce higher thrust.

2. Selection of Thrust Level

The gradually increasing north-south drift, because of moon and sun perturbations, of a geostationary spacecraft can be corrected by thrusting in a north or south direction around the orbital nodes [Ref. 23: pp. 127-129], as shown in Figure 21. However, the IPS must operate for an appreciable time to provide the necessary impulse, and the total efficiency (η_T) of the process decreases with increasing angle of thrust period (β) from the nodes. This issue is further evaluated in Chapter VII. Consequently, since reducing the thrust level decreases the mass of the propulsion subsystem while also degrading its efficiency, a compromise must be reached between thrust and operating time. In arriving at such compromise, criteria other than system mass and thrusting efficiency must also be taken into account. For example, the use of a large thruster necessitates the provision of increased power and, for short thrusting periods, proportionally more propellant is wasted during startup and shutdown [Ref. 24: p. 147]. With regard to the latter point, it is likely that the shortest times for these parts of the operational cycle will be about 5 and 3 minutes, respectively, and so it is reasonable to assume that the equivalent of 2 to 3 minutes of normal propellant flow will be wasted during each thrusting period. This represents a 1.5 to 2.5 reduction of mass utilization efficiency (η_m) over a 2-hour cycle, [Ref. 25: p. 76] which is probably acceptable and effectively fixes the upper thrust level.

3. Available Ion Thrusters

Only four of the available ion thrusters in the world are considered for analysis in this study. These are shown in Figure 22 and they are: 1) the UK-10 developed by Culham Laboratory in the UK, 2) the MELCO ion thruster developed in Japan, 3) the RIT-10 developed in Germany, and 4) the U.S.

Hughes Research Laboratories HRL-13 [Ref. 14]. The operating parameters of these thrusters are shown in Table 4. Individual mass breakdowns are shown in Table 5 for UK-10, Table 6 for Hughes, Table 7 for RIT-10, while none are available for MELCO. Appendix A is the analysis for HRL-13, Appendix B for MELCO, Appendix C for UK-10. The analysis for RIT-10 was not considered because of its obvious high specific mass and high specific power.

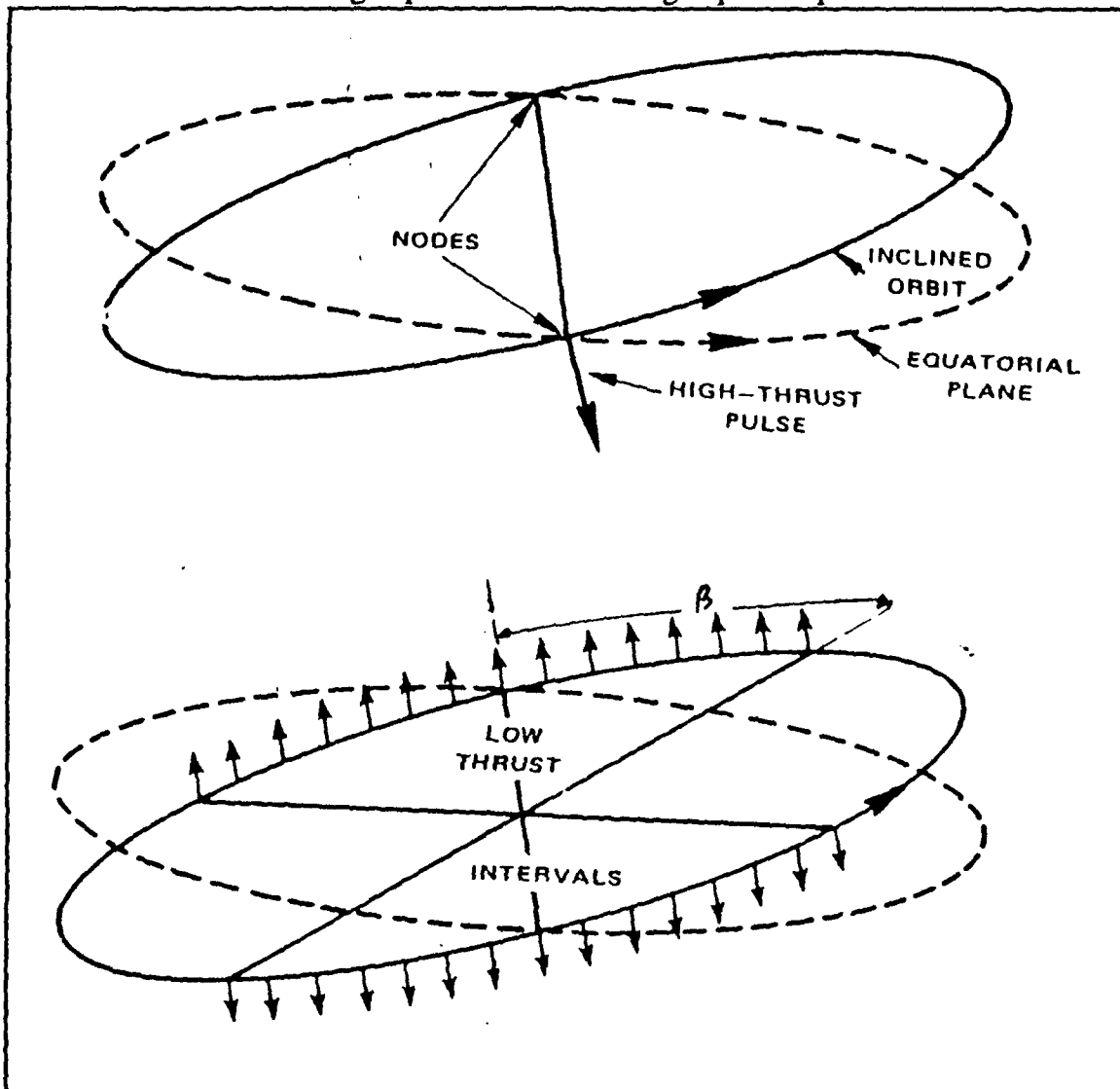
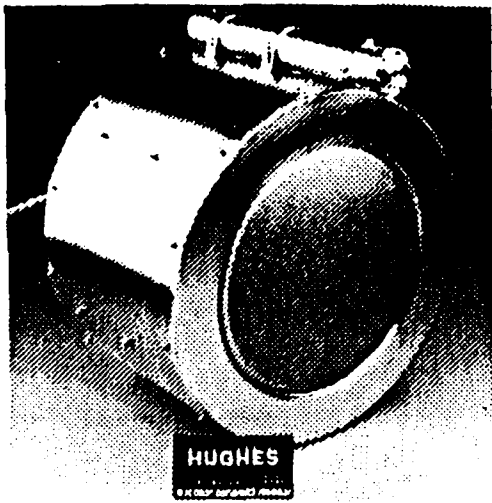
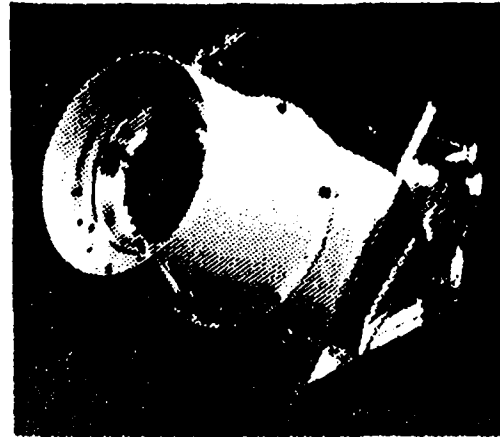


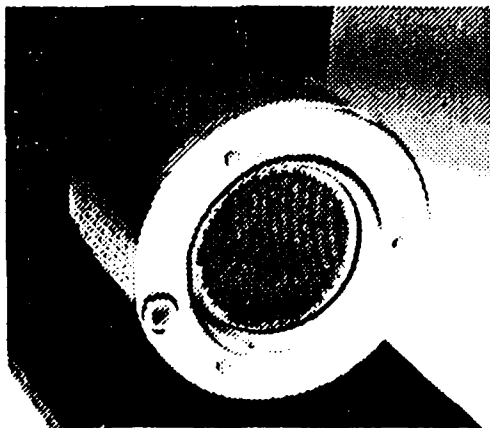
Figure 21. Thrust Program for North-South Station Keeping
a. High Thrust, b. Low Thrust [Ref. 24]



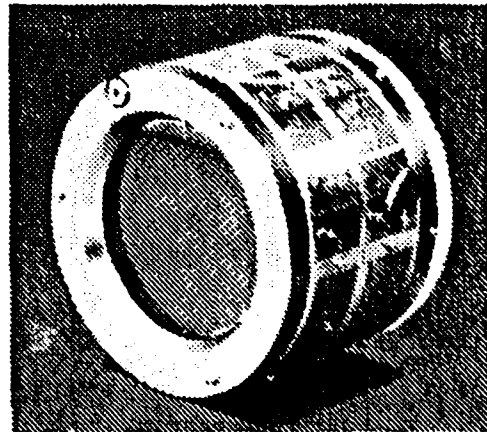
Hughes/US (ADM)



MBB/Germany (RIT-10)



Marconi-Culham/UK (UK-10)



MELCO/Japan (XIES)

Figure 22. Different Electrostatic Ion Thrusters [Ref. 9]

TABLE 4. THRUSTERS' PARAMETERS

TYPE	HRL-13	UK-10	RIT-10	MELCO
Output, mN	17.7	25	15	23.3
Power Consumption, W	427	644	460	745
Specific Power, W/mN	24.1	25.8	30.7	32
Dry Mass, kg (for four thrusters)	69.1	100	128.9*	84**
Specific Mass, kg/mN	3.9	4	8.6	3.6

* Does not include gimbal mass

** Not certain if gimbal mass is included

Summary of calculations are presented in Table 8 and Table 9 for the HRL-13, chosen for this study.

E. LOCATION OF ION THRUSTERS

When replacing chemical thrusters with ion thrusters, location and "plume" direction remain important considerations. Rapidly expanding chemical exhaust plumes present heating, torque, and chemical deposition problems. These problems do not go away with the ion thruster, although ion thruster has more collimated ion beam. As shown in Figure 23 and Figure 24, the half angle beam divergence of the ion thruster to contain 100% of the beam is 21°. Likewise, 95% of the beam is contained in 14° half angle divergence. [Ref. 20: p. 7 and Ref. 21: p. 147] If 95% of the beam is used as the criteria, Figure 23 shows that the solar array needs 1.7 meters clearance from the north panel of the satellite. In this case, sputtering resistant strip can be installed at the solar array basement, yoke side, to protect the solar cells from the remaining 5% of the ion beam. Another option is install plume shield, not recommended, as shown in Figure 25. Because the solar panels rotate about the north-south axis and always face the

sun, the ion beam impinging on the affected solar cells is less than 5%. If the full 42° is considered, 3 meters is needed to totally clear the solar panels from plume impingement, as shown in Figure 24. If extending the boom is not feasible nor practical to offset the degradation due to plume impingement, making the solar panels narrower and longer should solve the problem. The affected area, as shown in Figure 24, constitutes about 2% of the total north solar panels. Also, the position shown in Figure 24 is the worst case and this occurs only during the solstice periods.

Other factors affecting the selection of thruster configurations [Ref. 26: p. 217] are:

- 1) the primary component of the thrust must be along the North-South axis to perform inclination control,
- 2) the effect of thrust in the orbit plane must be negligible or averaged out,
- 3) the torques induced by ion thrusters must be as small as possible,
- 4) the plume impingement on other elements of the spacecraft must be minimized,
- 5) the ion thrusters must avoid as much as possible taking room where payloads are usually located, and
- 6) the beam of particles from the thrusters must be kept away from the payload to avoid electrical interference.

Ideally if the conditions above are all to be met for a three axis satellite NSSK control, the only possible option is place the thrusters at the end of each solar wing, as shown in Figure 26. Initially, all of the above conditions may be satisfied but a minor shift of the center of mass will have a tremendous impact on the torque because the moment arms of the thrusters are long. Problems with

propellant lines also exist because the lines have to be folded along with the solar panels during launch.

TABLE 5. UK-10 IPS MASS BUDGET

Equipment	Unit Mass, kg	Number	Total Mass, kg
THRUSTER	1.0	4	4.0
PCCE			
Beam Supply	2.5	1	
Controller	0.4	1	
PSME Electronics	0.4	1	
TLM Conditioning	0.2	1	
Remaining Supplier	2.1	set	
Baseplate	1.2	1	
Cover	0.4	1	
PCCE TOTAL	7.2	4	28.8
PSME			
Regulator Valve	0.1	5	
Plenum	0.25	2	
Transducer	0.05	3	
Latch Valve	0.45	1	
PSME TOTAL	1.6	4	6.4
Pipework	2.0	set	2.0
Cabling	2.0	set	2.0
Brackets	5.0	set	5.0
PSE			
Regulator Valve	0.25	4	
Plenum	0.25	1	
Transducer	0.05	3	
F/D Valve	0.12	1	
Relief Valve	0.25	1	
Xenon Tank	9.5	2	
PSE Electronics	1.0	1	
PSE TOTAL		1	21.77
IPS TOTAL		1	70.0
IMPLEMENTATION:			
Gimbal Mechanism	2.5	4	10
Structure and Brackets			10
Thermal Control			5
Sensors			2
Harness			2
Extra TLM			1
IMPLEMENTATION TOTAL			30
TOTAL IPS IMPACT			100

TABLE 6. HUGHES 13-CM ION THRUSTER MASS BREAKDOWN

[REF. 20]

Unit	Unit Mass, kg	No. per Spacecraft	Mass per Spacecraft
Ion Thruster	5.0	4	20.0
Power Processor Unit	7.1	4	28.4
Xenon Tank	2.0	2	4.0
Pressure Regulator	0.8	2	1.6
Other Feed Components	3.5		3.5
Gimbal	2.2	4	8.8
Structure	2.8		<u>2.8</u>
Total Mass			69.1

TABLE 7. RITA MASS BUDGET [REF. 15]

Unit	Unit Mass, kg	No. per Spacecraft	Mass per Spacecraft
Propulsion Unit	2.85	4	11.4
Power Supply Unit	12.6	4	50.4
Xenon Tank	7.35	2	14.7
Digital Automatic Control Unit	6.0	4	24
Radio Frequency Generator	1.5	4	6
Flow Control Unit	3.5	4	14
RITA Dedicated Harness	2.10	4	<u>8.4</u>
Total Mass			128.9

**TABLE 8. SUMMARY OF CALCULATIONS OF APPENDIX A
AND APPENDIX H COMPARING ION AND BIROPELLANT
PROPULSION SUBSYSTEM MASS FOR NSSK USING HUGHES ION
THRUSTER**

Maneuver Life (Years)	10	15	20
Spacecraft BOL Mass=kg (with Bipropellant Subsystem NSSK)	1471.42	1644.04	1831.93
Bipropellant Mass for NSSK, kg	211.44	356.38	514.47
BOL Mass =kg (with Ion Propulsion for NSSK)	1331.05	1352.76	1374.1
Xenon Mass, kg	24.8	39.5	53.9
Ion Subsystem Dry Mass , kg	80.15	82.62	85.1
Thruster Firing Time/Day (Hrs)	1.98	2.1	2.16
Total Hrs in Operation (Ion)	5445	8663	11,880
Energy Required (Watt-Hr)	1691	1794	1845
GTO Mass=kg, Ariane IV Launch (Bipropellant NSSK)	2461.18	2787.2	3136.92
GTO Mass=kg, Ariane IV Launch (Ion NSSK)	2226.39	2250.23	2298.39
GTO Mass Saving (Biprop - Ion) Ariane IV	234.79	536.97	838.53
GTO Mass=kg, ETR Launch (Bipropellant NSSK)	2824.64	3220.26	3642.08
GTO Mass=kg, ETR Launch (Ion NSSK)	2541.84	2588.95	2635.15
GTO Mass Saving =kg, (Bipropellant -Ion) ETR	282.8	631.31	1006.93

**TABLE 9. SUMMARY OF CALCULATIONS OF APPENDIX A
AND APPENDIX H FOR ION PROPULSION WITH
BIPROPELLANT BACKUP DURING ECLIPSE USING
HUGHES ION THRUSTER**

Maneuver Life (Years)	10	15	20
Spacecraft BOL Mass=kg(for Bipropellant NSSK)	1471.42	1644.04	1831.93
Thruster Firing Time/Day (Hrs) Combo	1.48	1.61	1.69
BOL Mass, kg for Ion/Bipropellant Combo	1380.55	1433.1	1485.16
Reduction in Mass due to Bipropellant backup , kg	90.87	210.94	346.77
Energy (w-hr) for Ion with COMBO (Ion/Bipropellant)	1264	1375	1444
Total Ion Thruster Hrs during (COMBO)	4070	6642	9295
Remaining Years in Operation with total Ion Propulsion Failure at (BOL)	2.465	3.7	4.93

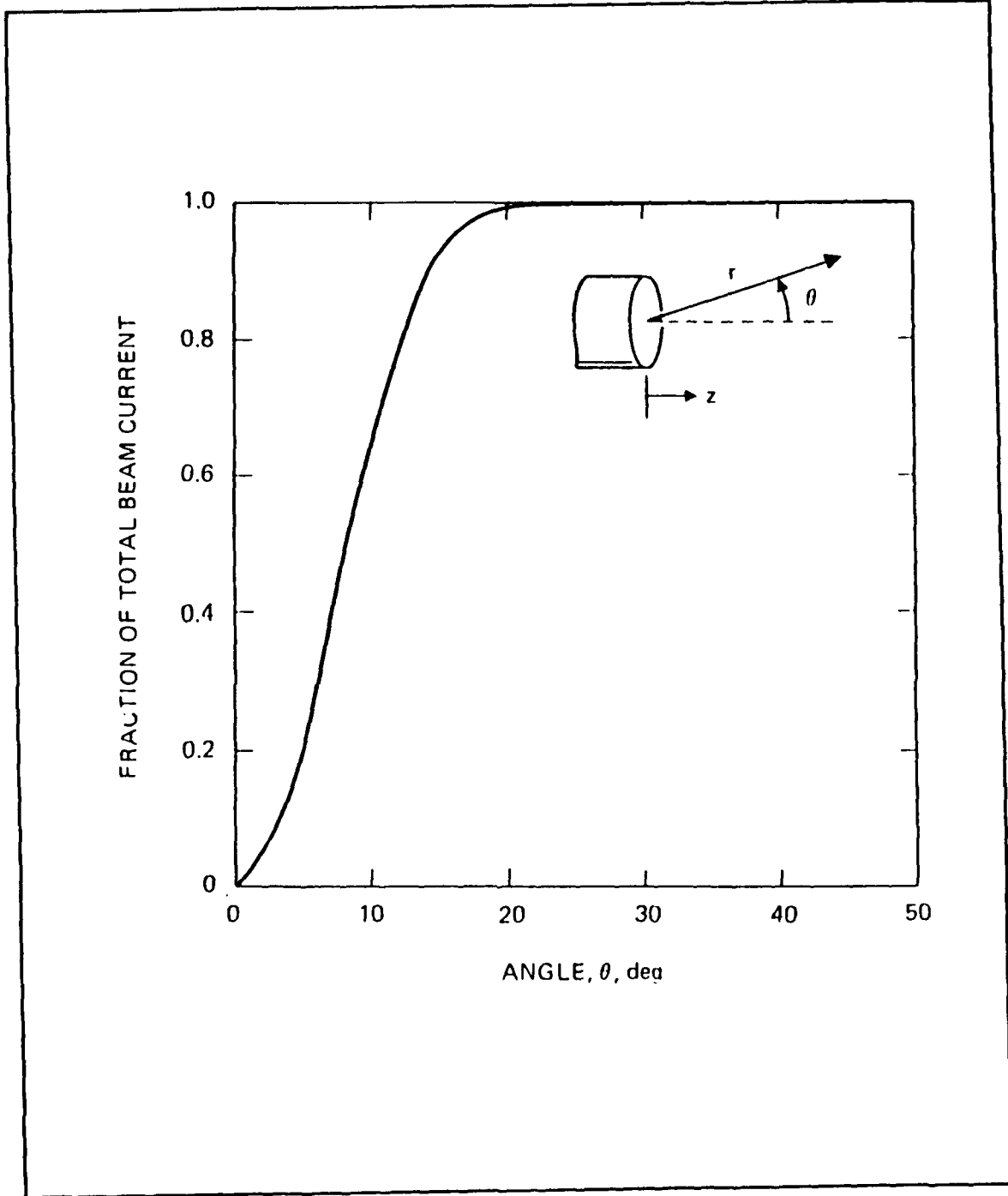


Figure 23. Hughes Thruster Beam Divergence Characteristics
[Ref. 21]

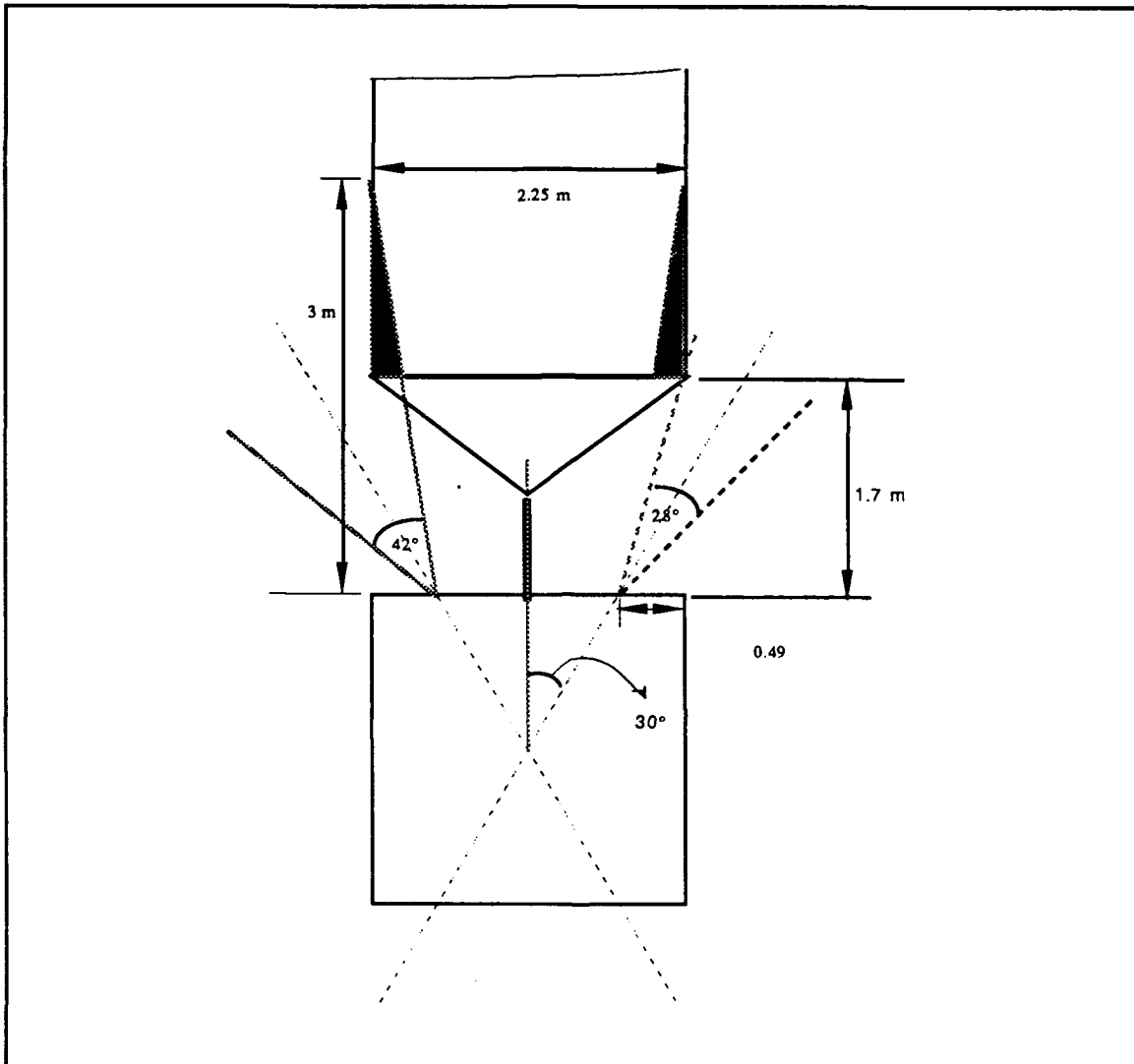


Figure 24. Plume Impingement Geometry

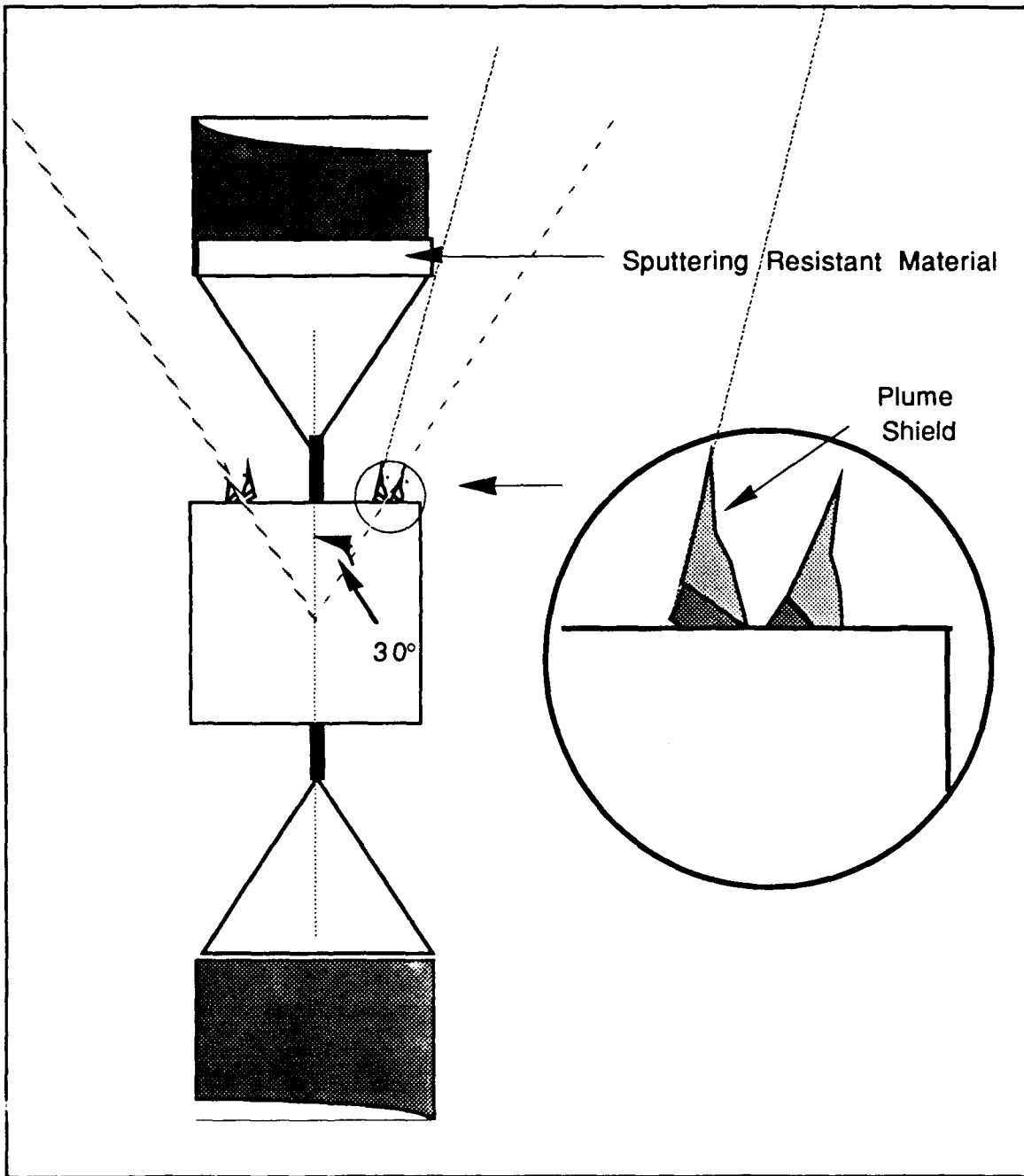


Figure 25. Thruster Configuration with Plume Shield and Sputtering Resistant Material

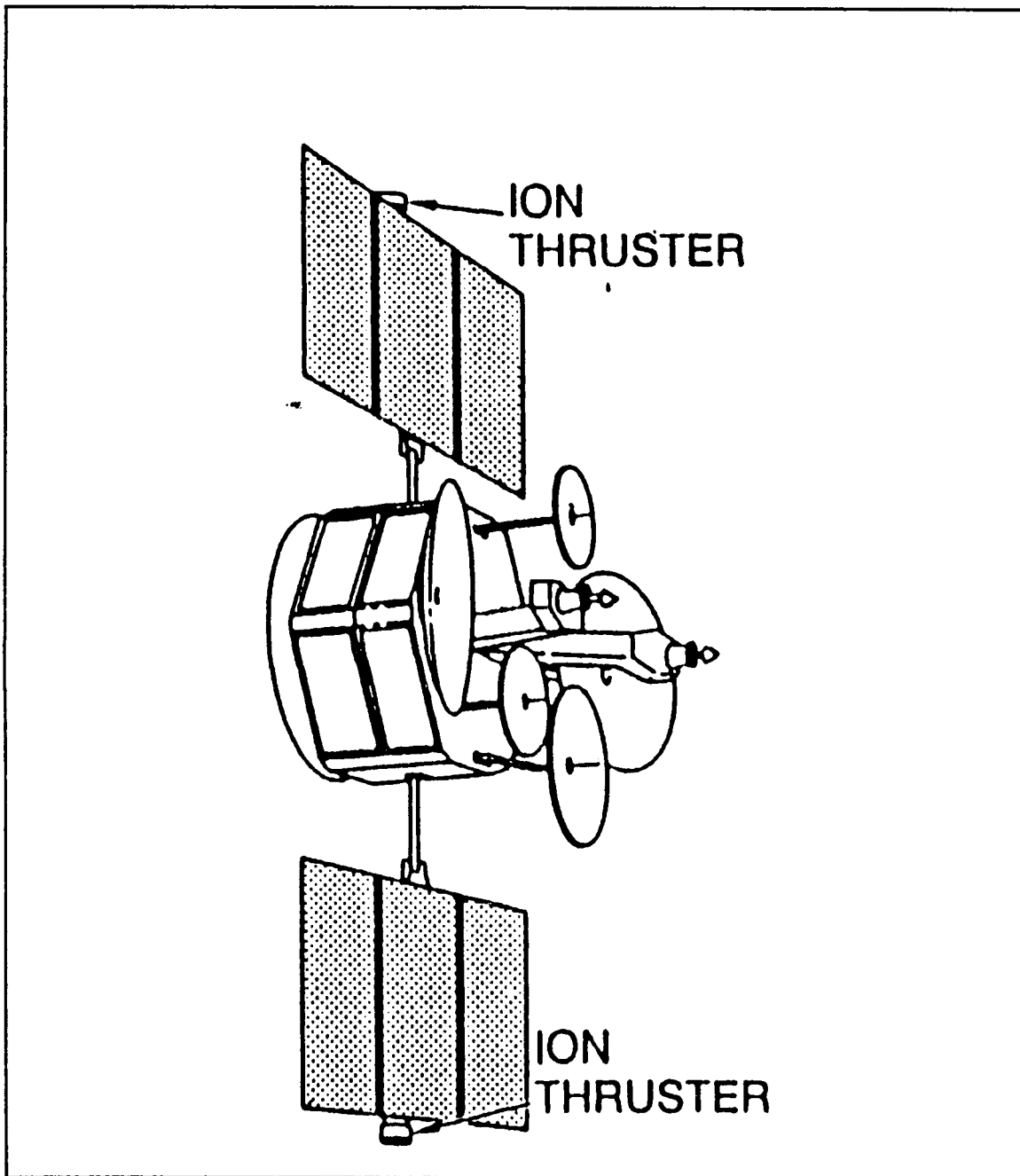


Figure 26. Thrusters at Ends of Solar Panels [Ref. 14]

In addition to the constraints mentioned above, making use of redundant operating modes to increase reliability remains a big factor when selecting the location of ion thrusters.

With a given thruster configuration, a variety of operating modes are possible for NSSK and EWSK corrections using either all thrusters or a reduced number of thrusters after a single thruster failure. Since this study is purely directed toward NSSK, only three configurations will be analyzed. As shown in Figure 27, the thruster configurations 1 and 2 can be used for NSSK and EWSK, while configuration 3, as further illustrated in Figure 28, is restricted to NSSK only because its thrust vectors do not pass through the center of mass. If the thrust vectors do not pass through the center of mass, torque will produce attitude disturbance if there is a thrust imbalance when the thrusters are fired (single thruster firing is not possible). One advantage with configuration 3 in Figure 27 is that the location of the thrusters contributes the least to plume impingement on the solar array compared to configurations 1 and 2.

If one thruster in configuration 1 fails, the north-south correction is continued at one orbital node only. If the diagonal pair is used, the east-west component for the correction will not cancel out but an eccentricity buildup will result, as shown in Figure 29. [Ref. 27: pp. 490-491]

In all the thruster configurations shown in Figure 27, the system fulfills its task if either all four thrusters are intact (configuration with system failure after one single thruster failure have been excluded), or if the system operates with two intact thrusters. Thus, the equation [Ref. 27: p. 491] for system reliability is

$$R_{\text{syst}} = R^4 + \left(\frac{4}{3}\right)R^3(1 - R) + R_{\text{syst}}(2 \text{ failures}) \quad (4-1)$$

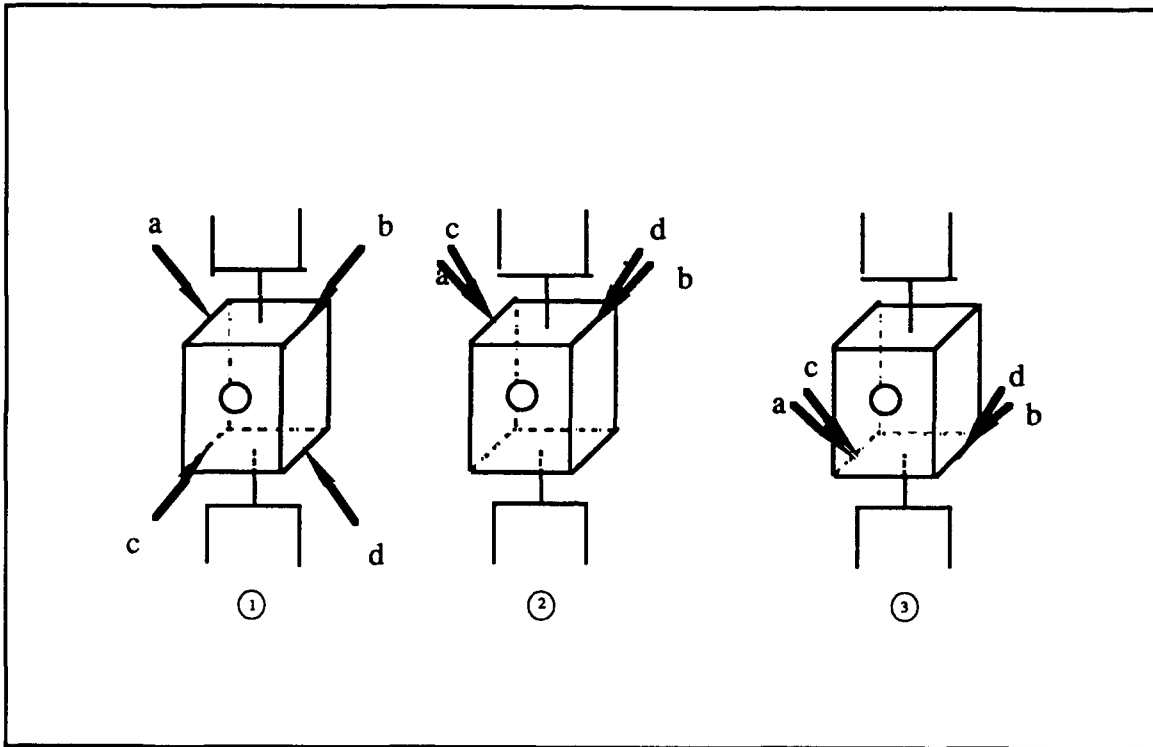


Figure 27. Possible Configuration for NSSK Ion Thrusters [Ref. 27]

where

R is the reliability value for each thruster (assumed the same for all thrusters)

$R_{\text{sys}}(2 \text{ failures})$ is the probability that the system fulfills its duty with only two intact thrusters.

The first two terms are the same for all three thruster configurations, so the difference between the effectiveness of each configuration is based on the last term. The last term can be evaluated by

$$R_{\text{sys}}(2 \text{ failures}) = (n/6)R^2(1-R)^2 \quad (4-2)$$

where n is the number of crosses from Table 10.

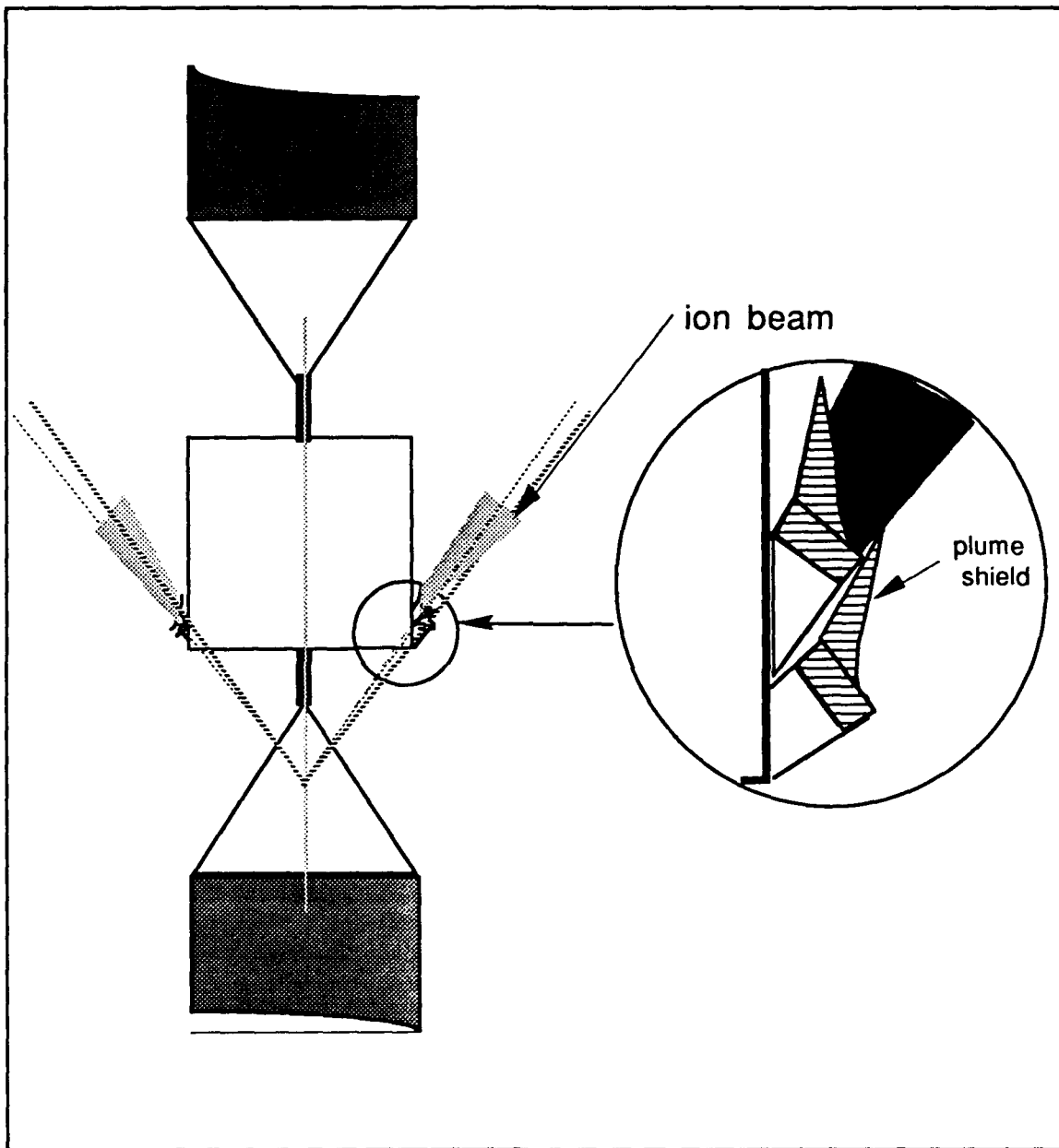


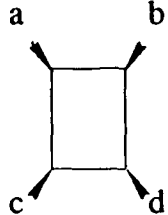
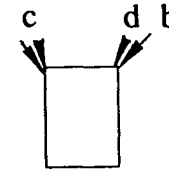
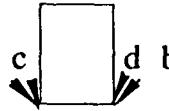
Figure 28. NSSK Thruster Location without EW Station Keeping Capability

As can be seen from Table 10, configuration 2 has more crosses than configurations 1 and 3, and therefore making it more reliable (i.e., more redundancy features). Configurations 1 and 2 will be less efficient if the satellite has a cube-like configuration, as shown in Figure 30. With this configuration the thrusters must have a 45° cant angle if the thrust vectors have to pass through the center of mass. To be more efficient, in the case of configuration 2, at the expense of solar degradation due to plume impingement, the thrusters must be moved inboard toward the center on the north panel with cant angle adjusted accordingly. The chosen configuration for this study is the modified configuration 2 with a cant angle of 30° , as seen in Figure 25.

1. Ion Thrusters on Gimbals

Torque introduced by thruster firing creates disturbance to the antennas' pointing accuracy. Setting the thrusters on gimbals, as shown in Figure 31, minimizes the disturbance by providing unlimited control to the thrust vectors of the thrusters. Single-axis gimbals, as shown in Figure 31 (a), will be sufficient in correcting thrust imbalance between two thrusters; however, when the center of mass starts to change due to depletion of propellant, the dual-axis gimbal is always the choice, as shown in Figure 31 (b). The latter, however, will need more parts and will be more complex to operate. Interface with other sensors is necessary to provide a feedback loop if automatic operation is to be incorporated with the gimbals systems. For example, the actuators that control the gimbals can receive input from a "star sensor". Since the thruster firing will always take place in the same inertial position, the sensor will always view the same part of the sky during the maneuver [Ref. 28: p. 3].

**TABLE 10. THE INFLUENCE OF DUAL THRUSTER FAILURES
ON THE SYSTEM CAPABILITY OF PERFORMING NSSK (+),
EWSK (+) OR BOTH (+) [REF. 27]**

CONFIGURATION																		
FAILURE OF THRUSTERS	a	c	a	a	b	b	a	a	b	c	a	b	a	a	b	c	a	b
	+	+	+	+	+	+	+	+	+	+	+	+	+	+	+	+	+	+
	b	d	d	c	c	d	b	d	c	d	c	d	b	d	c	d	c	d
STATION KEEPING POSSIBLE	north/south																	
	+	+					+	+	+	+			+	+	+	+		
	east/west																	
	+	+	+	+	+		+	+	+	+	+							
SYSTEM OPERABLE	+	+					+	+	+	+								

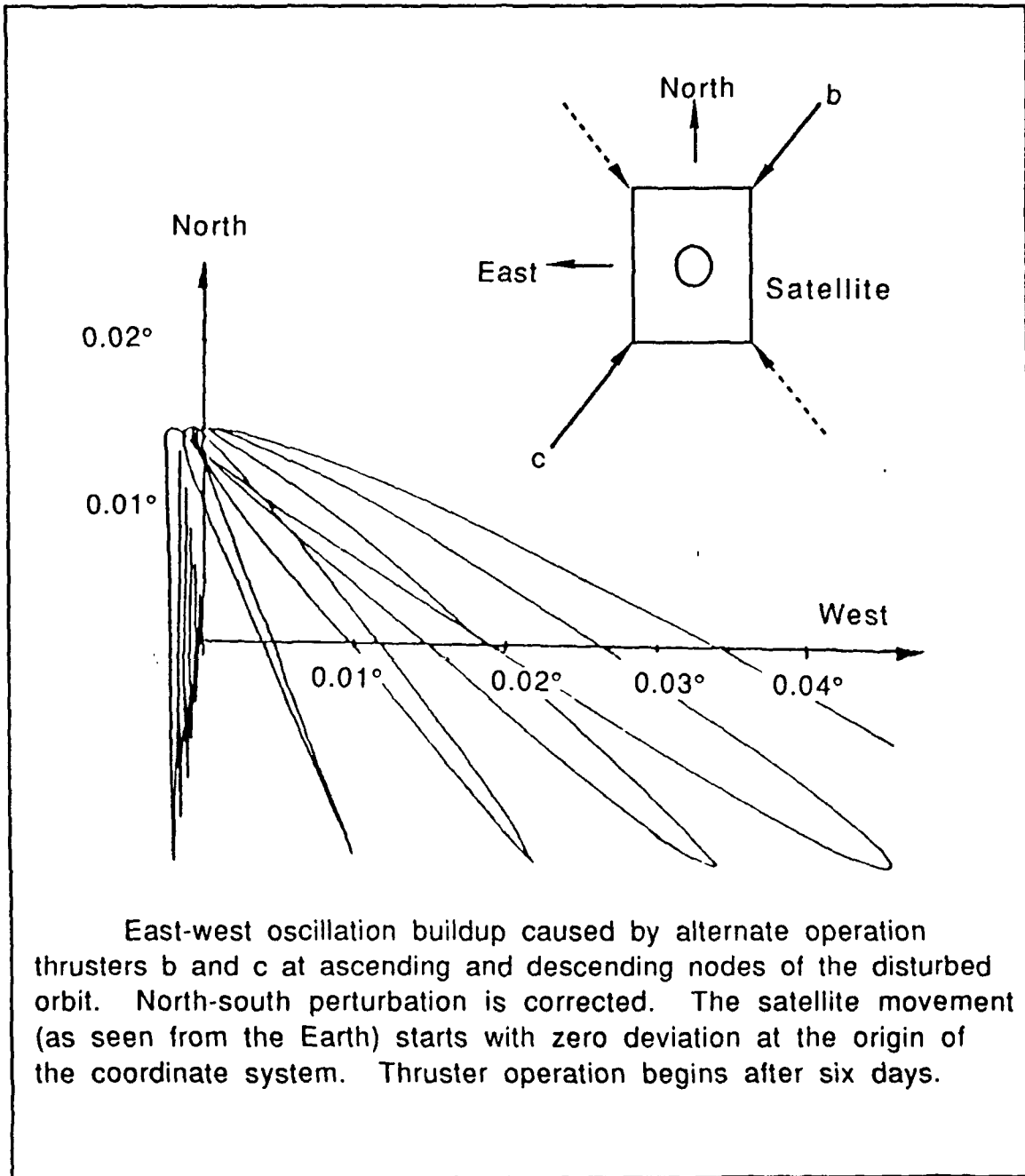


Figure 29. Eccentricity Buildup Due to Diagonal Thruster Firing
 [Ref. 27]

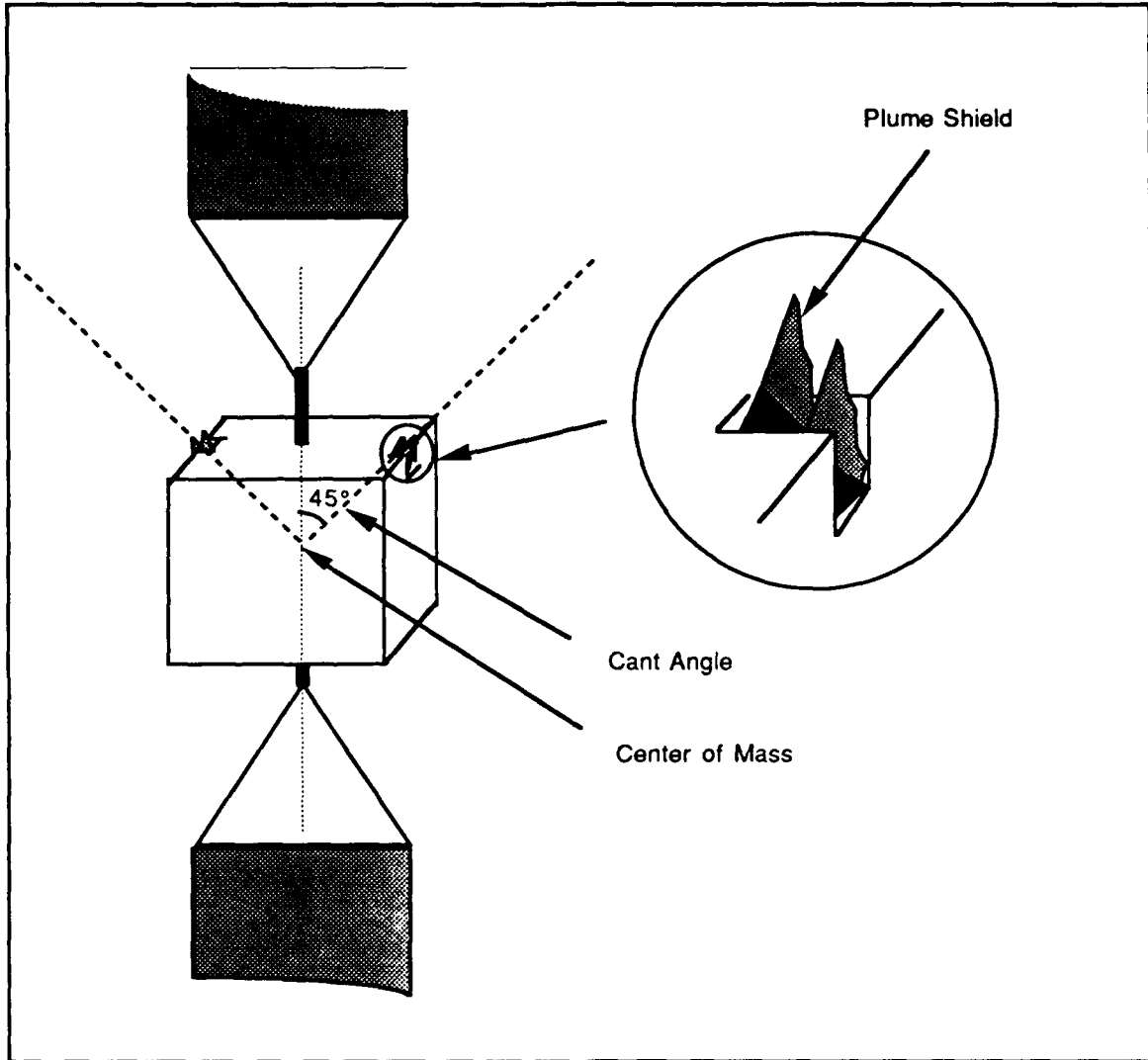


Figure 30. Ion Thruster Location with EW Station Keeping Capability [Ref. 22]

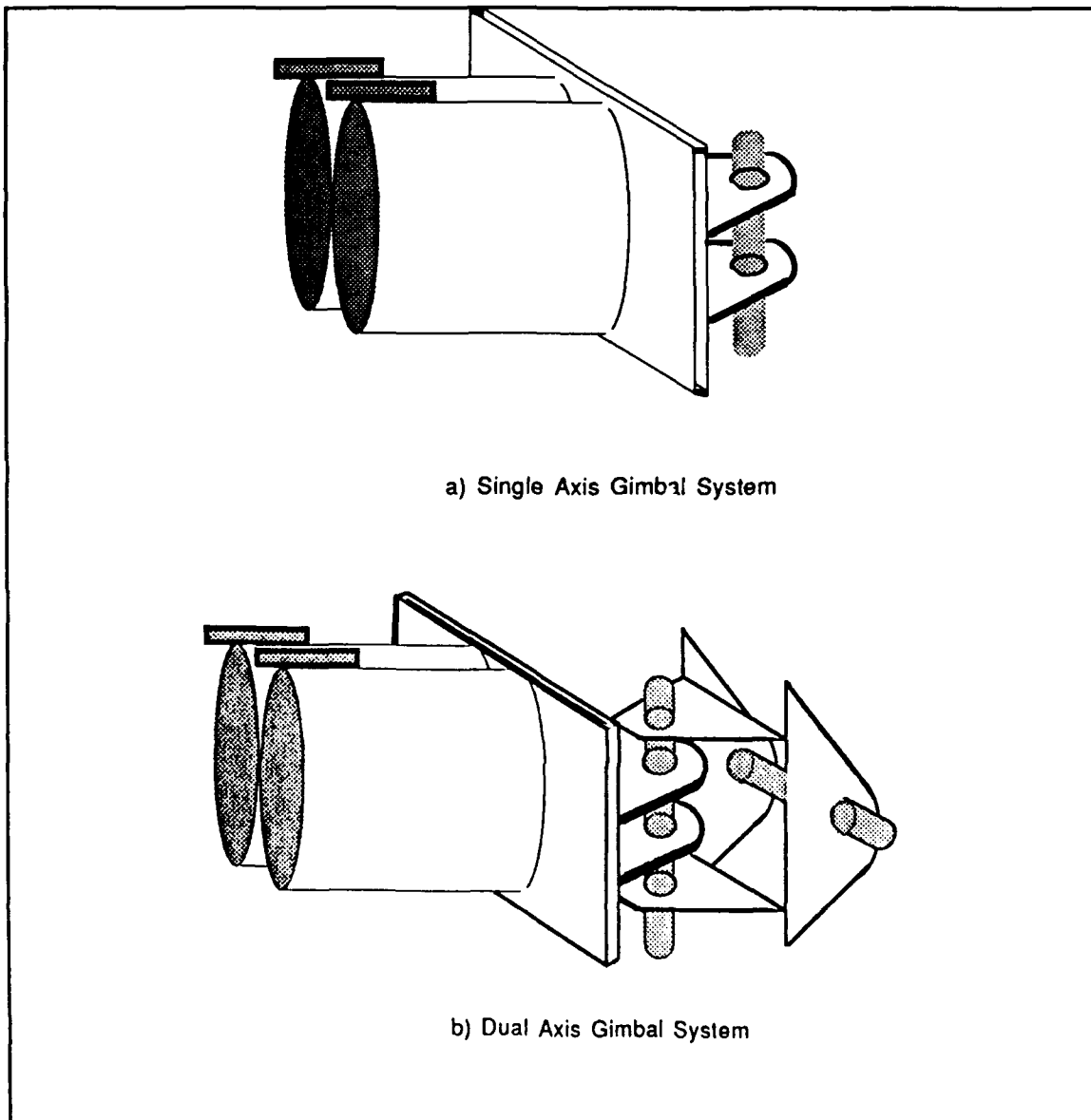


Figure 31. Ion Thrusters with Gimbals

V. STATION KEEPING

A geostationary orbit is one whose satellite track on the earth is a point on the equator that does not move. This requires that the satellite's orbit be circular (eccentricity = 0°), equatorial (inclination = 0°), and possessing a period equal to that of the earth's rotation [Ref. 29: p. 307]. Assuming at the BOL the satellite is on a geostationary orbit, the attraction of the sun and the moon on the satellite causes a long period (52 years) precessional drift [Ref. 30: p. 2] of the orbital plane in a north-south direction with nodal drift as well. The non-uniform gravitation field of the (triaxial) earth causes east-west drift, and solar radiation (from one side) causes changes in eccentricity and contributes to attitude disturbances. In case an initial geosynchronous orbit is allowed to drift without any orbit correction, the inclination will gradually increase to a maximum value of approximately 15° [Ref. 3: p. 80]. Around 0° (with respect to the equator) the drift rate varies from year to year, as shown in Table 11, as does the impulse associated with nullifying the rate [Ref. 30: p. 2].

A. NORTH-SOUTH STATION KEEPING (NSSK)

For a communications satellite with a small beam angle or that requires fine pointing accuracy, it is necessary to keep the orbital elements within allowable limits. For the chosen spacecraft, north-south inclination limit of 0.1° and east-west longitude tolerance of $\pm 0.1^\circ$ are assumed. Assuming the satellite is launched in January 1993, with 10, 15, and 20 mission years, the ΔV s required are 429.21, 676, and 912.1 m/s respectively, as calculated in Appendix G. The perturbing forces due to the moon and the sun cause the inclination drift.

TABLE 11. INCLINATION DRIFT RATES

Date	Ω moon	i_l	Ω_l	$\frac{di}{dt} _{\text{moon}}$	$\frac{di}{dt} _{\text{Total}}$
January 1	(Deg.)	(Deg.)	(Deg.)	(Deg./Year)	(Deg./Year)
1993	260.526	23.135	-13.023	0.565	0.834
1994	241.198	21.423	-12.436	0.533	0.802
1995	221.870	19.898	-10.138	0.506	0.775
1996	202.542	18.793	-6.132	0.487	0.756
1997	183.161	18.311	-0.903	0.479	0.748
1998	163.833	18.557	4.504	0.483	0.752
1999	144.505	19.476	8.993	0.498	0.767
2000	125.177	20.888	11.875	0.523	0.792
2001	105.796	22.568	13.006	0.554	0.823
2002	86.468	24.287	12.581	0.587	0.856
2003	67.139	25.865	10.929	0.619	0.888
2004	47.821	27.162	8.379	0.645	0.914
2005	28.481	28.078	5.218	0.664	0.933
2006	9.141	28.546	1.710	0.674	0.943
2007	349.801	28.532	-1.907	0.673	0.942
2008	330.461	28.039	-5.402	0.663	0.932
2009	311.121	27.100	-8.537	0.644	0.913
2010	291.781	25.783	-11.048	0.617	0.886
2011	272.441	24.191	-12.642	0.585	0.854
2012	253.101	22.469	-12.987	0.552	0.821
2013	233.761	20.801	-11.763	0.522	0.791
2014	214.421	19.409	-8.783	0.497	0.766
2015	195.081	18.523	-4.216	0.482	0.751
2016	175.741	18.318	1.215	0.479	0.748
2017	156.401	18.838	6.390	0.487	0.756
2018	137.061	19.973	10.313	0.507	0.776
2019	117.721	21.515	12.513	0.535	0.804
2020	98.381	23.233	13.010	0.567	0.838

1. Perturbation Forces

The perturbation forces are defined as those which change the orbital elements of the satellite with respect to the earth. The satellite will experience perturbation forces due to the gravitational effects of the sun and the moon. The perturbation force from a perturbing body is the difference between the gravitational force due to the perturbing body at the satellite and the gravitational force the satellite would experience if it were at the center of the earth. [Ref. 3: p. 73]

B. EAST-WEST STATION KEEPING

A satellite on geostationary orbit will tend to drift from its longitudinal position mainly because of the long-term tangential perturbing force due to the earth's triaxiality or elliptical shape [Ref. 29: p. 308]. The sun, which moves only $0.986^\circ/\text{day}$, contributes very little to the drift acceleration. The moon, which moves approximately $13.2^\circ/\text{day}$, contributes to the longitude drift acceleration term with a period equal to half of the rotational period (27.3 days). The periodic drift acceleration due to the moon for large longitude tolerance can be ignored because the time between maneuvers spans several lunar cycles. [Ref. 3: p. 83]

Considering second-order gravity effects only [Ref. 3: pp. 88-89], the longitudinal drift acceleration $\ddot{\lambda}$ due to the ellipticity of the earth at the equator is

$$\ddot{\lambda} = -0.00168 \sin 2(\lambda - \lambda_s) \text{ deg/day}^2 \quad (5-1)$$

where

$\ddot{\lambda}$ = longitudinal drift acceleration, deg/day^2

λ = satellite longitude, degree

$\lambda_s =$ stable longitude, 75° and 255°E

and the time interval T between successive maneuvers can be calculated as follows

$$T = 4 \left(\frac{\Delta \lambda}{|\dot{\lambda}|} \right)^{1/2} \quad (5-2)$$

where

$\Delta \lambda =$ allowable longitude deviation of the satellite

The velocity increment per year ($\Delta V|_{\text{year}}$) required to change the drift rate [Ref 3: p. 90] is

$$\Delta V|_{\text{year}} = 1.74 \sin 2(\lambda - \lambda_s) \text{ ms}^{-1}/\text{yr} \quad (5-3)$$

C. STATION REPOSITIONING

When a geosynchronous communications satellite is required to move from one longitude to another longitude to replace another satellite or pure change of station, two maneuvers are performed. The first maneuver involves the change in orbit velocity to reach the new location at geosynchronous radius. When in the vicinity of the new location with the required radius the second maneuver is performed to circularize the orbit. Longitudinal repositioning must usually be accomplished in a relatively short maneuver time (days to weeks), which requires high thrust over a short period of time. As shown in Appendix E, even if there is a dedicated set of thrusters, the size of that used for NSSK, it will still

take more than 10 hours of thruster firing per day for 30 days to do the 180° longitudinal repositioning. Therefore, this particular maneuver is not ideal using ion propulsion.

D. NSSK STRATEGY

Assuming an average inclination drift rate of 0.8455°/yr, as shown in Appendix G, the inclination incurred during eclipse period is given [Ref 3: p. 87] by

$$i = \frac{45 \times \frac{di}{dt}}{2 \times 365.25} \quad (5-4)$$

$$i = \frac{45 \times 0.8455}{2 \times 365.25}$$
$$i = 0.052^\circ$$

Since the thrusters are only fired during the non-eclipse periods, one half of the total drift is arrested during the first period and the other half of the drift during the second period, as shown in Figure 32. During the 137.5 days the thrusters are firing, not only do they nullify the drift incurred during those days (total of 0.318°) but also the drift (total of 0.104°) incurred while they are not firing during the eclipse period. The strategy consists of placing the inclination at the bottom of the station keeping window (in this case 0.052°), letting it drift freely and at the end of the eclipse period starting again the corrections that will bring the secular component of inclination near the top of the window at the beginning of the next eclipse period, as shown in Figure 32. As can be seen, the

drift does not start at $i = 0^\circ$, but due to over correction strategy, the satellite is placed on an inclination of 0.052° at the beginning of the eclipse period and let it drift a total of 0.104° (from an inclination of $+0.052^\circ$ to -0.052°) within a period of 45 days.

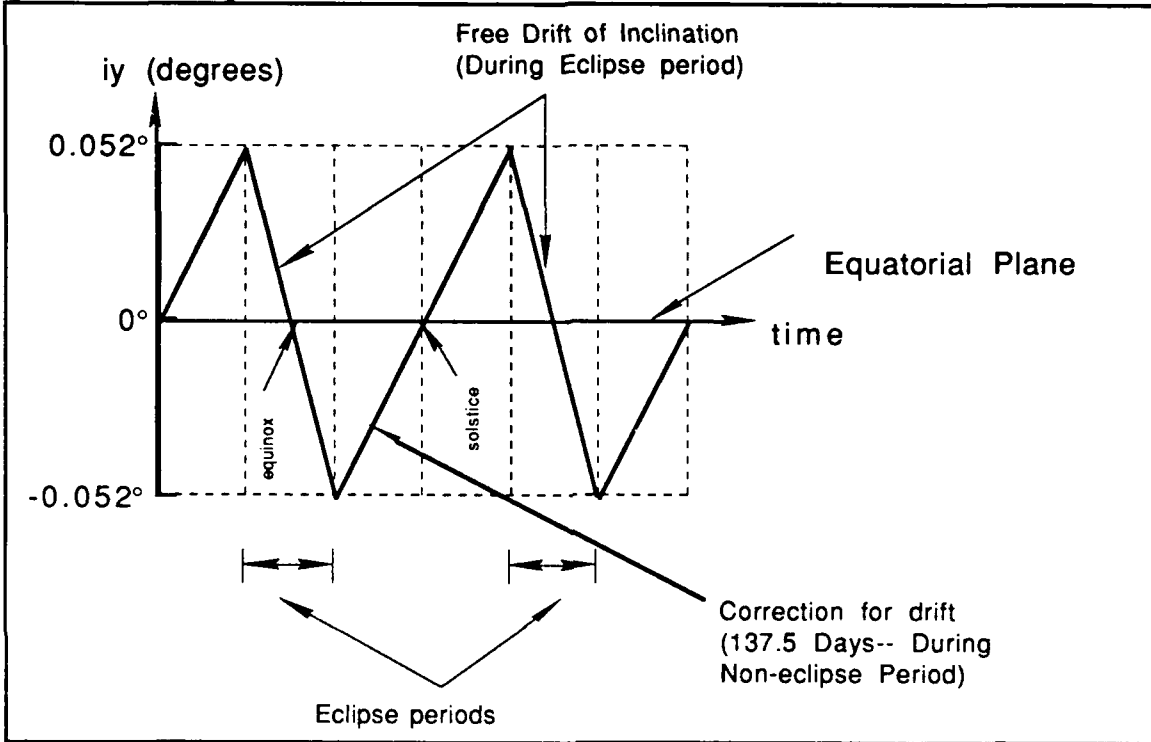


Figure 32. NSSK Strategy

VI. SOLAR ARRAY/BATTERY TRADE-OFF AS POWER SOURCE FOR ION THRUSTER

Geosynchronous satellites receive majority of their electrical power from the solar array. The only time the solar array cannot provide power to the satellite is during eclipse period by the earth. The battery is used as backup during eclipse periods and is charged when the satellite is out of the earth's shadow. Since the battery is required to provide power during eclipse period, it must have all the energy (plus reserve) required by the satellite for that period. For example, if a satellite requires 1 kilowatt (kW) of power during eclipse period, the battery must have at least 1.3 kW-hr ($1 \times 72/60 \times 0.65$) of energy capacity if the satellite has to function the whole time during eclipse period using 65% depth of discharge (DOD) for the battery.

In 1973, Free and Dunlop [Ref. 31: p. 212] proposed that ion thrusters on communications spacecraft should be operated on batteries. With the advances in Nickel-Hydrogen (Ni-H₂) battery technology, many communications satellites are presently equipped with sizable batteries in the kilowatt-hour (kW-hr) range, which makes them very attractive for providing power to the ion thrusters during eclipse period. This occurs twice a year, one in spring and another in autumn. As shown in Figure 33, each eclipse lasts about 45 days with a maximum shadow time of 72 minutes. [Ref. 32: p. 104]

Many benefits are derived from using the batteries as the sole provider of power to the IPS. There is the obvious benefit that ion propulsion power demands are satisfied with essentially zero mass and cost. Furthermore, since the stored electrical energy can be released more rapidly than it is

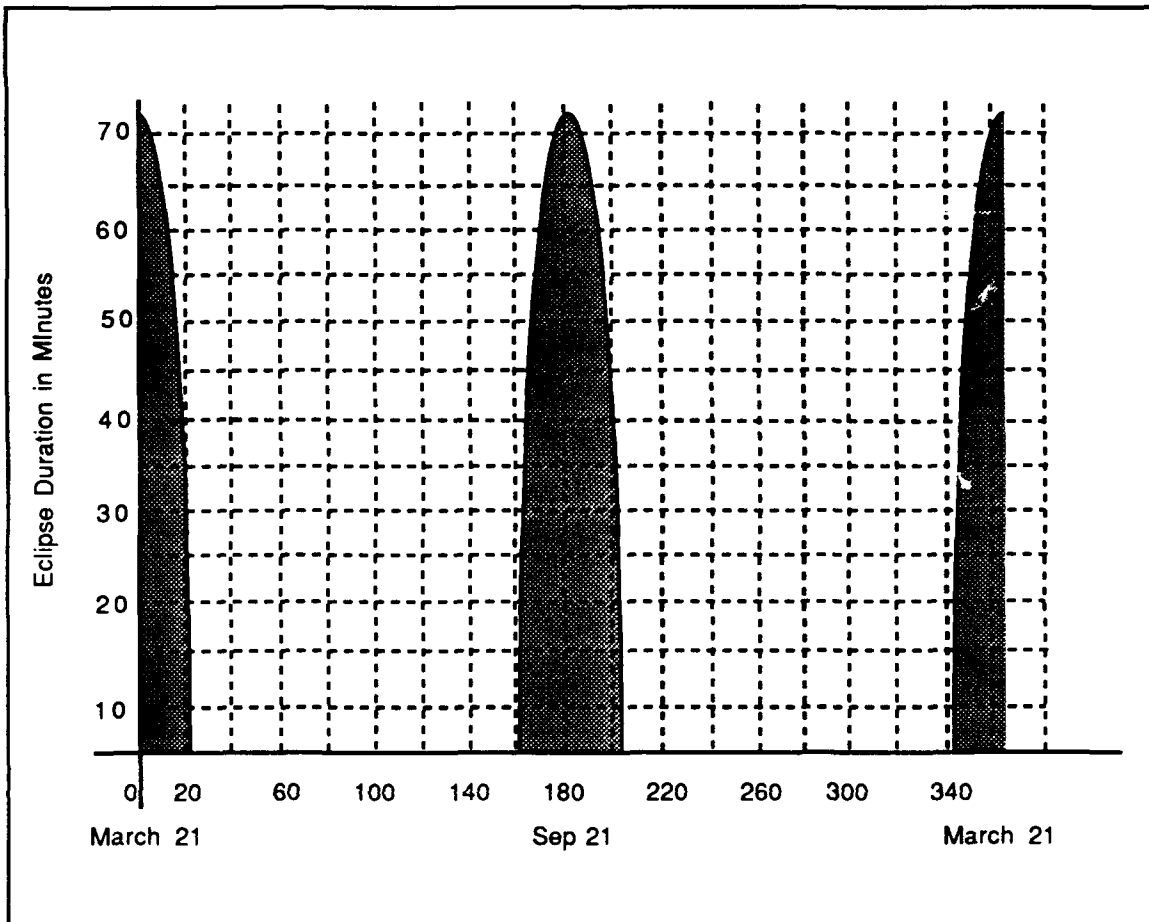


Figure 33. Eclipse Season in Geosynchronous Orbit [Ref. 32]

accumulated, larger thrusters can be employed than would be possible if the power were taken directly from the limited output of the spacecraft solar array. [Ref. 33: p. 165]

A. SOLAR ARRAY

Except during solar eclipse, the solar panels provide all the necessary electrical power for communications payloads and spacecraft housekeeping. The solar panels, made of silicon cells, convert solar energy into electric power.

Long mission years on a geosynchronous orbit degrade the performance of the solar panels due to solar radiation and plume impingement from the exhaust of the thrusters. The design output power of the solar array is based on the end of life (EOL) power requirement of the satellite due to degradation problems, therefore, excess power is available at BOL.

1. Solar Array Description

The solar array has two wings with three panels per wing, as shown in the deployed configuration in Figure 2 and stowed configuration breakdown in Figure 1. The effective area of the entire array (2 wings) is approximately 29 m². The solar array with the single bus regulated voltage is capable of providing 2350 watts at summer solstice EOL and 2500 watts at autumnal equinox EOL, as shown in Figure 34 (data extrapolated from Figure 9 of Ref. 14). Assuming the satellite has a constant power requirement of 2200 watts throughout its lifetime, it will have 150 and 300 watts margin during summer solstice and autumnal equinox respectively at EOL.

2. Solar Array as Power Source for IPS

It is obvious that the power margin at EOL is not even close to the 854 watts requirement of the IPS. However, going back to Figure 34, the excess power produced by the solar array during the early years is large enough to augment the battery in providing power to the IPS. This option will further decrease the battery DOD (the lower this number the better). The available power tapers down to the EOL values after twenty years and this means that a power management unit (PMU) will be required if the power sharing option is selected to operate the IPS.

Another option is to increase the size of the solar array to provide power to the IPS during the entire mission and use the battery as backup. If this

array. Typical power density is 20 W/kg [Ref. 3: p. 176]. Therefore, an additional 42.5 kg will be required for the solar the array mass to provide the entire power needed by the ion thrusters.

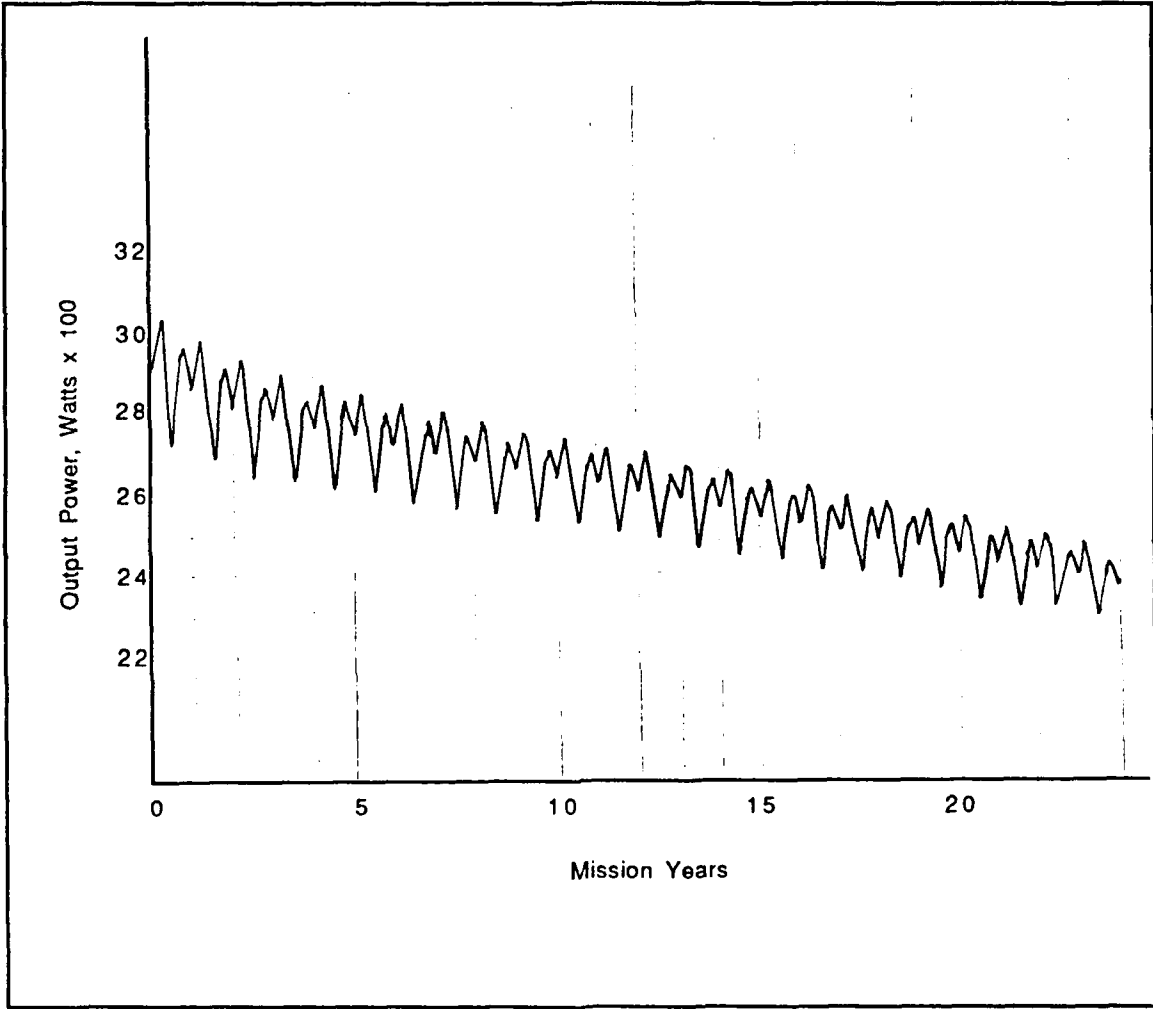


Figure 34. Projected Output of Solar Array

B. BATTERY

The battery selected for the satellite is Ni-H₂ type. This has been promoted as the most advanced, long life, rechargeable battery technology over the last 50 years. Unlike the solar panels, the battery is an energy storage unit. The

reliability of the Ni-H₂ battery depends on the number of charge/discharge cycles over a period of time, the average DOD, and the operating temperature. Normally, geosynchronous satellites use batteries only during the two eclipse periods to handle all electrical power requirements of the spacecraft. With the introduction of IPS as the primary NSSK propulsion subsystem for satellites, the charge/discharge cycles will quadruple, assuming the thrusters are fired once a day except during eclipse periods.

1. Battery Description

The Ni-H₂ battery is divided into four packs of 6 cells and are located as shown in Figure 1. It has a capacity of 123 ampere hours. The average eclipse voltage per cell is 1.24 volts. The allowable DOD is 70%. Theoretically, the battery can store 3.66 kW-hr ($123 \times 24 \times 1.24/1000$) of energy; however, because of the allowable DOD restriction, only 2.56 kW-hr (0.7×3.66) of the available stored energy can be used. Assuming one of the 24 battery cells fails and the satellite power requirement during eclipse is 2 kW, with the allowable DOD of 70%, the battery can provide 2.46 kW-hr ($0.70 \times 123 \times 23 \times 1.24/1000$). Since the maximum eclipse lasts about 72 minutes (1.2 hours), the spacecraft will need 2.4 kW-hr (2×1.2) from the battery. The allowance for this particular scenario is 60 watts (2460 - 2400).

2. Battery as Power Source for IPS

If the battery is the main source of power for IPS, the thrusters must only be used during the non-eclipse periods, when the solar panels provide the electrical power to the rest of the spacecraft. The two thrusters require 854 watts [Ref. 21: p. 8] when they operate. As shown in Appendix A, the total firing time per maneuver is 2.1 hr (for 20 year mission) plus 3.6 minutes for start-up. The energy required is about 1.824 kW-hr ($2.16 \times 854/1000$), and

Figure 35 shows that the battery can easily support the required 7300 (20 x 365) cycles for a 20 year mission, assuming an average of 56% DOD (i.e., 50% DOD for thruster firing during non-eclipse periods and 70% DOD for communications payload during eclipse period). This is a conservative figure since the satellite does not spend 1.2 hours everyday in the earth's shadow during the eclipse period.

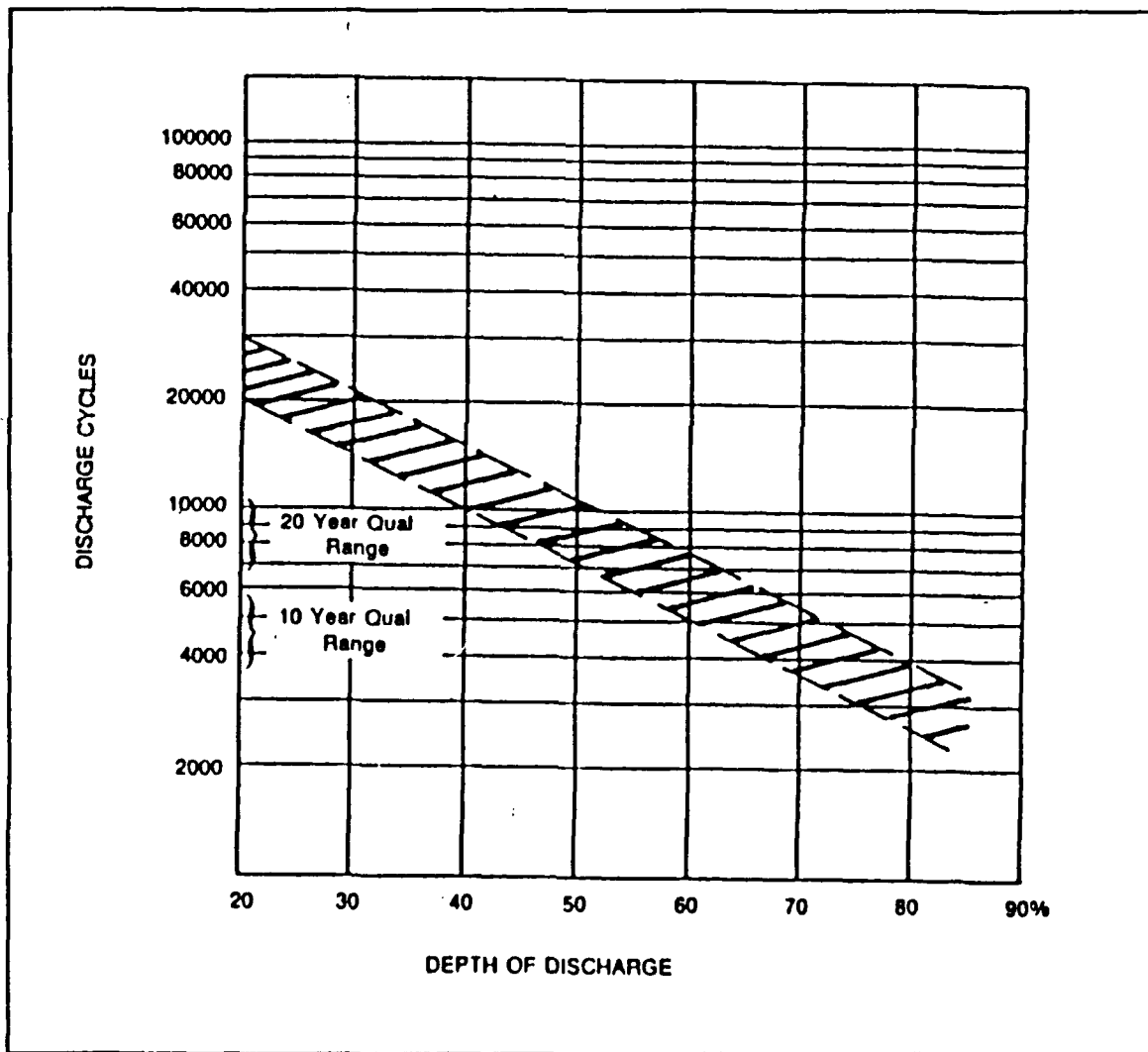


Figure 35. Battery Cycle Capability [Ref. 14]

VII. BIPROPELLANT AND ION PROPULSION TRADE-OFF

This chapter will examine the trade-off between BPS and IPS as implemented for NSSK on a spacecraft with 1200 kg dry mass. The thrust is most effective in removing orbit inclination at the orbit nodes, as shown in Figure 21. Between the nodes and antinodes, the effective thrust is equal to the normal component of the thrust, T_N , multiplied by the cosine of the angle (β) between the line of nodes and the satellite position vector. The mean effective thrust T_e is given by the equation [Ref. 23: p.131 and Ref. 3: p. 175]

$$T_e = \frac{T_N \int_0^\beta \cos\beta \, d\beta}{\int_0^\beta d\beta} = T_N \frac{\sin \beta}{\beta} \quad (5-1)$$

Assuming the thrusters are ON every day for two periods centered around nodes, except during eclipse periods, the thrusters for the descending and ascending nodes will be different because of opposite thrust directions. It is assumed that the lifetime of the current ion thrusters is 12,000 hours. The number of days allowed for a thruster to be ON, excluding eclipse periods, is 275 days/year. Therefore, the maximum period for each thruster ON, T_{ON} , is

$$T_{ON} = \frac{(12,000)}{20 \times 275} = 2.18 \text{ hr per day for 20 yr}$$

Assume that each thruster is on for 2 hours per day or 30° ($360^\circ \times 2/24 = 30^\circ$) and that the cant angle (α) is 30 degrees. The efficiency (τ_i) for the ion thruster becomes

$$\eta = \cos \alpha \frac{\sin \beta}{\beta} \quad (5-2)$$

$$\eta = \cos 30^\circ \frac{\sin 15^\circ}{\pi/12} = 0.856 \quad \text{if ON for 2 hours}$$

$$\eta = \cos 30^\circ \frac{\sin 22.5^\circ}{\pi/8} = 0.844 \quad \text{if ON for 3 hours}$$

$$\eta = \cos 30^\circ \frac{\sin 11.25^\circ}{\pi/16} = 0.8604 \quad \text{if ON for 1.5 hrs}$$

By using equation

$$M_p = m_i (1 - e^{-\left(\frac{\Delta V}{\eta l g}\right)}) \quad (5-3)$$

$$= m_f (e^{\left(\frac{\Delta V}{\eta l g}\right)} - 1) \quad (5-4)$$

As a preliminary analysis assume:

$\Delta V \approx 45 \text{ m/s}$ per year for NSSK

$I = 2850$ sec and 285 sec, specific impulse of Ion Propulsion and bipropellant respectively

where

M_p = mass of propellant, kg

m_i = initial mass of the spacecraft, kg

m_f = final mass of the vehicle after burnout, kg

ΔV = required velocity change, m/s

I = specific impulse of the propellant, s

g = gravitational acceleration, (9.806 m/s^2)

η = engine efficiency, (use eq. (A-3) for ion thrusters)

α = the thruster cant angle

β = the angle between the line of nodes and satellite position, as shown in

Figure 21

for 20 year NSSK

$$M_p = 1200(1 - e^{-(920/0.844 \times 2850 \times 9.806)})$$

$$= 47.7 \text{ kg for } \eta = 0.844$$

$$= 47 \text{ kg for } \eta = 0.856$$

$$= 46.82 \text{ kg for } \eta = 0.86$$

$$473 \text{ kg for bipropellant}$$

For the IPS, the average ΔV removed by each thruster during one maneuver is

for twenty year NSSK

$$\Delta V = 920/20 \times 275 \times 2 \times 0.844 = 0.09909 \text{ m/s (if ON for 3 hrs)}$$

$$= 0.097706 \text{ m/s (if ON for 2 hrs)}$$

$$= 0.09725 \text{ m/s (if ON for 1.5 hrs)}$$

for 15 year NSSK

$$\begin{aligned} &= 0.09909 \text{ m/s (if ON for 3 hrs)} \\ &= 0.097706 \text{ m/s (if ON for 2 hrs)} \\ &= 0.09725 \text{ m/s (if ON for 1.5 hrs)} \end{aligned}$$

for 10 year NSSK

$$\begin{aligned} &= 0.09909 \text{ m/s (if ON for 3 hrs)} \\ &= 0.097706 \text{ m/s (if ON for 2 hrs)} \\ &= 0.09725 \text{ m/s (if ON for 1.5 hrs)} \end{aligned}$$

The thrust required for the thruster, T_e , is

$$T_e = \frac{\text{BOL}_{\text{mass}} \times \Delta V_{\text{removed per day}}}{\text{Time thruster firing}} \quad (5-4)$$

$$\begin{aligned} \frac{1247 \times 0.09909}{3 \times 60 \times 60} &= 0.0115 \text{ N (ON for 3 hrs)} \\ &= 0.0169 \text{ N (ON for 2 hrs)} \\ &= 0.0225 \text{ N (ON for 1.5 hrs)} \end{aligned}$$

The total operating hours for each thruster are:

25 Years:

$$1.5 \times 275 \times 25 = 10,313 \text{ hrs (1.5 hours firing time)}$$

$$2 \times 275 \times 25 = 13,750 \text{ hrs (2 hours firing time,}$$

borderline)

$$3 \times 275 \times 25 = 20,625 \text{ hrs (3 hours firing time, Too$$

high, unacceptable)

20 Years:

$$1.5 \times 275 \times 20 = 8250 \text{ hours}$$

$$2 \times 275 \times 20 = 11,000 \text{ hrs}$$

$$3 \times 275 \times 20 = 16,500 \text{ hrs (Too high, unacceptable)}$$

15 Years:

$$1.5 \times 275 \times 15 = 6187.5 \text{ hrs}$$

$$2 \times 275 \times 15 = 8250 \text{ hrs}$$

$$3 \times 275 \times 15 = 12,375 \text{ hrs (Marginal)}$$

10 Years:

$$1.5 \times 275 \times 10 = 4125 \text{ hrs}$$

$$2 \times 275 \times 10 = 5500 \text{ hrs}$$

$$3 \times 275 \times 10 = 8250 \text{ hrs}$$

Assume a power/thrust ratio of 25 W/mN, as shown in Figure 35, the power required for these thrusters are: 563 W (22.5 mN), 425 W (16.9 mN) and 288 W (11.5 mN). Since there are two nodes to perform this maneuver, the thrust levels have to be doubled to complete the maneuver. Since the power/thrust ratio used is the same for all three thrusters, the required power from the battery will be approximately the same (≈ 1.7 kW-hr). As can be seen from Table 4, this is not always the case because different thrusters have different values for the same parameter. This is an important factor when considering which thruster is best suitable for the job.

All the computed values presented in this chapter are simple approximations and serve as guide only. The actual values, as calculated in Appendices A, B, and C, are summarized in Table 8 and Table 9 for HRL-13, Table 12 for UK-10, and Table 13 for MELCO.

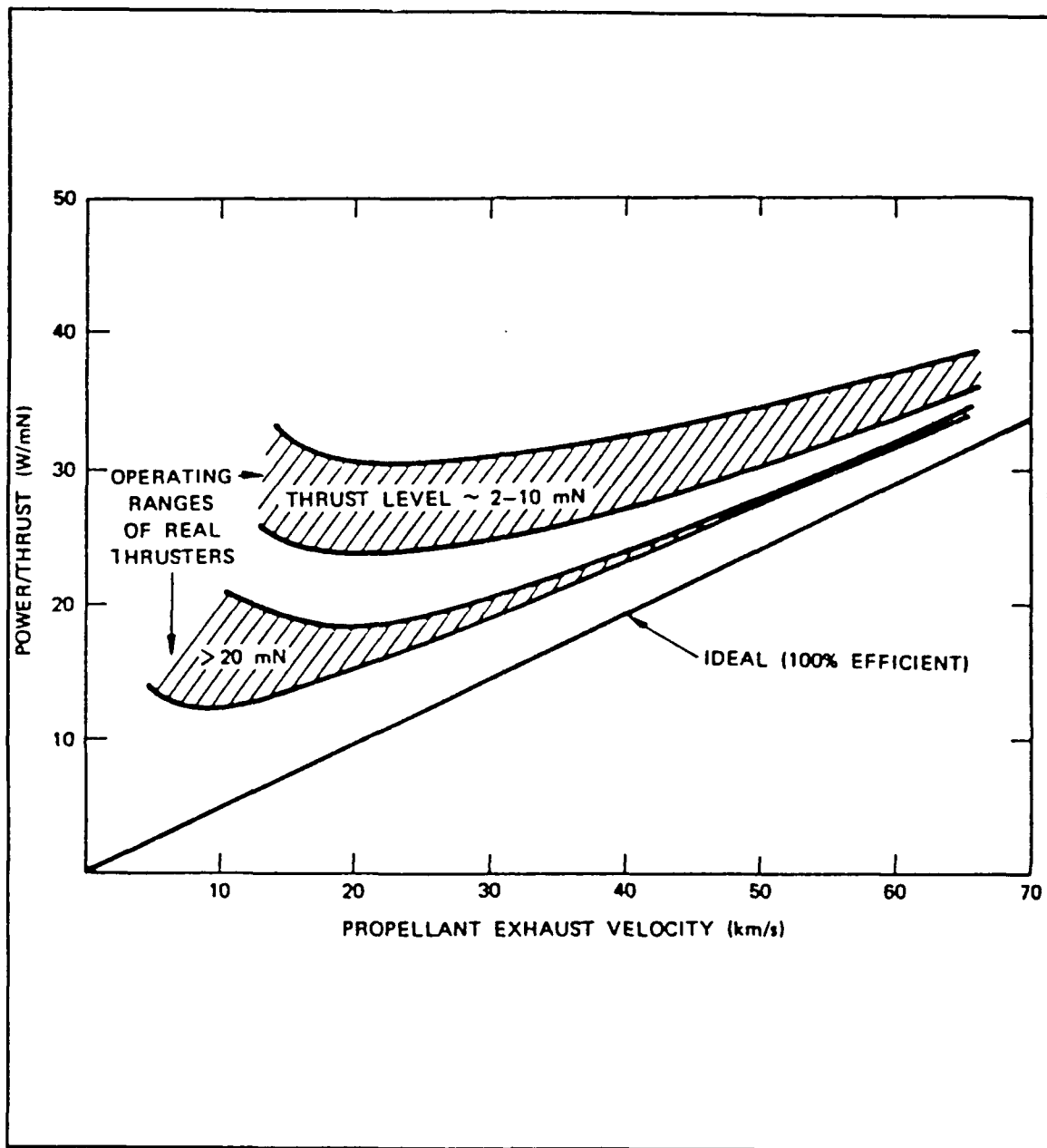


Figure 36. Power/Thrust Ratios for Ion Thrusters [Ref. 24]

**TABLE 12. SUMMARY OF CALCULATIONS OF APPENDIX B
AND APPENDIX H COMPARING ION AND BIROPELLANT
PROPULSION SYSTEMS MASS FOR NSSK USING UK-10
THRUSTER**

Maneuver Life (Years)	10	15	20
Spacecraft BOL Mass=kg (with Bipropellant Subsystem NSSK)	1471.42	1644.04	1831.93
Bipropellant Mass for NSSK, kg	211.44	356.38	514.47
BOL Mass =kg (with Ion Propulsion for NSSK)	1359.18	1377.23	1395
Xenon Mass, kg	19.68	31.27	42.62
ion Subsystem Dry Mass , kg	113.35	115.32	117.25
Thruster Firing Time/Day (Hrs)	1.43	1.52	1.56
Total Hrs in Operation (Ion)	3933	6270	8580
Energy Required (Watt-Hr)	2171	2307	2368
GTO Mass=kg, Ariane IV Launch (Bipropellant NSSK)	2461.18	2787.2	3136.92
GTO Mass=kg, Ariane IV Launch (Ion NSSK)	2777.23	2303.63	2333.35
GTO Mass Saving (Biprop - Ion) Ariane IV	183.95	483.57	803.57
GTO Mass=kg, ETR Launch (Bipropellant NSSK)	2835.36	3220.26	3642.08
GTO Mass=kg, ETR Launch (Ion NSSK)	2602.82	2641.93	2680.46
GTO Mass Saving =kg, (Bipropellant -Ion) ETR	232.51	578.33	961.62

**TABLE 13. SUMMARY OF CALCULATIONS OF APPENDIX C
AND APPENDIX H COMPARING ION AND BIROPELLANT
PROPULSION SYSTEMS MASS FOR NSSK USING MELCO
THRUSTER**

Maneuver Life (Years)	10	15	20
Spacecraft BOL Mass=kg (with Bipropellant Subsystem NSSK)	1471.42	1644.04	1831.93
Bipropellant Mass for NSSK, kg	211.44	356.38	514.47
BOL Mass =kg (with Ion Propulsion for NSSK)	1345.62	1365.9	1386.8
Xenon Mass, kg	23.1	37.18	50.67
Ion Subsystem Dry Mass , kg	96.33	98.72	101
Thruster Firing Time/Day (Hrs)	1.51	1.62	1.65
Total Hrs in Operation (Ion)	4153	6683	9075
Energy Required (Watt-Hr)	2250	2414	2459
GTO Mass=kg, Ariane IV Launch (Bipropellant NSSK)	2461.18	2787.2	3136.92
GTO Mass=kg, Ariane IV Launch (Ion NSSK)	2250.76	2284.7	2319.63
GT) Mass Saving (Biprop-Ion) Ariane IV	210.42	502.5	817.29
GTO Mass=kg, ETR Launch (Bipropellant NSSK)	2746.98	3220.26	3642.08
GTO Mass=kg, ETR Launch (Ion NSSK)	2573.43	2617.38	2662.69
GTO Mass Saving =kg, (Bipropellant -Ion) ETR	173.55	602.88	976.39

VIII. IMPLEMENTATION IMPACT ON PRESENT SUBSYSTEMS

Subsystem design strategy is delineated as a balance (or compromise) among thrust level, maneuver frequency/time, specific impulse, available/added power, number and redundancy of thrusters, and other technical and operational factors [Ref. 30: p.1].

A. PROPULSION

The addition of IPS to the UHF Follow-On class satellite will not have an impact on the bipropellant propulsion subsystem operation. Since the north panel will not have any bipropellant thrusters, plume contamination on the ion thrusters will be non-existent. Removal and installation of the IPS will be easy, and no extensive piping or rewiring is required.

B. ELECTRIC POWER

If the battery is selected to provide power to the IPS, charge/discharge cycles increase four times (from 90 to 365 times a year). Present capability of the Ni-H₂ battery indicates that these additional cycles can be handled since the average DOD of the battery stays at 50% during non-eclipse and 70% during eclipse periods. To further reduce the average DOD it may be necessary to add another pack of cells to supplement the four that are already in the spacecraft.

As discussed in Chapter VI, if the solar array is to provide power to the IPS, present solar array configuration is not capable of providing full power to the ion thrusters. Therefore, additional panels will be required to provide the necessary power to the IPS. This choice will have more impact on other subsystems than adding a pack of cells to the battery because of the solar array's size. If 29 m² of solar array can provide 2400 watts power at EOL, this means

that approximately 10 m² more is required to supplement the present configuration.

C. THERMAL CONTROL

The power processing unit (PPU) and the ion thrusters dissipate about 10-15% of the total power of the IPS [Ref. 34: p. 210]. Temperature control of the xenon thrusters on orbit is by radiative heat transfer to space via the grids. Depending on the bulk of the temperature of the xenon thruster when operating, a small radiation shield and local fixed solar panel blanket can be implemented to minimize the thermal interaction with adjacent equipment. PPU's are located on the south side panel with a full view of space; therefore, thermal dissipation is also via radiative heat transfer to space. Thermostatically controlled heaters for the PPU's and thrusters will be incorporated to keep the units within the design operating temperature range (-20°C to 75°C).

To maintain the xenon propellant tanks within the predicted temperature range of 18° to 42° C, one heater per tank is required during on-orbit operation.

Although the PPU's and the ion thrusters have both approximately 100 watts of power to dissipate when they operate, they introduce minimal heat interactions with other subsystems because their locations allow them to radiate most of the heat directly into space. The radiators, also located on the north and south panels, need to be resized because of the sections removed from them to accommodate the PPU's and the thrusters, as shown in Figure 1. As mentioned above, most of the heat generated by the PPU's and the ion thrusters is dissipated directly into space, but because of their co-location with the radiators, conductive heat transfer is also possible between the IPS (ion thrusters and PPU's) and the radiators. For this reason, the thrusters and the PPU's are protected from the

radiators by multilayer insulation (MLI) blanket. In addition, the radiators will need more area to dissipate the absorbed heat generated by the IPS.

D. STRUCTURES

For this study, it was assumed that the present structure subsystem is only capable of supporting the dry mass of the spacecraft and the bipropellant for the AKM. To support the additional propellant mass for station keeping, both for bipropellant and ion propulsion subsystems, the structures will require an additional mass. It was also assumed that the allowance for structural mass will be approximately 10% of any additional mass to the baseline dry mass of 1200 kg. Although determination of the exact structural support will necessitate a much more detailed study than the present one, this estimate is generally thought to hold true for spacecraft of this type.[Ref. 3: p. 48]

As shown in Figure 1, the IPS mass is distributed around the Z-axis of the spacecraft to give the least amount of disturbance to the center of mass of the spacecraft. As shown in Table 6, the thrusters with their gimbals have almost the same mass as the PPU's. Placing the thrusters with their gimbals opposite the PPU's, as shown in Figure 1, solves the problem of concentrating the IPS mass on one side of the spacecraft (i.e., disturbing the baseline center of mass). Not only the locations for the thrusters and PPU's solve the center of mass problem, but also are considered favorable for dissipating heat and providing easy access for removal and replacement of the parts. Regarding the xenon tanks, movement of the center of mass due to depletion of the xenon tanks should be negligible because their location is in the vicinity of the center of mass of the spacecraft.

E. TELEMETRY, TRACKING AND CONTROL (TT&C)

IPS performance can be monitored on the ground with the aid of the TT&C signals. Some of the important performances associated with the successful

operation of the ion thrusters are: 1) automatic operation of the ion thrusters 2) state of charge/discharge of the battery to achieve the predicted lifetime, 3) downlink/uplink information on the gimbals to avoid unnecessary corrections for attitude disturbance, and 4) shorts and arcing produced by the thruster grids or PPU's. As can be seen above, TT&C plays an important role in the successful operation of the ion thrusters.

F. ATTITUDE CONTROL

Thrust vector misalignment, thrust imbalance, and movement of the satellite's center of mass introduce disturbance forces that must be nullified by the attitude control. Although the thrusters are initially aligned, the thrust vectors could change dramatically due to launch vibration, thermal distortion (most notably that of the grid system), or accelerator grid wear [Ref. 35: p. 216]. Thrust vector misalignment can be solved by mounting the ion thrusters on gimballed platform, as shown in Figure 31.

Due to redundancy consideration, four pairing combinations are possible but not without penalty to the attitude control subsystem. Out of these four combinations, only two sets can be operated as matched set. When these two sets are not used, thrust imbalance occurs between the two firing thrusters. This can be corrected by the gimbals system and/or thrust adjustment of the thruster.

Movement of the center of mass from BOL to EOL is minimal because the bipropellant tanks will almost be empty at BOL (no bipropellant for NSSK required). The remaining bipropellant will be used for EWSK and, worst case, for repositioning. The total subsystem mass of the remaining propellant for EWSK and repositioning, as shown in Appendix A, is approximately 30 kg. In the case of IPS, the total mass, including the propellant, is only 139 kg for a 20

year mission. The total xenon propellant available at BOL is 54 kg. Therefore, the contribution of IPS to the shift of center of mass is also negligible.

IX. ENVIRONMENTAL IMPACT

Ion propulsion can offer significant advantages over chemical propulsion due to its high specific impulse on the order of a magnitude. However, the plasma environment produced by electric propulsion devices can significantly affect sensitive spacecraft surfaces, such as sensors, solar cells, and thermal control devices. Therefore, consideration of impact to other subsystems is necessary when designing the installation of IPS to the spacecraft.

A. PARTICULATE CONTAMINATION

Contamination caused by the ion propulsion system is one of the significant parameters for the satellite system design, especially for the power system and thermal control. Degradation of the solar array due to plume impingement cannot be ignored especially if the satellite has to remain in service for a long period of time. The same is true for the effectiveness of the exterior MLI to protect the interior equipment from solar radiation.

1. Contamination Process

Sputter erosion of discharge-chamber surfaces has been identified as an important life-limiting process in electron bombardment ion thrusters [Ref. 36: p. 375] and any mass expelled from a spacecraft is liable to be deposited on surfaces if surface conditions (chemical potential, temperature and electrical fields) allow it. When the system cannot tolerate the deposition or resulting symptoms, there is a contamination problem. The most obvious and easily avoided contamination is the direct impingement of north-south pointing ion beam on north-south oriented solar panels where high energy Xe^+ would directly erode panel material. However, three grid thrusters that have tightly collimated beams with 100% of measured plasma within half angles of about 21°

can be canted at reasonable angles providing a good margin for avoiding impingement. [Ref. 14: p. 14]

Ions produced in the discharge chamber are accelerated and expelled by the static electrical field formed by the grid-system. In the discharge chamber, the portion of the cathode potential, such as the baffle and screen grid, is sputtered by ions of relatively low energy ($\sim 35\text{eV}$). On the other hand, the accelerator grid of negative potential in the grid system is sputtered by the charge exchange ions which is of relatively high energy ($\sim 500\text{ eV}$). [Ref. 37: p. 1]

The complexity of the thruster induced environment becomes apparent when it is considered that 1) neutral atoms, 2) primary charged beam ions, 3) multiple charged ions, 4) charge exchanged ions, and 5) sputtered thruster components metal atoms are all present in an operating thruster. Upon reaching a surface these components may 1) coat it, 2) erode it, 3) participate in bulk chemical reactions, and/or 4) diffuse into the solid surface to change its metallurgy [Ref. 38: p.368]. In the case of the Space Electric Rocket Test (SERT)-II mission, although the powered solar array test panel was in clear view of its mercury ion thrusters, no adverse effects were observed.

Contamination due to particles is caused by bombardment of the grid by low energy xenon ions that are created immediately downstream of the thruster as a result of collisions between neutral xenon propellant and ions in the beam. The ions produced by the collision are attracted to the negatively charged accelerator grid, and on impact dislodge atoms from the grid (made of molybdenum). The molybdenum atoms then tend to become permanently deposited in the vicinity of the thruster. [Ref. 39: p. 552]

The use of xenon allows rapid ON/OFF cycling with a single command, bringing the thruster to full operation in three minutes. Development and qualification testing, while requiring cryopumping capability, has considerably fewer problems than those caused by mercury [Ref. 20: p. 6]. Since inert gases do not condense on material surfaces, problems of discharge-chamber flooding and requirements for extended extraction-grid bakeout (which can occur with mercury ion thrusters) are avoided with xenon. This immunity is expected to result in considerable simplification in the control algorithm (and associated hardware) required for autonomous thruster operation. The noncondensable quality of inert gases offers systematic advantages for spaceflight in the capability for essentially instantaneous startup and shutdown, and by essentially eliminating concern over spacecraft contamination. [Ref. 33: p. 165]

The rate and total amount of material generated is time dependent and a strong function of thruster design and operating conditions (ionization voltage, ionization efficiency and thrust density) and of thruster materials (sputter energy threshold). Thus, quantifying the contamination potential of any ion thruster would need to rely on data from qualification/life test program and would depend on the specific thruster/spacecraft installation and layout including shields. Erosion is monitored by measuring the weight of the grid before and after or at any point during the test period. [Ref. 14: p 14]

a. Production of Positive Ions

Whatever the ionization mechanism, a certain average amount of energy must be expended to create each ion at the source. This is by no means simply the ionization potential of the atom, but includes all thermal and radiative losses associated with maintaining the environment in which the ions are created. The source must be highly selective in restricting its emission to ions rather than

neutral particles. Small fractions of the latter, unaffected by the accelerating field, migrate relatively slowly through the gap and tend to disturb the ion trajectories. Specifically, ions from the source may suffer charge-exchange collisions with these ambient neutrals, thereby producing ions which are "out of focus" in the accelerating system and fast neutrals which are uncontrolled by the fields. These ions may then strike the accelerating electrode, causing sputtering erosion and contamination of its surface. Even at the modest prevailing temperatures, an alkali-contaminated accelerator surface may emit electrons, which then return to the ion source, causing a current drain on the power supply with no corresponding useful thrust. [Ref. 11: p. 4]

Doubly charged ions have been found to be undesirable in the discharge chambers of electron bombardment ion thrusters, primarily because they increase the rate of sputtering damage to discharge-chamber components. [Ref. 40: p. 264]

B. ELECTROMAGNETIC INTERFERENCE (EMI)

PPU start/stop and restart power switching transients caused by high voltage breakdown and grid shorts produce radiated and conducted EMI [Ref. 14: p. 12].

Tests have recently been conducted at Culham Laboratory on the UK-10 thruster operating with xenon, using laboratory power supplies. Noise measurements were made in the frequency range of up to 300 MHz and no significant signals were detected on any electrode under any condition. In this respect, the thruster performs better than with mercury. No signal greater than the noise of the measuring equipment, 2 mV, was found in the range 1-300MHz with operation at 10 mN. At lower frequencies, 16-20 and 904-907 kHz, values were generally in the range of 10-100 mV. Even at high thrust, noise signals in

the 1-300 MHz range were always below 30 mV. Nothing was found which could adversely affect thruster spacecraft integration.

SERT-II, ATS-6 and SCATHA, all experimental spacecraft using ion thrusters, did not not experience any anomalies on their telemetry, command or control [Ref. 13: p. 13].

C. ELECTROSTATIC CHARGING AND DISCHARGING (ESD)

Ion thrusters have a significant influence on the electrostatic charge levels of orbiting satellites. The effect is caused by the charge-exchange plasma that is generated in the main beam just downstream of the thruster. A small amount of xenon, about 10 to 20% depending on ionization efficiency, escapes the chamber without being ionized. Charge-exchange reactions between these atoms and the very energetic beam ions result in ions and atoms that possess only thermal (i.e. low) energy. These charge-exchange ions are strongly influenced by weak electric fields in the beam and leave the beam in a radial direction. The Xe^+ and their space charge neutralizing electrons (e^- at about 1 eV) constitute a charge-exchange plasma that can migrate about the spacecraft under the influence of differentially charged surface areas.

A simplified dielectric spacecraft model consists of a conductive inner structure (electrical ground with an attached ion thruster), surrounded by an outer dielectric cover much of which is thermal blanket [Ref. 14: p. 13]. As is well known, the ambient magnetosphere plasma at geosynchronous altitude contributes electrons that cause surface charge buildup throughout the spacecraft, resulting in sunlight voltage differentials of the order of 1kV, with the surface at -2kV and the structural ground at -1kV. These charge levels, which can be predicted using the NASA lumped element model Charging Analyzer Program (NASCAP), then increase upon entering an eclipse due to surface effects,

producing an increased voltage differential, possibly 2kV, with the surface at about -10kV. Thus, the eclipse is a worst case for electrostatic discharge events. [Ref. 41: p. 469 and Ref. 42: p. 532]

However, when the thruster and its neutralizer are activated, their operation quickly pulls the structural ground up to about zero volt, and at the same time the charge-exchange plasma fully forms, migrates and surrounds the spacecraft. This plasma, which is more dense than the ambient space plasma, contains highly mobile Xe^+ and e^- that are attracted to oppositely charged surfaces on the spacecraft, bringing them to near neutrality. Thus, ion thruster operation beneficially reduces and controls electrostatic charge buildup. [Ref. 14 :pp. 13-14]

Two other possible effects caused by the surrounding plasma are solar panel charge buildup and charge accumulation within electronic boxes. The first is a function of "exposed" panel area and potential and that for low voltage panels (<100V) the increase is minor and does not affect panel output. The second problem is solved by combining "electron (so called Faraday) shielding" requirements (i.e., hole or screen mesh openings less than the Debye length of several millimeters) with those for box venting to obtain an integrated design meeting both requirements. [Ref. 14: p. 14]

1. Neutralization of the Beam

To produce a useful level of thrust, an ion engine must emit many amperes of positive ion current, yet the total electrical capacitance of a typical ion-propelled spacecraft will probably not exceed 10^{-9} farad; hence, if no provision for neutralization of the beam were made, the spacecraft would acquire a negative potential at a rate 10^9 volts/(sec)(amp of ion current) [Ref. 11: p. 165]. This gross charging could be inhibited by the emission of an identical

electron current from any convenient location on the spacecraft. Somewhat more subtle, however, is the need for detailed neutralization of the ion beam itself before it gets very far from the exit electrode, lest the positive space-charge potentials within the beam cause it to stall or reflect upon itself.

2. The Acceleration and Deceleration Concept

The possibility of the injected electrons from the neutralizer migrating backward upstream past the accelerating electrode cannot be tolerated. Once beyond this electrode, the electrons would be vigorously accelerated toward the ion plane by the same electric field which drives the ions downstream. This electron flux would constitute a current drain on the power supply, with no corresponding thrust power. To preclude upstream migration of electrons into the acceleration gap, a region of increase potential aft of the accelerator seems to work. This would also provide a means of reducing ion exhaust speeds without a corresponding loss in space-charge current, and thereby preserving higher thrust densities at a lower specific impulse levels. [Ref. 11: p. 173]

3. Charge-Exchange Plasma Flow

When the xenon is ionized in a discharge chamber and accelerated through ion optics which produces the thrust, a small amount of approximately 10% Xe neutral escapes from the discharge chamber without being ionized [Ref. 43: p. 457 and Ref. 44: p. 571]. Charge exchange interactions between the primary ion beam and the neutral efflux downstream of the thruster optics form ions with only thermal energy. These ions, aside from sputtering the material from the accel grid, leave the beam radially with directed energy of from a few tenths to a few electron volts because of internal fields in the primary beam [Ref. 24: p. 151]. These ions with neutralizing electrons, constitute a charge-exchange plasma that can flow upstream around the spacecraft.

X. RISKS AND BENEFITS OF ION PROPULSION

A. REQUIREMENTS FOR GROUND TESTING

A major feature of the use of any IPS, due to low thrust, is that long operating times are necessary, with values of thousands of hours covering the requirements of most missions. In the case of this study, approximately 12,000 hours are required. Consequently, lengthy and time-consuming life-testing is mandatory for space qualification purposes, and ideally this should be carried out on a number of complete systems to gain statistically important information regarding operational reliability. Qualification tests, usually for 1.5 x mission life, are a major expense [Ref. 14: p. 6]. In the case of the Hughes thruster, with a daily firing of 2.16 hours and a total thruster firing time of 11,880 hours in a period of 20 years, the thruster would require a qualification test of 17,820 hours. Assuming an accelerated ON/OFF cycle of 2.4 hr ON/1 hr OFF (seven cycle/day) and a conservative 300 test days/year [Ref. 14: p. 6], the qualification program would require more than 42 months.

What is unique with the ion thruster is the long operating times needed, which therefore require extremely durable components and consequently, very long and expensive ground life-tests. Depending on how long the thruster has been in operation during the ground test period, the lifetime can be projected by extrapolating the results to reduce the extensive and expensive testing.

The cost of xenon used at Hughes Research Laboratories (HRL) is \$17 to \$20 per liter [Ref 45] while the propellant consumption of the thruster under test was 1 liter per hour. Assuming 17,820 hours are required for the ground test, the total cost of propellant alone will be around \$303,000 (using \$17/liter).

Another problem with ground testing is that it cannot completely duplicate the space environment, especially in terms of gravity and vacuum. As an example, during the SERT-II ion thruster ground testing [Ref. 35: p. 221] some fragments of the grids became detached due to sputtering and would tend to fall off rather than short the grids because the thruster was vertically oriented. That particular problem may be controlled by repositioning the neutralizer or by providing increased current capability to burn out shorts.

B. UNCERTAINTIES IN FLIGHT OPERATION

The lifetimes of previous thrusters flown showed some problems and did not match the performance showed during the ground test. In the case of the Applied Technology Satellite (ATS)-6 thrusters (using cesium as propellant), thousands of hours were demonstrated on the ground, but during flight test its propellant tank developed some thermal problems (propellant freezing) and stopped the space tests at only 92 hours [Ref 46: p. 654]. On the other hand, the better of the two SERT-II thrusters (using Hg as propellant) operated for 3879 hours when a short disabled it [Ref. 47: p. 245]. As mentioned previously, the outer space condition is hard to duplicate during ground testing.

It has been quite a long time since the last satellite flew with an ion thruster: SCATHA (U.S.) was launched in Jan 79; SERT-II (U.S.) operated until 1981; and ETS -3 (Japan) was launched in September 82 [Ref 35]. The next satellite, the Japanese ETS-6, is not schedule to be launched until 1992. In Europe, a combined effort is being organized to launch SAT-2 that will use two kinds of thrusters, the UK's UK-10 (Kaufman type) and West Germany's RIT-10 (RF type). Different satellite companies have already undertaken studies for a possible inclusion of IPS into their propulsion subsystem. The final decision will

not probably be made by the unconvinced decision-makers until the outcome of the flight performance of ETS-6 and SAT-2 is known.

C. COST AND BENEFITS

The cost of IPS integration will be high if this will be done on: 1) only one satellite, instead of a class of satellites wherein the cost for qualification of hardwares and ground testing can be equally distributed, and 2) on a satellite that has been designed without room for growth (i.e., relocating a lot of parts just to accommodate another).

The net monetary benefit that is accrued from replacing chemical with ion propulsion for NSSK arises from the 1 to 10 increase in specific impulse that significantly reduces on-orbit propulsion mass. Bipropellant mass for NSSK constitutes very close to 28 % of the BOL mass of the spacecraft with 20 mission years. For mission of this length, more than 500 kg of bipropellant is required for NSSK. In the case of BPS, the additional dry mass for structural support and tankage is almost as close as that of the XIPS dry mass of about 85 kg, as shown Table 8. Replacing BPS with IPS produces a net BOL mass saving of 458 kg. The net mass benefit from the satellite can be considered in a form of currency that can be utilized in several ways. Some possibilities include: reduction in the launch satellite cost, increased communications payload, and extension of satellite life; singly or in combination [Ref. 30: p. 8]. Assigning a monetary value to these options is highly arbitrary and subjective. As a "wholesale" value of the net mass benefit, the incremental value of inserting mass into geosynchronous orbit is assumed to be on the order of \$30,000 /kg [Ref. 48: p. 2]. This means a saving of about \$25M (\$30K x 838) for an Ariane launch with a satellite of 20 year mission. See Figure 37 for mass savings using Ariane IV, and Figure 38 for mass savings when launching at ETR in Florida.

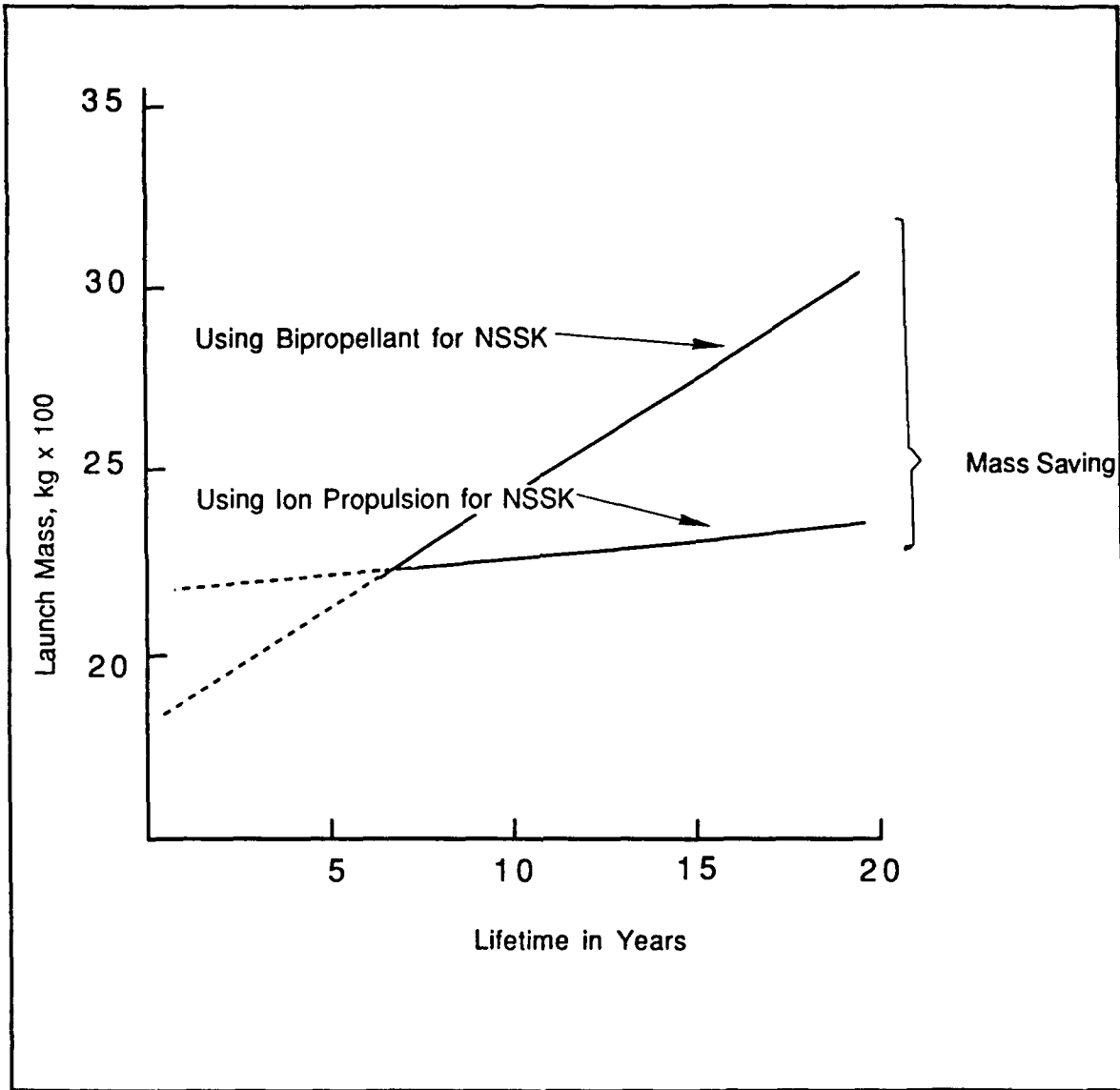


Figure 37. Ariane GTO Capability vs Spacecraft Lifetime

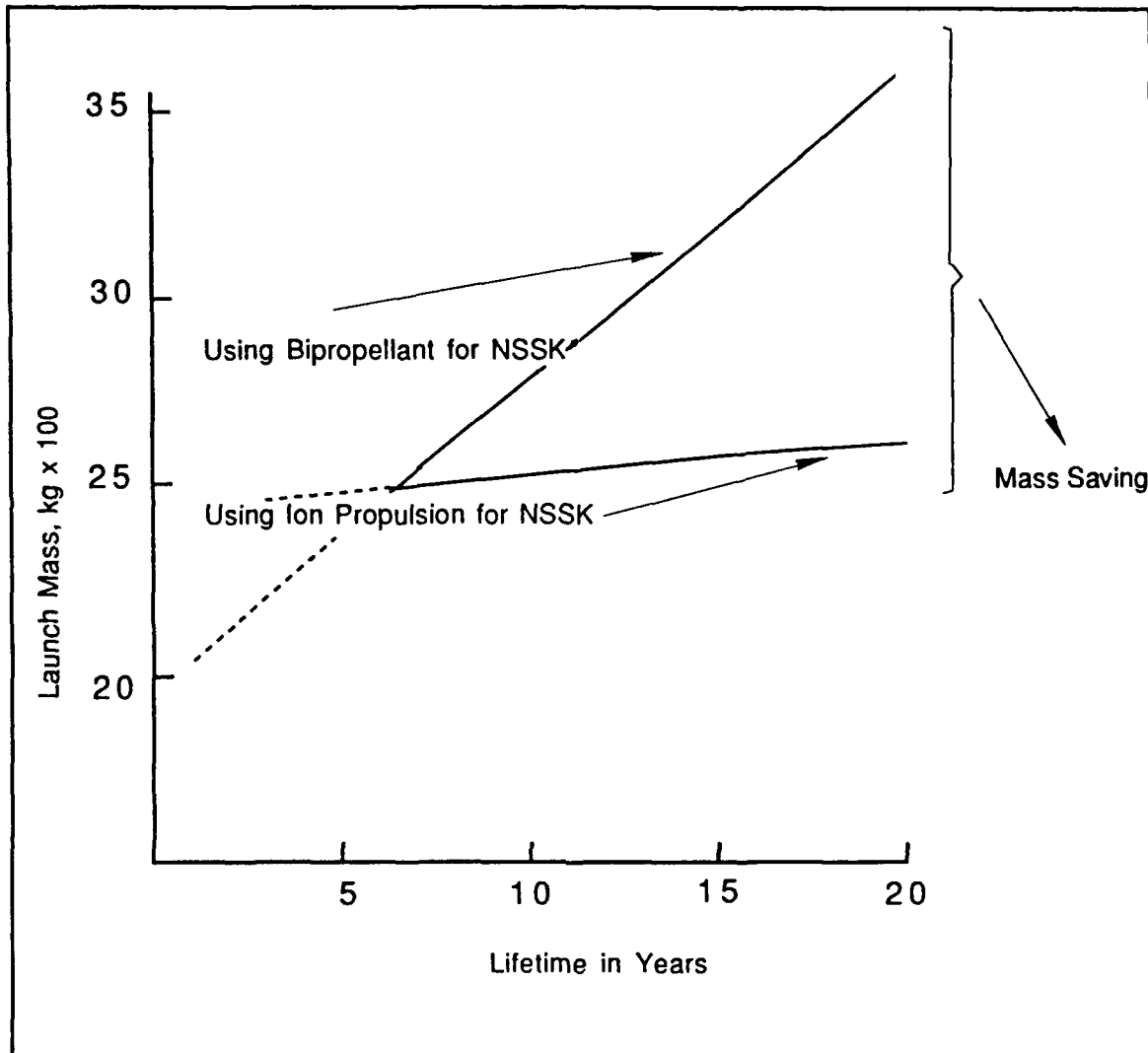


Figure 38. ETR GTO Capability vs Spacecraft Lifetime

XI. SUMMARY AND CONCLUSIONS

The xenon ion propulsion subsystem proposed herein will enable the UHF Follow-On class satellite to achieve the extended lifetime of 20 years while maintaining compatibility with other subsystems. This ability will be accomplished by adding ion thrusters, associated equipment, and xenon propellant primarily for NSSK while deleting the equivalent mass of bipropellant.

A. BIPROPELLANT AND ION PROPULSION TRADE-OFF

Ion propulsion system has an specific impulse (Isp) of an order of magnitude higher than that of the bipropellant propulsion systems. As a result, the propellant consumption of the ion thrusters is an order of magnitude lower than that of the bipropellant subsystem. For station keeping consideration, NSSK uses more than 90% of the bipropellant. For a satellite of this size with a lifetime of 20 years, the bipropellant requirement for NSSK is about 514 kg. If IPS is chosen over the BPS, the total IPS mass will only be 27% of the bipropellant mass.

B. IMPACT ON OTHER SUBSYSTEMS

The major impact of IPS will be primarily on the electrical power subsystem. The satellite has to provide the high power requirement, aside from the nominal power requirement of the payload, by the ion thrusters. The battery employed in the satellite is of Ni-H₂ type, which is capable of providing several thousands of deep charge/discharge cycles, therefore, making it attractive for long mission years and DOD. The solar array is another alternative, but to provide the required 854 W by the ion thrusters it is necessary to add another 10

m² of solar cells to augment the present configuration. This will have more impact on other subsystems than just adding a pack of cells to the battery to lower its depth of discharge (DOD).

Several options were investigated in selecting the location of the ion thrusters. Each has its own advantages and disadvantages. The chosen location has the least impact on the attitude control subsystem because the thrust vectors pass through the center of mass of the spacecraft. The thrust loss is minimized by canting the thrusters 30° with the north-south axis. The ion thruster's components are distributed around the spacecraft's Z-axis so that the IPS removal can be accomplished easily and with minimum impact on the spacecraft balance.

Impingement of the ion beam on solar array was also investigated, and it is recommended that sputtering resistant material be installed at the solar array basement to protect the solar cells (about 1% of the total array is affected) from the 5% ion beam, that may hit the affected solar cells. Plume shield was not adopted because of its protruding configuration and the efficiency loss due to shielding.

C. ENVIRONMENTAL IMPACT

The introduction of xenon as an ion propulsion propellant in the 80's makes IPS more attractive in terms of environmental concern because the gas is inert and, under normal condition, does not produce any chemical reaction with other materials. Problems with shorts in the grids and with high voltage electronics due to propellant leakage is also avoided with the use of xenon.

Previous data on flight tested ion thrusters indicated that interference contributed by the thrusters was minimal to non-existent. In the case of ESD, the

ion thrusters will help in unloading the charged spacecraft, due to magnetosphere plasma in the geosynchronous orbit. The plasma produced by the thrusters, which is more dense than the ambient space plasma, contains highly mobile xenon ions and electrons that are attracted to oppositely charged surfaces on the spacecraft, bringing them to near neutrality.

D. RISKS AND BENEFITS

There is no doubt that the risks involved in integrating ion propulsion are high. Several million dollars have already been spent on its development and testing, including several experimental satellites that had flown with ion thrusters as a part of their propulsion subsystems; yet, no commercial applications have been flown because of the risks involved. Since ion thrusters are best suited for NSSK, their operational failure will render the total spacecraft useless. It is this risk, the satellite industries' executives are most worried about.

On the other hand, if all the uncertainties are overcome by a proven demonstrated product, the benefits that can be gained are also very high. As an example, about 838 kg in launch mass can be saved by replacing BPS with IPS, the latter having a total mass of only 139 kg. If the mass saving is converted into monetary value, the launch cost saving is about \$25M. Several combinations of benefits can also be derived if the mass allowance, as a result of the mass saving, is used in adding more transponders for the satellite and/or extending the lifetime of the satellite.

**APPENDIX A: BIPROPELLANT AND ION PROPULSION
TRADE-OFF FOR NORTH-SOUTH STATION KEEPING
USING HUGHES 13cm ION THRUSTER**

To obtain the propellant mass [Ref. 3: p. 164] use

$$M_p = m_i (1 - e^{-\frac{\Delta V}{\eta I g}}) \quad (A-1)$$

$$= m_f (e^{\frac{\Delta V}{\eta I g}} - 1) \quad (A-2)$$

$$\eta = \cos \alpha \frac{\sin \beta}{\beta} \quad (A-3)$$

where

M_p = mass of propellant, kg

m_i = initial mass of the spacecraft, kg

m_f = final mass of the vehicle after burnout, kg

ΔV = required velocity change, m/s

I = specific impulse of the propellant, s

g = gravitational acceleration, (9.806 m/s²)

η = engine efficiency, (use eq. (A-3) for ion thrusters)

α = the thruster cant angle

β = the angle between the line of nodes and satellite position, as shown in

Figure 21

A. CASE I: PURE XENON ION PROPULSION

ION THRUSTER by Hughes Research Laboratories [Ref. 21]

Size = 13 cm with 17.7 mN (35.4 mN for two)

Power = 427 watts per thruster

Isp = 2718 sec

Cant Angle = 30 deg

Dry weight = 69 kg + 6.9 kg for allowance + 17% of propellant for support and tankage (10% for support and 7 % for tankage)

1. For 10 Year Mission

ΔV removed per day = Total ΔV in ten years / number of days

$$429.1/10 \times 275 = 0.156 \text{ m/s}$$

BOL mass of satellite with ion propulsion = 1226.5 + (69 + 6.9 + 24.9 + 4.25)

$$= 1331.05 \text{ kg}$$

Mean time for thruster firing is

$$1331.05 \times 0.156 / 35.4 \times 10^3 \times 60 \times 60 = 1.63 \text{ hr}$$

The thruster firing angle is

$$360 \times 1.64 / 24 = 24.45^\circ$$

The efficiency is

$$\eta = \cos 30^\circ \frac{\sin \frac{24.45^\circ}{2}}{\frac{24.45^\circ \times \pi}{2 \times 180^\circ}} = 0.859$$

Taking efficiency into consideration, the time for thruster firing is

$$1.64/0.859 = 1.91 \text{ hrs}$$

The new thruster firing angle

$$360 \times 1.91 / 24 = 28.65^\circ$$

The final efficiency is

$$\eta = \cos 30^\circ \frac{\sin \frac{28.65^\circ}{2}}{\frac{28.65^\circ \times \pi}{2 \times 180^\circ}} = 0.857$$

The final thruster firing time with 0.06 hr for start-up is

$$0.06 + 1.64 / 0.857 = 1.98 \text{ hrs}$$

The propellant required is

$$m_f = (1226.15 + 69 + 6.9 + 0.17M_p)$$

$$M_p = (1311.04 + 0.17M_p)(e^{(429.21/2718 \times 9.806 \times 0.856)} - 1)$$

$$= 24.8 \text{ kg}$$

$$\text{Therefore, BOL} = 1226.15 + 69 + 6.9 + 25 + 4.25$$

$$= 1331.05 \text{ kg}$$

a. Assume ETR Launch

Assuming the spacecraft is launched at ETR

For apogee kick motor (AKM) propellant, assuming bipropellant is

used

$$I_{sp} = 300 \text{ s, from Table 14}$$

$$\Delta V = 1836.49 \text{ m/s from Appendix F}$$

$$\eta = 100\%$$

$$m_f = 1331.05 + 0.16(M_p - 989.76)$$

$$M_p = (1172.69 + 0.16M_p)(e^{(1836.49/300 \times 9.806 \times 1)} - 1)$$

$$= 1180.3 \text{ kg}$$

$$\text{GTO Mass} = 2541.84 \text{ kg}$$

**TABLE 14. SPECIFIC IMPULSE (SECONDS) OF VARIOUS
PROPULSION [REF. 3]**

Propulsion System	Function		
	High-Thrust Steady State (>450 N) Apogee Injection	Low -Thrust Steady State (0.05 -22 N) Station Keeping	Low-Thrust Pulse (0.05 -22 N) Attitude Control
Monopropellant hydrazine (N ₂ H ₄)	235	220	135
Electrothermal hydrazine	-	290	-
Bipropellant (N ₂ O ₄ -MMH)	300	285	175
Ion thruster		3000	
Solid propellant	285		

b. Assume Ariane IV Launch

For apogee kick motor (AKM) propellant, assuming bipropellant is used

$$I_{sp} = 300 \text{ s, from Table 14}$$

$$\Delta V = 1513.3 \text{ m/s from Appendix F}$$

$$\eta = 100\%$$

$$m_f = 1331.05 (e^{(1513.3/300 \times 9.806 \times 1)} - 1)$$

$$= 895.34 \text{ kg}$$

$$\begin{aligned} \text{GTO Mass} &= 895.34 + 1331.05 \\ &= 2226.39 \text{ kg} \end{aligned}$$

2. For 15 Year Mission

$$\Delta V = 676 \text{ m/s}$$

$$676/15 \times 275 = 0.164 \text{ m/s } \Delta V \text{ removed per day}$$

$$\text{BOL} = 1230.64 + 69 + 6.9 + 39.5 + 0.17(39.5)$$

$$= 1352.76 \text{ kg}$$

Mean time for thruster firing

$$1352.76 \times 0.164 / 35.4 \times 10^{-3} \times 60 \times 60 = 1.74 \text{ hrs}$$

$$360 \times 1.74 / 24 = 26.1^\circ$$

The efficiency is

$$\eta = \cos 30^\circ \frac{\sin \frac{26.1^\circ}{2}}{26.1^\circ \times \pi} = 0.8586$$

Taking efficiency into consideration, the total time for thruster firing is

$$1.74/0.8586 = 2.03 \text{ hrs}$$

The final orbit angle

$$360 \times 2.03 / 24 = 30.45^\circ$$

The final efficiency is

$$\eta = \cos 30^\circ \frac{\sin \frac{30.45^\circ}{2}}{30.45^\circ \times \pi} = 0.856$$

The final thruster firing time is

$$0.06 + 1.74/0.856 = 2.1 \text{ hrs}$$

The propellant required is

$$m_f = 1230.64 + 69 + 6.9 + 0.17 M_p$$

$$M_p = (1306.64 + 0.17M_p)(e^{(676/2718 \times 9.806 \times 0.856)} - 1)$$

$$= 39.5 \text{ kg}$$

$$= 1352.76 \text{ kg}$$

a. Assume ETR Launch

Assuming the spacecraft is launched at ETR

For apogee kick motor (AKM) propellant

$$I_{sp} = 300 \text{ s}$$

$$\Delta V = 1836.49 \text{ m/s}$$

$$\eta = 100\%$$

$$m_f = 1352.76 + 0.16(M_p - 980.76)$$

$$M_p = (1194.4 + 0.16M_p)(e^{(1836.49/300 \times 9.806 \times 1)} - 1)$$

$$= 1202.2 \text{ kg}$$

$$\text{GTO Mass} = 1194.4 + 1.16(1202)$$

$$= 2588.95 \text{ kg.}$$

b. Assume Ariane IV Launch

For apogee kick motor (AKM) propellant

$$I_{sp} = 300 \text{ s}$$

$$\Delta V = 1513.3 \text{ m/s}$$

$$\eta = 100\%$$

$$M_p = 1352.76 (e^{(1513.3/300 \times 9.806 \times 1)} - 1)$$

$$= 909.94 \text{ kg}$$

$$\text{GTO Mass} = 909.94 + 1340.29$$

$$= 2250.23 \text{ kg}$$

3. For 20 Year Mission

$\Delta V = 912.1$ m/s, see Appendix G

$912.1/20 \times 275 = 0.1658$ m/s ΔV removed per day

Mean time for thruster firing

BOL = $1235.14 + 69 + 6.9 + 53.9 + 0.17(53.9)$

= 1374.1 kg

$1374.1 \times 0.1658 / 35.4 \times 10^{-3} \times 60 \times 60 = 1.79$ hrs

The thruster firing angle is

$360 \times 1.79 / 24 = 26.85^\circ$

The efficiency is

$$\eta = \cos 30^\circ \frac{\sin \frac{26.85^\circ}{2}}{\frac{26.85^\circ \times \pi}{2 \times 180^\circ}} = 0.858$$

Time for thruster firing:

$1.79/0.858 = 2.09$ hrs

The new thruster firing angle

$360 \times 2.09 / 24 = 31.35^\circ$

The new efficiency is

$$\eta = \cos 30^\circ \frac{\sin \frac{31.35^\circ}{2}}{\frac{31.35^\circ \times \pi}{2 \times 180^\circ}} = 0.855$$

The final thruster firing time is

$0.06 + 1.79/0.855 = 2.16$ hrs

The propellant required is

$m_f = 1235.14 + 69 + 6.9 + 0.17 M_p$

$$M_p = (1311.04 + 0.17M_p)(e^{(912.1/2718 \times 9.806 \times 0.855)} - 1)$$

$$= 53.9 \text{ kg}$$

$$\text{BOL} = 1235.14 + 69 + 6.9 + 53.9 + 0.17(53.9)$$

$$= 1374.1 \text{ kg}$$

a. Assume ETR Launch

Assuming the spacecraft is launched at ETR

For apogee kick motor (AKM) propellant

$$I_{sp} = 300 \text{ s}$$

$$\Delta V = 1836.49 \text{ m/s}$$

$$m_f = 1374.1 + 0.16(M_p - 989.76)$$

$$M_p = (1215.74 + 0.16 M_p)(e^{(1836.49/300 \times 9.806 \times 1)} - 1)$$

$$= 1223.63 \text{ kg}$$

$$\text{GTO Mass} = 1215.74 + 1.16(1223.63)$$

$$= 2635.15 \text{ kg}$$

b. Assume Ariane IV Launch

For apogee kick motor (AKM) propellant

$$I_{sp} = 300 \text{ s}$$

$$\Delta V = 1513.3 \text{ m/s}$$

$$\eta = 100\%$$

$$M_p = 1374.1 (e^{(1513.3/300 \times 9.806 \times 1)} - 1)$$

$$= 924.29 \text{ kg}$$

$$\text{GTO Mass} = 924.29 + 1374.1$$

$$= 2298.39 \text{ kg}$$

B. CASE II: ION AND BIPELLANT COMBO

Ion thrusters used during non-eclipse and Bipropellant thrusters during eclipse

1. For 10 Year Mission

$$\Delta V[\text{bipropellant}] = 429.1 \times 90/365$$

$$= 105.81 \text{ m/s}$$

$$m_f = 1226.15 + 0.16M_p$$

$$M_p = (1226.15 + 0.16 M_p) (e^{(105.81/285 \times 9.806 \times .99)} - 1)$$

$$= 48.1 \text{ kg}$$

$$\Delta V[\text{ion}] = 429.1 - 105.81$$

$$= 323.29 \text{ m/s}$$

$$m_f = 1226.15 + 48.1 + 0.16(48.1) + 69 + 6.9 + 0.17 M_p$$

$$M_p = (1357.85 + 0.17M_p) (e^{(323.29/2718 \times 9.806 \times 0.857)} - 1)$$

$$= 19.4 \text{ kg}$$

2. For 15 Year Mission

$$\Delta V[\text{bipropellant}] = 676 \times 90 / 365$$

$$= 166.68 \text{ m/s}$$

$$m_f = 1230.64 + 0.16 M_p$$

$$M_p = (1230.64 + 0.16M_p) (e^{(166.68/285 \times 9.806 \times .99)} - 1)$$

$$= 77.2 \text{ kg}$$

$$\Delta V[\text{ion}] = 676 - 166.68$$

$$= 509.32 \text{ m/s}$$

$$m_f = 1230.64 + 1.16(77.2) + 69 + 6.9 + 0.17M_p$$

$$M_p = (1396.1 + 0.17M_p) (e^{(509.32/2718 \times 9.806 \times 0.856)} - 1)$$

$$= 31.6 \text{ kg}$$

3. For 20 Year Mission

$$\Delta V[\text{bi-propellant}] = 912.1 \times 90 / 365$$

$$= 224.9 \text{ m/s}$$

$$m_f = 1235.14 + 0.16M_p$$

$$M_p = (1235.14 + 0.16M_p) (e^{(224.9/285 \times 9.806 \times .99)} - 1)$$

$$= 106 \text{ kg}$$

$$\Delta V[\text{ion}] = 912.1 - 224.9$$

$$= 687.2 \text{ m/s}$$

$$m_f = 1235.14 + 1.16(106) + 69 + 6.9 + 0.17M_p$$

$$M_p = (1434 + 0.17 M_p) (e^{(687.2/2718 \times 9.806 \times 0.855)} - 1)$$

$$= 44.1 \text{ kg}$$

a. Assume ETR Launch

For apogee kick motor (AKM) propellant

$$I_{sp} = 300 \text{ s, from Table 14}$$

$$\Delta V = 1836.49 \text{ m/s from Appendix F}$$

$$\eta = 100\%$$

$$m_f = 1434 + 1.17(44.1) + 0.16(M_p - 989.76)$$

$$= 1327.24 + 0.16M_p \text{ kg}$$

$$M_p = [1327.24 + 0.16M_p](e^{(1836.49/300 \times 9.806 \times 1)} - 1)$$

$$= 1335.86 \text{ kg}$$

For perigee propellant

$$I_{sp} = 285 \text{ from Table 14}$$

$$\Delta V = 2454.57 \text{ m/s (from Appendix F)}$$

$$\eta = 100\%$$

$$m_f = 2876.84 \text{ kg}$$

$$M_p = (2876.84 + 0.07M_p) (e^{(2454.57/285 \times 9.806 \times 1)} - 1)$$

$$= 4489.14 \text{ kg}$$

$$\text{Solid propellant casing} = 0.07(4489.14) = 314.24 \text{ kg}$$

b. Assume Ariane IV Launch

For apogee kick motor (AKM) propellant

$$I_{sp} = 300 \text{ s, from Table 14}$$

$$\Delta V = 1513.3 \text{ m/s from Appendix F}$$

$$\eta = 100\%$$

$$m_f = 1434 + 1.17(44.1) + 0.16(M_p - 989.76)$$

$$= 1327.24 + 0.16M_p \text{ kg}$$

$$M_p = [1327.24 + 0.16(M_p)] (e^{(1513.3/300 \times 9.806 \times 1)} - 1)$$

$$= 1000.45 \text{ kg}$$

For perigee propellant

$$I_{sp} = 285 \text{ from Table 14}$$

$$\Delta V = 2454.57 \text{ m/s (from Appendix F)}$$

$$\eta = 100\%$$

$$m_f = 2487.76$$

$$M_p = (2487.76 + 0.07M_p) (e^{(2454.57/285 \times 9.806 \times 1)} - 1)$$

$$= 3882.02 \text{ kg}$$

$$\text{Solid propellant casing} = 0.07(3882.02) = 271.74 \text{ kg}$$

APPENDIX B. BIPELLANT AND ION PROPULSION TRADE-OFF FOR NORTH-SOUTH STATION KEEPING USING UK-10 ION THRUSTER

To obtain the propellant mass [Ref. 3: p. 164] use

$$M_p = m_i (1 - e^{-\frac{\Delta V}{\eta I g}}) \quad (B-1)$$

$$= m_f (e^{\frac{\Delta V}{\eta I g}} - 1) \quad (B-2)$$

$$\eta = \cos \alpha \frac{\sin \beta}{\beta} \quad (B-3)$$

where

M_p = mass of propellant, kg

m_i = initial mass of the spacecraft, kg

m_f = final mass of the vehicle after burnout, kg

ΔV = required velocity change, m/s

I = specific impulse of the propellant, s

g = gravitational acceleration, (9.806 m/s²)

η = engine efficiency, (use eq. (B-3) for ion thrusters)

α = the thruster cant angle

β = the angle between the line of nodes and satellite position, as shown in

Figure 21

A. USING PURE XENON ION PROPULSION

ION THRUSTER by UK [Ref. 48]

Size = 10 cm with 25 mN (50 mN for two)

Power = 759 watts per thruster

Isp = 3486 sec

Cant Angle = 30 deg

Dry weight = 100 kg + 10 kg (for allowance) + 17% of propellant for support and tankage (10% for support and 7 % for tankage)

1. For 10 Year Mission

ΔV removed per day = Total ΔV in ten years / number of days

$429.1/10 \times 275 = 0.156$ m/s

BOL mass of satellite with ion propulsion = $1226.5 + (100 + 10 + 1.17(19.68))$
 $= 1359.18$ kg

Mean time for thruster firing

$1359.18 \times 0.156 / 50 \times 10^3 \times 60 \times 60 = 1.18$ hr

The thruster firing angle

$360 \times 1.18 / 24 = 17.7^\circ$

The efficiency is

$$\eta = \cos 30^\circ \frac{\sin \frac{17.7^\circ}{2}}{\frac{17.7^\circ \times \pi}{2 \times 180^\circ}} = 0.863$$

Taking efficiency into consideration, the time for thruster firing is

$1.18/0.863 = 1.37$ hrs

The new thruster firing angle

$$360 \times 1.37 / 24 = 20.55^\circ$$

The final efficiency is

$$\eta = \cos 30^\circ \frac{\sin \frac{20.55^\circ}{2}}{\frac{20.55^\circ \times \pi}{2 \times 180^\circ}} = 0.861$$

The final thruster firing time with 0.06 hr for start-up is

$$0.06 + 1.18/0.861 = 1.43 \text{ hrs}$$

The propellant required is

$$m_f = (1226.15 + 100 + 10 + 0.17M_p)$$

$$M_p = (1336.15 + 0.17M_p)(e^{(429.21/3486 \times 9.806 \times 0.856)}) - 1)$$

$$= 19.68 \text{ kg}$$

$$\text{Therefore, BOL} = 1226.15 + 100 + 10 + 1.17(19.68)$$

$$= 1359.18 \text{ kg}$$

a. Assume ETR Launch

Assuming the spacecraft is launched at ETR

For apogee kick motor (AKM) propellant, assuming bipropellant is

used

$$I_{sp} = 300 \text{ s, from Table 14}$$

$$\Delta V = 1836.49 \text{ m/s from Appendix F}$$

$$\eta = 100\%$$

$$m_f = 1359.18 + 0.16(M_p - 989.76)$$

$$M_p = (1200.82 + 0.16M_p)(e^{(1836.49/300 \times 9.806 \times 1)} - 1)$$

$$= 1208.62 \text{ kg}$$

$$\text{GTO Mass} = 1200.82 + 1.16(1208.62)$$

$$= 2602.82 \text{ kg}$$

b. Assume Ariane IV Launch

For apogee kick motor (AKM) propellant

$$I_{sp} = 300 \text{ s}$$

$$\Delta V = 1513.3 \text{ m/s}$$

$$\eta = 100\%$$

$$m_f = 1359.18(e^{(1513.3/300 \times 9.806 \times 1)} - 1)$$

$$= 914.26 \text{ kg}$$

$$\text{GTO Mass} = 914.36 + 1359.18$$

$$= 2277.23 \text{ kg}$$

2. For 15 Year Mission

$$\Delta V = 676 \text{ m/s}$$

$$676/15 \times 275 = 0.164 \text{ m/s } \Delta V \text{ removed per day}$$

$$\text{BOL} = 1230.64 + 100 + 10 + 1.17(31.27)$$

$$= 1377.23 \text{ kg}$$

Mean time for thruster firing

$$1377.23 \times 0.164 / 50 \times 10^{-3} \times 60 \times 60 = 1.255 \text{ hrs}$$

$$360 \times 1.255 / 24 = 18.8^\circ$$

The efficiency is

$$\eta = \cos 30^\circ \frac{\sin \frac{18.8^\circ}{2}}{\frac{18.8^\circ \times \pi}{2 \times 180^\circ}} = 0.862$$

Taking efficiency into account, the time for thruster firing is

$$1.255/0.862 = 1.46 \text{ hrs}$$

The thruster firing angle

$$360 \times 1.46 / 24 = 22^\circ$$

The final efficiency is

$$\eta = \cos 30^\circ \frac{\sin \frac{22^\circ}{2}}{\frac{22^\circ \times \pi}{2 \times 180^\circ}} = 0.861$$

The final thruster firing time is

$$0.06 + 1.26/0.861 = 1.52 \text{ hrs}$$

The propellant required is

$$m_f = 1230.64 + 100 + 10 + 0.17 M_p$$

$$M_p = (1340.64 + 0.17M_p)(e^{(676/3486 \times 9.806 \times 0.856)} - 1)$$
$$= 31.27 \text{ kg}$$

$$\text{BOL} = 1230.64 + 100 + 10 + 1.17(31.27)$$

$$= 1377.23 \text{ kg}$$

a. Assume ETR Launch

Assuming the spacecraft is launched at ETR

For apogee kick motor (AKM) propellant

$$I_{sp} = 300 \text{ s}$$

$$\Delta V = 1836.49 \text{ m/s}$$

$$\eta = 100\%$$

$$m_f = 1377.23 + 0.16(M_p - 989.76)$$

$$M_p = (1218.87 + 0.16M_p)(e^{(1836.49/300 \times 9.806 \times 1)} - 1)$$
$$= 1226.78 \text{ kg}$$

$$\text{GTO Mass} = 1218.87 + 1.16(1226.78)$$

$$= 2641.93 \text{ kg}$$

b. Assume Ariane IV Launch

For apogee kick motor (AKM) propellant

$$I_{sp} = 300 \text{ s}$$

$$\Delta V = 1513.3 \text{ m/s}$$

$$\eta = 100\%$$

$$m_f = 1377.23(e^{(1513.3/300 \times 9.806 \times 1)} - 1)$$

$$= 926.4 \text{ kg}$$

$$\text{GTO Mass} = 926.4 + 1377.23$$

$$= 2303.63 \text{ kg}$$

3. For 20 Year Mission

$$\Delta V = 912.1 \text{ m/s, see Appendix G}$$

$$912.1/20 \times 275 = 0.1658 \text{ m/s } \Delta V \text{ removed per day}$$

$$\text{BOL} = 1235.14 + 100 + 10 + 1.17(42.62)$$

$$= 1395 \text{ kg}$$

Mean time for thruster firing

$$1395 \times 0.1658 / 50 \times 10^{-3} \times 60 \times 60 = 1.29 \text{ hrs}$$

The thruster firing angle is

$$360 \times 1.29 / 24 = 19.3^\circ$$

The efficiency is

$$\eta = \cos 30^\circ \frac{\sin \frac{19.3^\circ}{2}}{\frac{19.3^\circ \times \pi}{2 \times 180^\circ}} = 0.862$$

Time for thruster firing:

$$1.29/0.862 = 1.5 \text{ hrs}$$

The new thruster firing angle

$$360 \times 1.5/24 = 22.5^\circ$$

The new efficiency is

$$\eta = \cos 30^\circ \frac{\sin \frac{22.5^\circ}{2}}{\frac{22.5^\circ \times \pi}{2 \times 180^\circ}} = 0.86$$

The final thruster firing time is

$$0.06 + 1.29/0.86 = 1.56 \text{ hrs}$$

The propellant required is

$$m_f = 1235.14 + 100 + 10 + 0.17 M_p$$

$$M_p = (1345.14 + 0.17 M_p)(e^{(912.1/3486 \times 9.806 \times 0.855)} - 1)$$

$$= 42.62 \text{ kg}$$

$$\text{BOL} = 1235.14 + 100 + 10 + 1.17(42.62)$$

$$= 1395 \text{ kg}$$

a. Assume ETR Launch

Assuming the spacecraft is launched at ETR

For apogee kick motor (AKM) propellant

$$I_{sp} = 300 \text{ s}$$

$$\Delta V = 1836.49 \text{ m/s}$$

$$m_f = 1395 + 0.16(M_p - 989.76)$$

$$M_p = (1236.64 + 0.16 M_p)(e^{(1836.49/300 \times 9.806 \times 1)} - 1)$$

$$= 1244.67 \text{ kg}$$

$$\text{GTO Mass} = 1236.64 + 1244.67$$

$$= 2680.46 \text{ kg}$$

b. Assume Ariane IV Launch

For apogee kick motor (AKM) propellant

$$I_{sp} = 300 \text{ s}$$

$$\Delta V = 1513.3 \text{ m/s}$$

$$\eta = 100\%$$

$$M_p = 1395(e^{(1513.3/300 \times 9.806 \times 1)} - 1)$$

$$= 938.35 \text{ kg}$$

$$\text{GTO} = 2333.35 \text{ kg}$$

APPENDIX C. BIPROPELLANT AND ION PROPULSION TRADE-OFF FOR NORTH-SOUTH STATION KEEPING USING MELCO ION THRUSTER

To obtain the propellant mass [Ref. 3: p. 164] use

$$M_p = m_i \left(1 - e^{-\frac{\Delta V}{\eta I g}} \right) \quad (C-1)$$

$$= m_f \left(e^{\frac{\Delta V}{\eta I g}} - 1 \right) \quad (C-2)$$

$$\eta = \cos \alpha \frac{\sin \beta}{\beta} \quad (C-3)$$

where

M_p = mass of propellant, kg

m_i = initial mass of the spacecraft, kg

m_f = final mass of the vehicle after burnout, kg

ΔV = required velocity change, m/s

I = specific impulse of the propellant, s

g = gravitational acceleration, (9.806 m/s²)

η = engine efficiency, (use eq. (C-3) for ion thrusters)

α = the thruster cant angle

β = the angle between the line of nodes and satellite position, as shown in

Figure 21

A. USING PURE XENON ION PROPULSION

ION THRUSTER by Japanese MELCO [Ref. 49]

Size = 12 cm with 23.3 mN (46.6 mN for two)

Power = 745 watts per thruster

Isp = 2906 sec

Cant Angle = 30 deg

Dry weight = 84 kg + 8.4 kg (for allowance) + 17% of propellant for support and tankage (10% for support and 7 % for tankage)

1. For 10 Year Mission

ΔV removed per day = Total ΔV in ten years / number of days

$$429.1/10 \times 275 = 0.156 \text{ m/s}$$

$$\begin{aligned} \text{BOL mass of satellite with ion propulsion} &= 1226.5 + 84 + 8.4 + \\ &1.17(23.14) \\ &= 1345.62 \text{ kg} \end{aligned}$$

Mean time for thruster firing

$$1345.62 \times 0.156 / 46.6 \times 10^3 \times 60 \times 60 = 1.25 \text{ hr}$$

The thruster firing angle

$$360 \times 1.25 / 24 = 18.75^\circ$$

The efficiency is

$$\eta = \cos 30^\circ \frac{\sin \frac{18.75^\circ}{2}}{\frac{18.75^\circ \times \pi}{2 \times 180^\circ}} = 0.862$$

Taking efficiency into consideration, the time for thruster firing is

$$1.25/0.862 = 1.45 \text{ hrs}$$

The new thruster firing angle

$$360 \times 1.45 / 24 = 21.75^\circ$$

The final efficiency is

$$\eta = \cos 30^\circ \frac{\sin \frac{21.75^\circ}{2}}{\frac{21.75^\circ \times \pi}{2 \times 180^\circ}} = 0.861$$

The final thruster firing time with 0.06 hr for start-up is

$$0.06 + 1.25/0.861 = 1.51 \text{ hrs}$$

The propellant required is

$$m_f = (1226.15 + 100 + 10 + 0.17M_p)$$

$$M_p = (1336.15 + 0.17M_p)(e^{(429.21/2906 \times 9.806 \times 0.861)}) - 1)$$
$$= 23.14 \text{ kg}$$

$$\text{Therefore, BOL} = 1226.15 + 84 + 8.4 + 1.17(23.14)$$

$$= 1345.62 \text{ kg}$$

a. Assume ETR Launch

Assuming the spacecraft is launched at ETR

For apogee kick motor (AKM) propellant

$$I_{sp} = 300 \text{ s, from Table 14}$$

$$\Delta V = 1836.49 \text{ m/s from Appendix F}$$

$$\eta = 100\%$$

$$m_f = 1345.62 + 0.16(M_p - 989.76)$$

$$M_p = (1187.26 + 0.16M_p)(e^{(1836.49/300 \times 9.806 \times 1)} - 1)$$
$$= 1194.97 \text{ kg}$$

$$\text{GTO Mass} = 1187.26 + 1.16(1194.97)$$

$$= 2573.43 \text{ kg}$$

b. Assume Ariane IV Launch

For apogee kick motor (AKM) propellant

$$I_{sp} = 300 \text{ s}$$

$$\Delta V = 1513.3 \text{ m/s}$$

$$\eta = 100\%$$

$$M_p = 1345.62(e^{(1513.3/300 \times 9.806 \times 1)} - 1)$$

$$= 905.14 \text{ kg}$$

$$\text{GTO Mass} = 905.14 + 1345.62$$

$$= 2250.76 \text{ kg}$$

2. For 15 Year Mission

$$\Delta V = 676 \text{ m/s}$$

$$676/15 \times 275 = 0.164 \text{ m/s } \Delta V \text{ removed per day}$$

$$\text{BOL} = 1230.64 + 84 + 8.4 + 1.17(37.18)$$

$$= 1365.9 \text{ kg}$$

Mean time for thruster firing

$$1365.9 \times 0.164 / 46.6 \times 10^{-3} \times 60 \times 60 = 1.34 \text{ hrs}$$

$$360 \times 1.34 / 24 = 20.1^\circ$$

The efficiency is

$$\eta = \cos 30^\circ \frac{\sin \frac{20.1^\circ}{2}}{\frac{20.1^\circ \times \pi}{2 \times 180^\circ}} = 0.861$$

Taking efficiency into account, the time for thruster firing is

$$1.34/0.861 = 1.56 \text{ hrs}$$

The thruster firing angle

$$360 \times 1.56 / 24 = 23.34^\circ$$

The final efficiency is

$$\eta = \cos 30^\circ \frac{\sin \frac{23.34^\circ}{2}}{\frac{23.34^\circ \times \pi}{2 \times 180^\circ}} = 0.86$$

The final thruster firing time is

$$0.06 + 1.34/0.86 = 1.62 \text{ hrs}$$

The propellant required is

$$m_f = 1230.64 + 84 + 8.4 + 0.17 M_p$$

$$M_p = (1230.64 + 0.17M_p)(e^{(676/2906 \times 9.806 \times 0.856)} - 1)$$

$$= 37.18 \text{ kg}$$

$$\text{BOL} = 1230.64 + 84 + 8.4 + 1.17(37.18)$$

$$= 1365.9 \text{ kg}$$

a. Assume ETR Launch

Assuming the spacecraft is launched at ETR

For apogee kick motor (AKM) propellant

$$I_{sp} = 300 \text{ s}$$

$$\Delta V = 1836.49 \text{ m/s}$$

$$\eta = 100\%$$

$$m_f = 1365.9 + 0.16(M_p - 989.76)$$

$$M_p = (1207.54 + 0.16M_p)(e^{(1836.49/300 \times 9.806 \times 1)} - 1)$$

$$= 1215.38 \text{ kg}$$

$$\text{GTO Mass} = 1207.54 + 1215.38$$

$$= 2617.38 \text{ kg}$$

b. Assume Ariane IV Launch

For apogee kick motor (AKM) propellant

$$I_{sp} = 300 \text{ s}$$

$$\Delta V = 1513.3 \text{ m/s}$$

$$\eta = 100\%$$

$$M_p = 1365.9(e^{(1513.3/300 \times 9.806 \times 1)} - 1)$$

$$= 918.8 \text{ kg}$$

$$\text{GTO Mass} = 918.8 + 1365.9$$

$$= 2284.7 \text{ kg}$$

3. For 20 Year Mission

$$\Delta V = 912.1 \text{ m/s, see Appendix G}$$

$$912.1/20 \times 275 = 0.1658 \text{ m/s } \Delta V \text{ removed per day}$$

Mean time for thruster firing

$$\text{BOL} = 1235.14 + 84 + 8.4 + 1.17(50.67)$$

$$= 1386.8$$

$$1386.8 \times 0.1658 / 46.6 \times 10^{-3} \times 60 \times 60 = 1.37 \text{ hrs}$$

The thruster firing angle is

$$360 \times 1.37 / 24 = 20.55^\circ$$

The efficiency is

$$\eta = \cos 30^\circ \frac{\sin \frac{20.55^\circ}{2}}{\frac{20.55^\circ \times \pi}{2 \times 180^\circ}} = 0.861$$

Time for thruster firing:

$$1.37/0.861 = 1.59 \text{ hrs}$$

The new thruster firing angle

$$360 \times 1.59/24 = 23.85^\circ$$

The new efficiency is

$$\eta = \cos 30^\circ \frac{\sin \frac{23.85^\circ}{2}}{\frac{23.85^\circ \times \pi}{2 \times 180^\circ}} = 0.86$$

The final thruster firing time is

$$0.06 + 1.37/0.86 = 1.65 \text{ hrs}$$

The propellant required is

$$m_f = 1235.14 + 84 + 8.4 + 0.17 M_p$$

$$M_p = (1327.54 + 0.17M_p)(e^{(912.1/2906 \times 9.806 \times 0.855)} - 1)$$

$$= 50.67 \text{ kg}$$

$$\text{BOL} = 1235.14 + 84 + 8.4 + 1.17(42.62)$$

$$= 1386.8 \text{ kg}$$

a. Assume ETR Launch

Assuming the spacecraft is launched at ETR

For apogee kick motor (AKM) propellant

$$I_{sp} = 300 \text{ s}$$

$$\Delta V = 1836.49 \text{ m/s}$$

$$m_f = 1386.8 + 0.16(M_p - 989.76)$$

$$M_p = (1228.44 + 0.16M_p)(e^{(1836.49/300 \times 9.806 \times 1)} - 1)$$

$$= 1236.42 \text{ kg}$$

$$\text{GTO Mass} = 1228.44 + 1236.42$$

$$662.69 \text{ kg}$$

b. Assume Ariane IV Launch

For apogee kick motor (AKM) propellant

$$I_{sp} = 300 \text{ s}$$

$$\Delta V = 1513.3 \text{ m/s}$$

$$\eta = 100\%$$

$$M_p = 1386.8(e^{(1513.3/300 \times 9.806 \times 1)} - 1)$$

$$= 932.83 \text{ kg}$$

$$\text{GTO Mass} = 932.83 + 1386.8$$

$$= 2319.63 \text{ kg}$$

APPENDIX D. EAST-WEST STATION KEEPING

Considering second order effects only, the longitudinal drift acceleration λ due to the ellipticity of the earth (Ref. 3: p.88) at the equator is

$$\lambda = -0.00168 \sin 2(\lambda - \lambda_s) \text{ deg/day} \quad \text{D-1}$$

where λ = satellite longitude, deg

λ_s = stable longitude, 75° E

considering the worst case

$$\sin 2(\lambda - \lambda_s) = 1$$

$$\sin 2(\lambda - 75^\circ) = 1$$

$$\lambda = 120^\circ \text{ E}$$

$$\lambda = -0.00168 \sin 2(120^\circ - 75^\circ)$$

$$= -0.00168 \text{ deg/day}$$

The time interval

$$T = 4 \sqrt{\frac{\Delta\lambda}{|\lambda|}} \quad \text{D-2}$$

$$= 4 \sqrt{\frac{0.1}{0.00168}}$$

$$= 59.523 \text{ days}$$

ΔV required per year is

$$\Delta V = 1.74 \sin 2(120 - 75) \quad \text{D-3}$$

$$= 1.74 \text{ m/s-yr}$$

A. USING ION PROPULSION

ION THRUSTER by Hughes Aircraft Corporation [Ref. 21]

Size = 13 cm with 17.7 mN

Isp = 2718 sec

Cant Angle = 60 deg (the same thrusters used for NSSK)

For 20 year mission

$$\Delta V = 17.4 \times 2 = 34.8 \text{ m/s}$$

$$34.8/20 \times 275 = 0.00633 \text{ m/s } \Delta V \text{ removed per day}$$

Mean time for thruster firing

$$1203 \times 0.0063 / 35.4 \times 10^{-3} \times 60 \times 60 = 0.0597 \text{ hrs}$$

Considering $\eta = 0.50$

$$\text{Time for thruster firing} = 0.0597/0.5 = 0.1194 \text{ hr}$$

The propellant required is

$$M_p = 1203 (1 - e^{-(34.8/2718 \times 9.806 \times 0.5)})$$

$$= 3.14 \text{ kg for (BOL = 1203 kg)}$$

$$M_p = 1195.5(1 - e^{-(34.8/2718 \times 9.806 \times 0.5)})$$

$$= 3.12 \text{ kg for (BOL = 1195.5 kg)}$$

APPENDIX E. STATION REPOSITIONING

The equation for change in velocity for station repositioning [Ref.3: p. 91] is:

$$\Delta V = 5.66 \frac{\Delta \lambda}{n} \quad (\text{E-1})$$

where $\Delta \lambda$ = degrees traversed by satellite during the reposition (assume worst case of 180°)

ΔV = required velocity change for station repositioning

n = number of days required for the reposition

$$\begin{aligned} \Delta V &= 5.66 \frac{180}{30} \\ &= 33.96 \text{ m/s} \end{aligned}$$

A. USING PURE XENON ION PROPULSION

ION THRUSTER by Hughes Research Laboratories [Ref. 21]

Size = 13 cm with 17.7 mN

Power = 427 watts/thruster

Isp = 2718 sec

Cant Angle = 0°

$$\begin{aligned} \Delta V_{\text{removed per day}} &= 33.96/30 \\ &= 1.132 \text{ m/s} \end{aligned}$$

Mean time for thruster firing

$$1200 \times 1.132 / 35.4 \times 10^{-3} \times 60 \times 60 = 10.66 \text{ hrs}$$

With $\eta = 1$

Mean time for thrusting = $10.66/1 = 10.66 \text{ hr}$ (too long)

The propellant required is

$$M_p = 1200(1 - e^{-(33.96/2718 \times 9.806 \times 1)})$$

$$= 1.52 \text{ kg}$$

APPENDIX F. ORBIT VELOCITIES

See Figure 39 for the following analysis.

Velocity Requirements [Ref. 3: pp. 93-94]

The parking orbit velocity V_p is

$$V_p = \sqrt{\frac{\mu_e}{a}} \quad (\text{F-1})$$

where $\mu_e = 398,601.2 \text{ km}^3/\text{s}^2$

$a = 6578.2 \text{ km}$ see Figure 22

$$\begin{aligned} &= \sqrt{\frac{(398,601.2)}{6578.2}} \\ &= 7.78423 \text{ km/s} \end{aligned}$$

The orbit period τ_p is

$$\tau_p = 2\pi \sqrt{\frac{a^3}{\mu}} \quad (\text{F-2})$$

$$\begin{aligned} &= 2\pi \sqrt{\frac{6578.2^3}{398601.2}} \\ &= 5309.71459 = 1.47492 \text{ hr} \end{aligned}$$

The transfer orbit velocity V_{tp} at perigee is

$$V_{tp} = \sqrt{\frac{2\mu_e r_a}{(r_a + r_p)r_p}} \quad (\text{F-3})$$

where $r_a = 42,164.2 \text{ km}$, apogee distance, see Figure 39

$r_p = 6578.2 \text{ km}$ perigee distance, see Figure 39

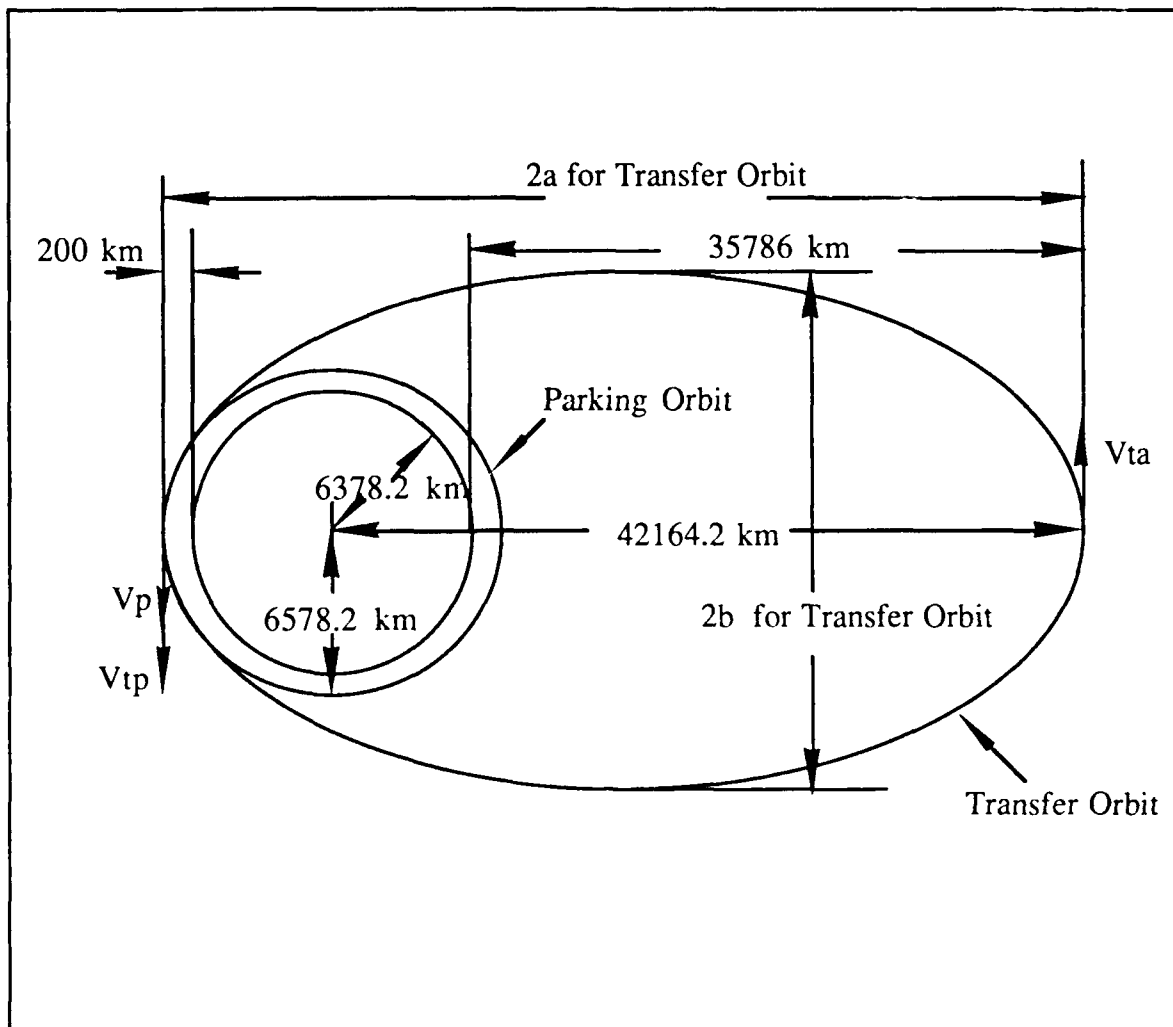


Figure 39. Orbital Parameters for Parking Orbit and Transfer Orbit [Ref. 3]

$$V_{tp} = \sqrt{\frac{(2 \times 398601.2 \times 42164.2)}{(42164.2 + 6578.2)(6578.2)}}$$

$$= 10.2388 \text{ km/s}$$

Hence, the velocity change required to transfer the satellite from parking orbit to the transfer orbit without a plane change is

$$\Delta V_{tp} = V_{tp} - V_p = (10.2388 - 7.78423)$$

$$\Delta V_{tp} = 2.45457 \text{ km/s}$$

The transfer orbit period τ_t is given by

$$\tau_t = 2\pi \frac{a^{3/2}}{m^{1/2}} \quad (\text{F-4})$$

where $a = \frac{r_a + r_p}{2}$, semi major axis

$$= 2\pi \sqrt{\frac{(r_a + r_p)^3}{(2)^3 \mu}}$$

$$= 2\pi \sqrt{\frac{(42164.2 + 6578.2)^3}{(2)^3 \times 398601.2}} = 37863.9517 \text{ s}$$

$$= \frac{37863.9517}{3600} = 10.5177 \text{ hrs}$$

The transfer orbit velocity V_{ta} at the apogee

$$\begin{aligned} V_{ta} &= V_{tp} \frac{r_p}{r_a} & (F-5) \\ &= 10.2388 \times \frac{6578.2}{42164.2} \\ &= 1.59738 \text{ km/s} \end{aligned}$$

The synchronous orbit velocity V_s is

$$V_s = \sqrt{\frac{\mu_e}{a}} \quad (F-6)$$

$$\text{where } \mu_e = 398,601.2 \text{ km}^3/\text{s}^2$$

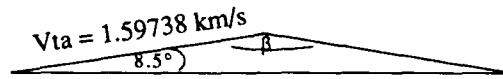
$$a = 42,164.2 \text{ km}$$

$$V_s = 3.07466 \text{ km/s}$$

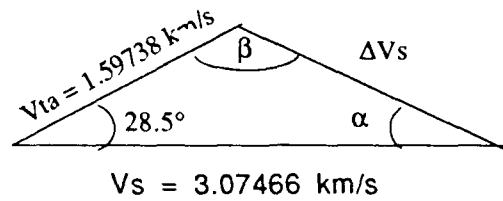
The velocity change (ΔV_s) provided by the apogee motor to transfer the satellite from the transfer orbit to synchronous orbit can be determined from the velocity vector diagram in Figure 40, for Eastern Test Range (ETR) in Florida at a latitude of 28.5° .

$$\begin{aligned} \Delta V_s &= \sqrt{(1.59738 \sin 28.5^\circ)^2 + (3.07466 - 1.59738 \cos 28.5^\circ)^2} \\ &= \sqrt{3.37271159} = 1.83649 \text{ km/s} \end{aligned}$$

$$\begin{aligned} \alpha &= \tan^{-1} \frac{1.59738 \sin 28.5^\circ}{3.07466 - 1.59738 \cos 28.5^\circ} \\ &= 24.521^\circ \end{aligned}$$



Velocity Vector Diagram at Apogee Burn (French Guiana Launch)



Velocity Vector Diagram at Apogee Burn (Eastern Test Range Launch)

Figure 40. Velocity Vector Diagram

$$\begin{aligned}\beta &= 180^\circ - (28.5^\circ + 24.521^\circ) \\ &= 126.978^\circ\end{aligned}$$

Therefore, the apogee motor is required to provide a velocity change of 1.83649 km/s at an angle 24.521° with respect to equatorial plane.

For Ariane, launch site is French Guiana at a latitude of approximately 5° with a transfer orbit inclination of 8.5° [Ref. 3: p. 24]

$$\begin{aligned}\Delta V_s &= \sqrt{(1.59738 \sin 8.5^\circ)^2 + (3.07466 - 1.59738 \cos 8.5^\circ)^2} \\ &= \sqrt{2.290248} = 1.5133 \text{ km/s}\end{aligned}$$

$$\alpha = \tan^{-1} \frac{1.5133 \sin 8.5^\circ}{3.07466 - 1.5133 \cos 8.5^\circ} = 8.068^\circ$$

$$\begin{aligned} \beta &= 180^\circ - (8.5^\circ + 8.068^\circ) \\ &= 163.432^\circ \end{aligned}$$

Therefore, for the Ariane, the apogee kick motor is required to provide a velocity change of 1.5133 km/s at an angle 8.068° with respect to equatorial plane.

APPENDIX G. NORTH-SOUTH STATION KEEPING

To solve for the average drift rate ($\frac{di}{dt}$), add the two consecutive total drift rates from Table 1-5 (last column), starting with 1993 and divide by two, as shown below, since spacecraft is assumed to be launched in Jan 1993. Also, the inclination tolerance (i) for NSSK is 0.1° .

$$1) \frac{0.834 + 0.802}{2} = 0.818$$

$$2) \frac{0.802 + 0.775}{2} = 0.7885$$

$$3) \frac{0.775 + 0.756}{2} = 0.7655$$

$$4) \frac{0.756 + 0.748}{2} = 0.752$$

$$5) \frac{0.748 + 0.752}{2} = 0.75$$

$$6) \frac{0.752 + 0.767}{2} = 0.7595$$

$$7) \frac{0.767 + 0.792}{2} = 0.7795$$

$$8) \frac{0.792 + 0.823}{2} = 0.8075$$

$$9) \frac{0.823 + 0.856}{2} = 0.8395$$

$$10) \frac{0.856 + 0.888}{2} = 0.872$$

$$11) \frac{0.888 + 0.914}{2} = 0.901$$

$$12) \frac{0.914 + 0.933}{2} = 0.9235$$

$$13) \frac{0.933 + 0.943}{2} = 0.938$$

$$14) \frac{0.943 + 0.942}{2} = 0.9425$$

$$15) \frac{0.942 + 0.932}{2} = 0.937$$

$$16) \frac{0.932 + 0.913}{2} = 0.9225$$

$$17) \frac{0.913 + 0.886}{2} = 0.8995$$

$$18) \frac{0.886 + 0.854}{2} = 0.87$$

$$19) \frac{0.854 + 0.821}{2} = 0.8375$$

$$20) \frac{0.821 + 0.791}{2} = 0.806$$

For the first ten years the average drift rate is 0.7932 °/yr

For 15 years, the average drift rate is 0.83826 °/yr

For 20 years, the average drift rate is 0.8455 °/yr

A. FOR 10 YEAR MISSION

Assuming an average inclination drift rate of 0.7932 °/yr, the average time interval T between the maneuvers is given [Ref 3: p. 87] by

$$T = \frac{2i}{\frac{di}{dt}} \times 365.25 \quad (G-1)$$

$$T = \frac{2 \times 0.1}{0.7932} \times 365.25 = 92.095 \text{ days}$$

The total number of maneuvers will be

$$\frac{\text{total inclination drift}}{2 \times \text{inclination tolerance}} = \frac{0.7932 \times 10}{2 \times 0.1} \approx 40$$

Assuming that the change in the right ascension of the orbital node caused by the maneuver is 180°. the velocity increment can be obtained by the equation

$$\Delta V = 6.148 \sin i \quad (G-2)$$

The total ΔV required is

$$\begin{aligned} & \text{number of maneuvers} \times \Delta V \text{ per maneuver} \\ &= 40 \times 6.148 \sin 0.1 \\ &= 429.21 \text{ m/s} \end{aligned}$$

B. FOR 15 YEAR MISSION

Assuming an average inclination drift rate of $0.83826^\circ/\text{yr}$, the average time interval T between the maneuvers is

$$T = \frac{2 \times 0.1}{0.83826} \times 365.25 = 87.145 \text{ days}$$

The total number of maneuvers will be

$$\frac{\text{total inclination drift}}{2 \times \text{inclination tolerance}} = \frac{0.83826 \times 15}{2 \times 0.1} \approx 63$$

The total ΔV required is

$$\begin{aligned} & \text{number of maneuvers} \times \Delta V \text{ per maneuver} = 63 \times 6.148 \sin 0.1^\circ \\ &= 676 \text{ m/s} \end{aligned}$$

C. FOR 20 YEAR MISSION

$$T = \frac{2 \times 0.1}{0.8455} \times 365.25 = 87.145 \text{ days}$$

The total number of maneuvers will be

$$\frac{\text{total inclination drift}}{2 \times \text{inclination tolerance}} = \frac{0.8455 \times 20}{2 \times 0.1} \approx 85$$

The total ΔV required is

$$\begin{aligned} \text{number of maneuvers} \times \Delta V \text{ per maneuver} &= 85 \times 6.148 \sin 0.1^\circ \\ &= 912.1 \text{ m/s} \end{aligned}$$

APPENDIX H. BIPROPELLANT MASS BUDGET FOR 10, 15 AND 20 YEAR MISSION

To obtain the propellant mass, [Ref 3: p 164], use

$$M_p = m_i (1 - e^{-\frac{\Delta V}{\eta I g}}) \quad (H-1)$$

$$= m_f (e^{\frac{\Delta V}{\eta I g}} - 1) \quad (H-2)$$

where

M_p = mass of propellant, kg

m_i = initial mass of the spacecraft, kg

m_f = final mass of the vehicle after burnout, kg

ΔV = required velocity change, m/s

I = specific impulse of the propellant, s

g = gravitational acceleration, (9.806 m/s²)

η = engine efficiency

A 1200 kg dry mass will be used, which does not include the additional tankage and structural support for station keeping propulsion. To account for this dry mass, an additional 7% and 9% of the propellant mass will be added for tankage and structural support respectively.

A. FOR 10 YEAR MISSION

1. For Station Repositioning

$$\Delta V = 33.96 \text{ m/s, see Appendix E}$$

$$\eta = 99\% \text{ due to } 7^\circ \text{ cant angle of the thrusters}$$

$$M_p = (1200 + 0.16 M_p) (e^{(33.96/285 \times 9.806 \times 0.99)} - 1)$$

$$M_p = (1200 + 0.16 M_p) (0.01235)$$

$$= 14.85 \text{ kg}$$

2. For East-West Station Keeping

$$\Delta V = 17.4 \text{ m/s (see Appendix D)}$$

$$I_{sp} = 285 \text{ s (from Table 14)}$$

$$\eta = 99\% \text{ due to } 7^\circ \text{ cant angle of the thrusters}$$

$$m_f = 1200 + 0.16(14.85) + 14.85$$

$$= 1217.23 \text{ kg}$$

$$M_p = (1217.23 + 0.16 M_p) (e^{(17.4/285 \times 9.806 \times 0.99)} - 1)$$

$$M_p = 7.69 \text{ kg}$$

3. For North-South Station Keeping:

$$\Delta V = 429.21 \text{ m/s, from Appendix G}$$

$$\eta = 99\% \text{ due to } 7^\circ \text{ cant angle of the thrusters}$$

$$m_f = 1217.13 + 0.16(7.69) + 7.69$$

$$= 1226.15 \text{ kg}$$

$$M_p = (1226.15 + 0.16 M_p) (e^{(429.21/285 \times 9.806 \times 0.99)} - 1)$$

$$= 211.44 \text{ kg}$$

$$\text{BOL} = 1226.15 + 1.16(211.44)$$

$$= 1471.42 \text{ kg}$$

4. Assuming the Spacecraft is Launched at French Guiana

For apogee kick motor (AKM) propellant, assuming bipropellant is used

$$I_{sp} = 300 \text{ s, from Table 14}$$

$$\Delta V = 1513.3 \text{ m/s from Appendix F}$$

$$\eta = 100\%$$

$$mf = 1226.15 + 0.16(211.44) + 211.44$$

$$= 1471.42$$

$$M_p = 1471.42 (e^{(1513.3/300 \times 9.806 \times 1)} - 1)$$

$$= 989.76 \text{ kg, } \underline{\text{this mass will be used as the baseline for tankage and}}$$

structural support limit

For perigee propellant, assuming solid propellant is used:

$$I_{sp} = 285 \text{ from Table 14}$$

$$\Delta V = 2454.57 \text{ m/s (from Appendix F)}$$

$$\eta = 100\%$$

$$mf = 1471.42 + 989.76$$

$$= 2461.18 \text{ kg (weight of the propellant tanks and support were included}$$

in the 1200 kg dry mass)

$$M_p = (2461.18 + 0.07M_p) (e^{(2454.57/285 \times 9.806 \times 1)} - 1)$$

$$= 3840.55 \text{ kg}$$

$$\text{Solid propellant casing} = 0.07(3840.55) = 268.84 \text{ kg}$$

5. Assuming the Spacecraft is Launched at ETR

For apogee kick motor (AKM) propellant, assuming bipropellant is used

$$I_{sp} = 300 \text{ s, from Table 14}$$

$$\Delta V = 1836.49 \text{ m/s from Appendix F}$$

$$\eta = 100\%$$

$$mf = 1226.15 + 0.16(211.44) + 211.44 + 0.16(M_p - 989.76)$$

$$= 1303.16 + 0.16M_p$$

$$M_p = (1303.16 + 0.16M_p) (e^{(1836.49/300 \times 9.806 \times 1)} - 1)$$

$$= 1311.62 \text{ kg}$$

For perigee propellant, assuming solid propellant is used:

$$I_{sp} = 285 \text{ from Table 14}$$

$$\Delta V = 2454.57 \text{ m/s (from Appendix F)}$$

$$\eta = 100\%$$

$$m_f = 1303.16 + 1.17(1311.62)$$

$$= 2824.64 \text{ kg}$$

$$M_p = (2853.36 + 0.07M_p) (e^{(2454.57/285 \times 9.806 \times 1)} - 1)$$

$$= 4407.71 \text{ kg}$$

$$\text{Solid propellant casing} = 0.07(4407.71) = 308.54 \text{ kg}$$

B. FOR 15 YEAR MISSION

1. For Station Repositioning

$$\Delta V = 33.96 \text{ m/s see, Appendix E}$$

$$\eta = 99\% \text{ due to } 7^\circ \text{ cant angle of the thrusters}$$

$$M_p = (1200 + 0.16 M_p) (e^{(33.96/285 \times 9.806 \times 0.99)} - 1)$$

$$M_p = (1200 + 0.16 M_p) (0.01235)$$

$$= 14.85 \text{ kg}$$

2. For East-West Station Keeping

$$\Delta V = 26.1 \text{ m/s (see Appendix D)}$$

$$I_{sp} = 285 \text{ s (from Table 14)}$$

$$\eta = 99\% \text{ due to } 7^\circ \text{ cant angle of the thrusters}$$

$$m_f = 1200 + 0.16(14.85) + 14.85$$

$$= 1217.23 \text{ kg}$$

$$M_p = (1217.23 + 0.16 M_p) (e^{(26.1/285 \times 9.806 \times 0.99)} - 1)$$

$$M_p = 11.65 \text{ kg}$$

3. For North-South Station Keeping:

$$\Delta V = 676 \text{ m/s, from Appendix G}$$

$$\eta = 99\% \text{ due to } 7^\circ \text{ cant angle of the thrusters}$$

$$m_f = 1217.13 + 0.16(11.65) + 11.65$$

$$= 1230.64 \text{ kg}$$

$$M_p = (1230.64 + 0.16M_p)(e^{(676/285 \times 9.806 \times 0.99)} - 1)$$

$$= 356.38 \text{ kg}$$

$$\text{BOL} = 1230.64 + 1.16(356.38)$$

$$= 1644.04 \text{ kg}$$

4. Assuming the Spacecraft is Launched at ETR

For apogee kick motor (AKM) propellant, assuming bipropellant is used

$$I_{sp} = 300 \text{ s, from Table 14}$$

$$\Delta V = 1836.49 \text{ m/s, from Appendix F}$$

$$\eta = 100\%$$

$$m_f = 1230.64 + 0.16(356.38) + 356.38$$

$$= 1644.04 \text{ kg}$$

$$M_p = [1644.04 + 0.16(M_p - 989.76)] (e^{(1836.49/300 \times 9.806 \times 1)} - 1)$$

where $(M_p - 989.76)$ is the mass that still needs to be supported

$$= (1485.68 + 0.16M_p)(e^{(1836.49/300 \times 9.806 \times 1)} - 1)$$

$$= 1495.33 \text{ kg}$$

For perigee propellant, assuming solid propellant is used:

$$I_{sp} = 285 \text{ from Table 14}$$

$$\Delta V = 2454.57 \text{ m/s (from Appendix F)}$$

$$\eta = 100\%$$

$$m_f = 1485.68 + 1.16(1495.33)$$

$$= 3220.26 \text{ kg}$$

$$M_p = (3220.26 + 0.07M_p) (e^{(2454.57/285 \times 9.806 \times 1)} - 1)$$

$$= 5025.05 \text{ kg}$$

$$\text{Solid propellant casing} = 0.07(5025.05) = 351.75 \text{ kg}$$

5. Assuming the spacecraft is launched at French Guiana

For apogee kick motor (AKM) propellant, assuming bipropellant is used

$$I_{sp} = 300 \text{ s, from Table 14}$$

$$\Delta V = 1513.3 \text{ m/s from Appendix F}$$

$$\eta = 100\%$$

$$m_f = 1230.64 + 0.16(356.38) + 356.38$$

$$= 1644.04 \text{ kg}$$

$$M_p = [1644.04 + 0.16(M_p - 989.76)](e^{(1513.3/300 \times 9.806 \times 1)} - 1)$$

$$= 1122 \text{ kg}$$

For perigee propellant, assuming solid propellant is used:

$$I_{sp} = 285 \text{ from Table 14}$$

$$\Delta V = 2454.57 \text{ m/s (from Appendix F)}$$

$$\eta = 100\%$$

$$m_f = 1644.04 + 0.16(1122 - 989.76) + 1122$$

$$= 2787.2 \text{ kg}$$

$$M_p = (2787.2 + 0.07M_p) (e^{(2454.57/285 \times 9.806 \times 1)} - 1)$$

$$= 4349.28 \text{ kg}$$

$$\text{Solid propellant casing} = 0.07(4349.28) = 304.45 \text{ kg}$$

C. FOR 20 YEAR MISSION

1. For Station Repositioning

$$\Delta V = 33.96 \text{ m/s see, Appendix E}$$

$$\eta = 99\% \text{ due to } 7^\circ \text{ cant angle of the thrusters}$$

$$M_p = (1200 + 0.16 M_p) (e^{(33.96/285 \times 9.806 \times 0.99)} - 1)$$

$$M_p = (1200 + 0.16 M_p) (0.01235)$$

$$= 14.85 \text{ kg}$$

2. For East-West Station Keeping

$$\Delta V = 34.8 \text{ m/s (see Appendix D)}$$

$$I_{sp} = 285 \text{ s (from Table 14)}$$

$$\eta = 99\% \text{ due to } 7^\circ \text{ cant angle of the thrusters}$$

$$m_f = 1200 + 0.16(14.85) + 14.85$$

$$= 1217.23 \text{ kg}$$

$$M_p = (1217.23 + 0.16 M_p) (e^{(34.8/285 \times 9.806 \times 0.99)} - 1)$$

$$M_p = 15.44 \text{ kg}$$

3. For North-South Station Keeping

$$\Delta V = 912.1 \text{ m/s, from Appendix G}$$

$$\eta = 99\% \text{ due to } 7^\circ \text{ cant angle of the thrusters}$$

$$m_f = 1217.23 + 0.16(15.44) + 15.44 + 0.16M_p$$

$$= 1235.14 \text{ kg} + 0.16M_p$$

$$M_p = (1235.14 + 0.16M_p)(e^{(912.1/285 \times 9.806 \times 0.99)} - 1)$$

$$= 514.47 \text{ kg}$$

$$\text{BOL} = 1235.14 + 1.16(514.47)$$

$$= 1831.93 \text{ kg}$$

4. Assuming the Spacecraft is Launched at ETR

For apogee kick motor (AKM) propellant, assuming bipropellant is used

$$I_{sp} = 300 \text{ s, from Table 14}$$

$$\Delta V = 1836.49 \text{ m/s from Appendix F}$$

$$\eta = 100\%$$

$$m_f = 1235.14 + 0.16(514.47) + 514.47$$

$$= 1831.93 \text{ kg}$$

$$M_p = [1831.93 + 0.16(M_p - 989.76)] (e^{(1836.49/300 \times 9.806 \times 1)} - 1)$$

$$= 1684.44 \text{ kg}$$

For perigee propellant, assuming solid propellant is used:

$$I_{sp} = 285 \text{ from Table 14}$$

$$\Delta V = 2454.57 \text{ m/s (from Appendix F)}$$

$$\eta = 100\%$$

$$m_f = 1831.93 + 0.16(1684.44 - 898.76) + 1684.44$$

$$= 3642.08 \text{ kg}$$

$$M_p = (3642.08 + 0.07M_p) (e^{(2454.57/285 \times 9.806 \times 1)} - 1)$$

$$= 5683.28 \text{ kg}$$

$$\text{Solid propellant casing} = 0.07(5683.28) = 397.83 \text{ kg}$$

5. Assuming the spacecraft is launched at French Guiana

For apogee kick motor (AKM) propellant

$$I_{sp} = 300 \text{ s, from Table 14}$$

$$\Delta V = 1513.3 \text{ m/s from Appendix F}$$

$$\eta = 100\%$$

$$m_f = 1235.14 + 0.16(514.47) + 514.47$$

$$= 1831.93 \text{ kg}$$

$$M_p = [1831.93 + 0.16(M_p - 989.76)] (e^{(1513.3/300 \times 9.806 \times 1)} - 1)$$

$$= 1261.51 \text{ kg}$$

For perigee propellant

$$I_{sp} = 285 \text{ from Table 14}$$

$$\Delta V = 2454.57 \text{ m/s (from Appendix F)}$$

$$\eta = 100\%$$

$$m_f = 1831.93 + 0.16(1261.51 - 989.76) + 1261.51$$

$$= 3136.92 \text{ kg}$$

$$M_p = (3136.93 + 0.07M_p) (e^{(2454.57/285 \times 9.806 \times 1)} - 1)$$

$$= 4895 \text{ kg}$$

$$\text{Solid propellant casing} = 0.07(4895) = 342.65 \text{ kg}$$

APPENDIX I. DETERMINATION OF INCLINATION DRIFT RATES

The right ascension of the ascending node of the lunar orbit measured in the ecliptic plane from the vernal equinox [Ref. 3: p. 77] is given by

$$\Omega = 178.78 - 0.05295 t \text{ (degrees)} \quad (\text{I-1})$$

where t is the number of days from January 1, 1960.

The lunar plane inclination i_l and the right ascension of the ascending node Ω_l are given by the equations

$$\cos i_l = \cos i_s \cos I_l - \sin i_s \sin I_l \cos \Omega \quad (\text{I-2})$$

$$\sin \Omega_l = \frac{\sin I_l \sin \Omega}{\sin i_l} \quad (\text{I-3})$$

where $i_s =$ inclination angle of the plane of ecliptic, 23.45°

$I_l =$ angle between the lunar orbit plane and ecliptic plane, 5.15°

With the equations above the values of i_l and Ω_l can be solved and are shown in Table 11.

A. DRIFT RATE DUE TO SUN'S PERTURBATION

The $\frac{di}{dt}|_{\text{sun}}$ can be solved using equation

$$\frac{di}{dt} \approx - \frac{3 \mu_s r^2}{4 h r_s^3} \sin \Omega \sin i_s \cos i_s \quad (\text{I-4})$$

where

$$\mu_s = 1.32686 \times 10^{11} \text{ km}^3 \text{ s}^{-2}$$

$$r_s = 1.49592 \times 10^8 \text{ km}$$

$$r = 42,164 \text{ km}$$

$$h = 129,640 \text{ km}^2 \text{ s}^{-1}$$

$$i_s = 23.45^\circ$$

It should be noted that the rate of change of the inclination depends on the right ascension of the satellite ascending node. The common strategy for the inclination station keeping is to let the satellite orbit drift from the orbit inclination at the allowable limit and with Ω in the neighborhood of 270° .

$$\begin{aligned} &\text{At } 270^\circ \\ \frac{di}{dt} \Big|_{\Omega = 270^\circ} &= -0.269^\circ \text{ yr}^{-1} \end{aligned}$$

$$\begin{aligned} &\text{Similarly, at } 90^\circ \\ \frac{di}{dt} \Big|_{\Omega = 90^\circ} &= 0.269^\circ \text{ yr}^{-1} \end{aligned}$$

B. DRIFT RATE DUE TO MOON'S PERTURBATION

Considering only the secular terms and assuming a geosynchronous orbit, the inclination can be approximated by

$$\frac{di}{dt} \approx -\frac{3}{4} \frac{\mu_l r^2}{h r_l^3} \sin(\Omega - \Omega_l) \sin i_l \cos i_l \quad (I-5)$$

where

$$\mu_l = 4.9028 \times 10^3 \text{ km}^3 \text{ s}^{-2}$$

$$r_l = 3.844 \times 10^5 \text{ km}$$

$$r = 42,164 \text{ km}$$

$$h = 129,640 \text{ km}^2 \text{ s}^{-1}$$

$$i_l = 18.30 \text{ to } 28.6^\circ$$

Then

$$\frac{di}{dt} \Big|_{i_l = 18.30^\circ, \Omega = 90^\circ, \Omega_l = 0} = 0.4780^\circ \text{ yr}^{-1}$$

and

$$\frac{di}{dt} \Big|_{i_l = 28.60^\circ, \Omega = 90^\circ, \Omega_l = 0} = 0.674^\circ \text{ yr}^{-1}$$

The last column of Table 11 is the sum of the inclination drift rates due to the moon and sun, and varies yearly between 0.943° and $0.747^\circ \text{ yr}^{-1}$.

LIST OF REFERENCES

1. Brewer, G. R., *Ion Propulsion Technology and Applications*, Gordon and Breach, Science Publishers, Inc., New York, 1970.
2. Poeschel, R. L., "Ion Propulsion for Communications Satellite," IEPC-Paper-84-43, Tokyo, Japan, May 1984.
3. Agrawal, Brij N., *Design of Geosynchronous Spacecraft*, Prentice-Hall, Inc., Englewood Cliffs, New Jersey, 1986, pp 459.
4. Ariane IV User's Manual, Arianspace, April 1983.
5. Stuhlinger, E., *Ion Propulsion for Spaceflight*, McGraw-Hill Book Co., 1964.
6. "Electric Propulsion," *Aerospace America*, v. 27, p. 78, December 1989.
7. Birkan, M., and Micci, M., "Survey of Electric Propulsion Thruster Applicability to Near Earth Space Missions," IEPC-Paper-88-065, 20th International Electric Propulsion Conference, Partenkirchen, Germany, October 1988.
8. Voulelikas G. D., "Electric Propulsion: A Review of Future Space Propulsion Technology," *Communications Research Centre*, Ottawa, Canada, October 1985.
9. Schreib, R., "Electric Propulsion: Implementation Issues," IEPC Paper-88-006, 20th International Electric Propulsion Conference, Partenkirchen, Germany, October 1988.
10. Yoshikawa, T., and others, "Continuous Operation of Quasi-Steady MPD Propulsion System with an External Magnetic Field," IEPC-Paper-88-056, 20th International Electric Propulsion Conference, Partenkirchen, Germany, October 1988.
11. Jahn, R. G., *Physics of Electric Propulsion*, McGraw-Hill Book Co., 1968.
12. Patterson, M. J., and Curran, F. M., "Electric Propulsion Options for 10 kW Class Earth-Space Missions," 1989 JANNAF Propulsion Meeting, v. 1, pp. 239-265, Cleveland, Ohio, 23-25 May 1989.

13. Byers, D. C., and Rawlin, V. K., "Critical Elements of Electron-Bombardment Propulsion for Large Space Systems," *Journal of Spacecraft and Rockets*, v.14, pp. 648-654, November 1977.
14. Schreib, R., "Readiness Appraisal: Ion Propulsion for Communication Satellites," AIAA-Paper-88-0777, March 1988.
15. Bassner, H. F., Berg, H. P., and Kukies, R., "Radiofrequency Ion Propulsion Application to Commercial Satellites," AIAA-Paper-89-2276, July 1989.
16. Kaufman, H. R., and Robinson R. S., "Electric Thruster Performance for Orbit Raising and Maneuvering," *Journal of Spacecraft and Rockets*, v. 21, pp. 180-186, March-April 1984.
17. Martin, A., "Electric Propulsion for Spacecraft," *Space*, v.2 pp.12-20, August 1986.
18. Schreib, R., "Planning for Ion Propulsion on Communication Satellites," IEPC Paper-84-42, Tokyo, Japan, May 1984.
19. Collier's Encyclopedia, v. 23, Macmillan Education Corp., New York, 1979.
20. Beattie, J. R., "Status of Xenon Ion Propulsion Technology for Station Keeping" Intelsat Symposium on Ion Propulsion for Communication Satellites, Monterey, Ca., July 13, 1989.
21. Beattie, J. R., Matossian, J. N., and Robson, R. R., "Status of Xenon Ion Propulsion Technology," *Journal of Propulsion and Power*, v. 6, pp. 145-150, March-April 1990.
22. Kaufman, H. R., "Technology of Electron-Bombardment Ion Thrusters," *Advances in Electronics and Electron Physics*, v. 36, Academic Press, New York, 1974, pp. 265-373.
23. Free, B. A., "Chemical and Electric Propulsion Tradeoffs for Communications satellites," *COMSAT Technical Review*, v. 2, pp123-145, Spring 1972.
24. Rees, T., and Fearn, D. G., "N-S Station Keeping by 10-cm Ion Thruster," *Journal of Spacecraft and Rockets*, v. 15, pp. 147-153, May-June 1978.

25. Hughes, R.C., and Hastings, R., "T4A Truster Starting Sequences and the Design of an Electromagnetic Sequencer for Cyclic Life Tests", AIAA-Paper-76-99, Key Biscayne, Fl., 1976.
26. Duhamel, T., Ricaud, P. H., Greff, P., "Design and Integration of an Electric Propulsion System on the Eurostar Spacecraft," IEPC-Paper-88-036, October 3-6, 1988.
27. Rex, D., and Kohhnecke, B., "Redundant Configuration of Electric Propulsion Systems for Station Keeping," *Journal of Spacecraft and Rockets*, v. 11, pp. 488-493, July 1974.
28. Duhamel, T. G., "Implementation of Electric Propulsion for North-South Station Keeping on the Eurostar Spacecraft," AIAA-Paper-89-2274, 25th Joint Propulsion Conference, Monterey, Ca., July 1989.
29. Anzel, B. M., "Controlling a Stationary Orbit Using Electric Propulsion," IEPC-Paper-88-051, 20th International Electric Propulsion Conference, Partenkirchen, Germany, October 1988.
30. Schreib, R., "Utility of Xenon Ion Station Keeping," AIAA-Paper-86-1849, June 1986.
31. Free, B. A., and Dunlop, J. D., "Battery-Powered Electric Propulsion for North Station Keeping," *COMSAT Technical Review*, v. 3, pp. 211-214.
32. Chetty, P. R. K., *Satellite Technology and Its Applications*, Tab Books Inc., Blue Ridge Summit, PA, 1988, pp. 418.
33. Hyman, J. Jr., "Hughes Research Laboratories Ion Propulsion Program," IEPC 84-25, Tokyo, Japan, May 1984.
34. Rulis, R. J., "SERT II: Design Requirements for Integrating Electric Propulsion into a Spacecraft," *Journal of Spacecraft and Rockets*, v. 8, pp. 209-212, March 1971.
35. Kerslake, W. R., Goldman, R. G., and Nieberding, W. C., "SERT II: Mission, Thruster Performance, and In-Flight Thrust Measurements," *Journal of Spacecraft and Rockets*, v. 8, pp. 213- 224, March 1971.
36. Williamson, W. S., and Hyman J. Jr., "Discharge-Charge Sputtering in Mercury Ion Thrusters," *Journal of Spacecraft and Rockets*, v. 15, pp. 375-380, November-December 1978.

37. Shimada, S., and others, "Ion Thruster Contamination Evaluation," AIAA-Paper-89-2269, July 1989.
38. Sperber, R., " Why Don't We Use Ion Propulsion," AIAA-Paper-84-0730.
39. King, H. J., and Schnelker, D. E., "Ion Thruster Systems with Thrust Vector Deflection," *Journal of Spacecraft and Rockets*, v. 8, pp. 553-554, May 1971.
40. Wilbur, P. J., and Kaufman H. R., "Double Ion Production in Argon and Xenon Ion Thrusters," *Journal of Spacecraft and Rockets*, v. 16, pp. 264-267, July-August 1979.
41. Olsen, R. C., "Modification of Spacecraft Potentials by Plasma Emission," *Journal of Spacecraft and Rockets*, v. 18, pp. 462-469, September-October 1981.
42. Olsen, R. C., "Modification of Spacecraft Potentials by Thermal Electron Emission on ATS-5," *Journal of Spacecraft and Rockets*, v. 18, pp. 527-532, November-December 1981.
43. Carruth , M. R. Jr., Gabriel, S. B., and Kitamura, S., "Ion Thruster Charge-Exchange Plasma Flow," *Journal of Spacecraft and Rockets*, v. 19, pp. 571-578, November-December 1982.
44. Carruth, M. R. Jr., and Brady, M. E., "Measurement of the Charge-Exchange Plasma Flow from an Ion Thruster," *Journal of Spacecraft and Rockets*, v.18, pp. 457-461, September-October 1981.
45. Interview between J. R. Beattie, Head, Plasma Source Section, Plasma Physics Department, Hughes Research Laboratories, Malibu, Ca., and the author, 4 May 1990.
46. Clark, K. E. "Survey of Electric Propulsion Capability" *Journal of Spacecraft and Rockets*, v. 12, pp 641-654, November 1975.
47. Kerslake, W. R., and Ignaczak L. R., "SERT II 1979-1981 Tests: Ion Thruster Performance and Durability," *Journal of Spaceraft and Rockets*, v. 19, pp. 241-245, May-June 1982.
48. Fearn, D. G., and Smith, S., "The Application of Ion Propulsion to Intelsat VII Class Spacecraft" AIAA-Paper-89-2275, July 1989.
49. Shimada, S., and others, "Ion Engine System Development of ETS-VI," AIAA-Paper-89-2267, July 1989.

INITIAL DISTRIBUTION LIST

	No. Copies
1. Defense Technical Information Center Cameron Station Alexandria, Virginia 22304-6145	2
2. Library, Code 0142 Naval Postgraduate School Monterey, California 93943-5002	2
3. Chairman, Code AA Department of Aeronautical and Astronautical Engineering Naval Postgraduate School Monterey, California 93943-5000	1
4. Curricular Officer, Code 39 Naval Postgraduate School Monterey, California 93943-5000	1
5. Prof. Brij N. Agrawal, Code AA/Ag Department of Aeronautical and Astronautical Engineering Naval Postgraduate School Monterey, California 93943-5000	2
6. Prof. Oscar Biblarz, Code AA/Bi Department of Aeronautical and Astronautical Engineering Naval Postgraduate School Monterey, California 93943-5000	1
7. Commander, Naval Research Laboratory ATTN: CDR Carl E. Josefson, Code 9110-4 4555 Overlook Ave., S.W. Washington, DC 20375	1
8. Commander, Naval Research Laboratory ATTN: LCDR Ronald S. Huber, Code 9120 4555 Overlook Ave., S.W. Washington, DC 20375	1

- | | | |
|-----|--|---|
| 9. | Commander, Naval Research Laboratory
ATTN: LCDR Michael L. Noble, Code 9120
4555 Overlook Ave., S.W.
Washington, DC 20375 | 1 |
| 10. | MAJ Charles C. Howard
166 Beechwood Drive
Oakland, California 94618 | 1 |
| 11. | LT Spotrizano D. Lugtu
USS Ranger, CV-61
FPO San Francisco, California 96601 | 2 |
| 12. | LT Spotrizano D. Lugtu
12906 Amaranth St.
San Diego, California 92129 | 2 |